

TARGET DETECTION AND COGNITIVE RADIO CAPACITY ANALYSIS  
BASED ON SENSOR NETWORKS

by

ISHRAT MAHERIN

Presented to the Faculty of the Graduate School of  
The University of Texas at Arlington in Partial Fulfillment  
of the Requirements  
for the Degree of

DOCTOR OF PHILOSOPHY

THE UNIVERSITY OF TEXAS AT ARLINGTON

May 2014

Copyright © by Ishrat Maherin 2014

All Rights Reserved

To my parents, Khojesta Akhter and Eradat Ullah,

My children, Zihan Hossain and Ahyan Hossain

and

My husband, Md Sahadat Hossain

for their support and encouragement

## Acknowledgements

I would like to express my deepest gratitude to my supervising professor, Dr. Qilian Liang. Dr. Liang continually and convincingly encourages and inspires me in all step of my research. He has knowledge and vision of a perfect researcher. He identified the strength inside me and encouraged me to work towards my interest. He conveyed his enthusiasm for research with positive encouragement, when the path was less obvious. Without his true guidance and mentorship this study would not have been possible.

I would like to express my sincere appreciation to all my committee members Dr. Jonathan Bredow, Dr. Kambiz Alavi, Dr. Saibun Tjuatja and Dr. Ioannis D. Schizas for their interest in my research and for taking time out to serve in my dissertation committee. My special acknowledgement to Dr. Bredow for teaching the valuable concept of radar, path loss and channel modeling. I would also like to thank Dr. Schizas for the valuable knowledge he introduced in estimation theory.

I would like to thank National Science Foundation(NSF) and office of Naval Research(ONR). This work was supported in part by U.S. National Science Foundation under Grants CNS-1247848, CNS-1116749, CNS-0964713, and U.S. Office of Naval Research under Grants N00014-13-1-0043, N00014-11-1-0865, N00014-11-1-0071.

I am thankful to all the current and the previous members of wireless communications and networking lab (WCNA) at UTA including Dr. Lei Xu, Dr. Davis

Kirachaiwanich, Dr.Jing Liang, Ji Wu, Junjie Chen, Xin Wang, Zhuo Li, Qiong Wu, Na Wu and Hao Liang.

Last but most importantly, I would like to express my gratefulness to my family. My parents unconditionally loved, encouraged and inspired me throughout my life. They taught me discipline, values and importance of education. My husband has built positive attitude inside me and supported me throughout the whole Ph.D. research. My children, specially my son is a wonderful child. I could work with full dedication because of his understanding and cooperation. I am so fortunate to have children like them. After all the hard work, they brought the smile in my face. I want to mention the support I got from my sister, Nuzhat Maherin. My family believed in me and I am determined because of their support and encouragement.

April 18, 2014

Abstract

TARGET DETECTION AND COGNITIVE RADIO CAPACITY ANALYSIS  
BASED ON SENSOR NETWORKS

Ishrat Maherin, Ph.D.

The University of Texas at Arlington, 2014

Supervising Professor: Qilian Liang

In this dissertation, we studied two topics which are focused on target detection through foliage and capacity analysis of cognitive radio. We propose a multi-step information theory based scheme for target detection through foliage, using ultra wide-band (UWB) radar sensor network (RSN). This method is motivated by the fact that echoes from the stationary target, obscured by foliage, are more random than the region without the target. This is resolved by three steps of information fusion. Information fusion and integration is the process of combining data from several radar sensors and can achieve results that are not possible by individual radar operating independently. For first step of information fusion, we propose to use Kullback-Leibler (K-L) divergence based weighting. By using the information theoretic criterion known as method of types, we proved that false alarm can be inversely proportional to the relative entropy or KL distance. In the second step, we propose to use Maximum Entropy Method(MEM) and mutual information based detection. Finally, we use Dempster and Shafer (D-S) theory of evidence for decision. We further investigated and applied another information theoretic criterion known

as Chernoff information to select the best radar sensor. We modified the algorithm we developed for RSN for single radar case and applied for human detection through wall. We successfully detected human behind a gypsum wall using single UWB radar. This proved that our method is not adhoc and applicable to various scenarios.

Cognitive radio is an intelligent wireless device that can exploit the side information and maximize the spectral utilization. Efficient spectrum sensing along with transmit power control can achieve the conflicting goal of increasing the capacity while keeping the interference under limit. In this dissertation, we propose a sensor network aided cognitive radio system which will reduce the missed detection and reduce the interference. The non-convex optimization problem is divided in two separate sub problems and solved to get a suboptimal solution. Mathematical analysis shows that interference between primary and secondary depends on spectral distance, when the parallel channels are orthogonal like an OFDM based system.

## Table of Contents

Acknowledgements . . . . .	iv
Abstract . . . . .	vi
List of Illustrations . . . . .	xii
List of Tables . . . . .	xvi
Chapter	Page
1. Introduction . . . . .	1
1.1 Preliminaries to UWB Based Detection . . . . .	3
1.2 Preliminaries to Target Detection Through Foliage . . . . .	4
1.3 Preliminaries to Radar Sensor Network and Preprocessing . . . . .	6
1.4 Preliminaries to Decision Fusion . . . . .	7
1.5 Preliminaries to Opportunistic Sensing Using Chernoff Information . . . . .	8
1.6 Preliminaries to Human Detection . . . . .	9
1.7 Preliminaries to Capacity Analysis of Sensor Aided Cognitive Radio . . . . .	10
1.8 Organization . . . . .	11
2. Information Theory Based Target Detection . . . . .	14
2.1 Introduction . . . . .	14
2.2 Data Measurement and Analysis . . . . .	15
2.2.1 Data Measurement . . . . .	15
2.2.2 Data Analysis . . . . .	18
2.3 Information Theory Based Detection . . . . .	22
2.3.1 Maximum Entropy Method Based Target Detection . . . . .	23
2.3.2 Mutual Information Based Target Detection . . . . .	26



2.3.3	Algorithm for Information Theory Based Target Detection . . .	27
2.4	Simulation Results . . . . .	28
2.5	Conclusion . . . . .	32
3.	Radar Sensor Network and KL Based Preprocessing . . . . .	33
3.1	Introduction . . . . .	33
3.2	Preprocessing . . . . .	33
3.2.1	Simple Weight Preprocessing . . . . .	33
3.2.2	Information Fusion by Information Theory . . . . .	34
3.2.3	False Alarm Rate for Continuous Case . . . . .	40
3.3	Simulation Results . . . . .	42
3.3.1	Computational Complexity . . . . .	47
3.4	Conclusion . . . . .	48
4.	Decision Fusion Based on Dempster Shafer's Theory and Bayesian Network	50
4.1	Introduction . . . . .	50
4.2	Block Diagram . . . . .	51
4.3	Decision Fusion . . . . .	52
4.3.1	DS Theory . . . . .	52
4.3.2	Proportional Conflict Redistribution Rule 5 . . . . .	55
4.3.3	Bayesian Network . . . . .	56
4.3.4	Computational Complexity . . . . .	58
4.4	Simulation Results . . . . .	58
4.4.1	Conclusion . . . . .	59
5.	Sensor Selection Based on Chernoff Information . . . . .	65
5.1	Introduction . . . . .	65
5.2	System Model . . . . .	66

5.3	Design and Performance Analysis Based on Chernoff Information and Chernoff Stein Lemma . . . . .	68
5.4	Simulation Results . . . . .	72
5.5	Conclusion . . . . .	74
6.	Human Detection Based on Information Theory . . . . .	78
6.1	Introduction . . . . .	78
6.1.1	Measurement Setup . . . . .	79
6.2	Four Step Method . . . . .	83
6.3	Simulation Results . . . . .	85
6.4	Conclusions . . . . .	88
7.	Throughput Optimization of Cognitive Radio Using Sensor Network and Power Allocation . . . . .	93
7.1	System Model . . . . .	94
7.2	WSN Based Spectrum Sensing . . . . .	95
7.2.1	Decision Fusion by OR Logic . . . . .	97
7.2.2	Majority rule . . . . .	97
7.2.3	Log Likelihood Ratio . . . . .	98
7.3	Throughput Analysis with Sensing Time and Interference Constraint . . . . .	99
7.4	Power Control and Sensing Time Design . . . . .	102
7.4.1	Power Allocation . . . . .	102
7.4.2	Sensing Time Design . . . . .	104
7.5	Simulation Results . . . . .	105
7.6	Conclusion . . . . .	106
8.	Conclusion and Future Works . . . . .	110
8.1	Summary . . . . .	110
8.2	Future Direction . . . . .	114

8.2.1	Extending Information Theory Based Target Detection in Multi-target Environment . . . . .	114
8.2.2	Applying Chernoff Information and KL Based Processing in Big Data . . . . .	115
8.2.3	Interweaved Cognitive Radio for Optimizing the Femto Macro Capacity . . . . .	115
Appendix		
A.	Closed Form Approximation Between Rician and Gaussian for KL . . . . .	118
B.	Closed Form Approximation of Chernoff Information Between Rician and Uniform Distribution . . . . .	121
	References . . . . .	124
	Biographical Statement . . . . .	138

## List of Illustrations

Figure	Page
1.1 Target detection with Radar Sensor Network (RSN) . . . . .	2
2.1 Target (A Trihedral Reflector) is shown 300 feet away . . . . .	17
2.2 This figure shows the lift of the experiment . . . . .	18
2.3 Reflected echoes for two different cases: (a) no target (b) with target	20
2.4 Reflected echoes of sample index 13001 to 15000 for two different cases: (a) no target (b) with target . . . . .	21
2.5 Expanded view of the echo difference. Signature of the target is de- tected around sample 13900 . . . . .	22
2.6 Expanded view of the echo difference. Signature of the target is not detected around sample 13900 . . . . .	23
2.7 3-D representation of the transition of the echoes in different state . .	24
2.8 Entropy of reflected echoes collected by single Radar for two different cases: (a) good signal (b) poor signal . . . . .	29
2.9 Quantized signature of target . . . . .	30
2.10 Conditional entropy given the background . . . . .	30
2.11 Mutual information of echoes with two different condition (a) good signal (b) poor signal . . . . .	31
3.1 Reflected echo difference on a single radar in position 1 . . . . .	34
3.2 Block diagram of multi-step information fusion . . . . .	38
3.3 Clutter distribution in the farfield for the last 5000 samples collected by 9 different radars with 20 bin . . . . .	41

3.4	Clutter distribution in the farfield for the last 5000 samples collected by 9 different radars with 100 bin . . . . .	42
3.5	Entropy of echoes of poor signal with power based weighted RSN for two quantization level: (a) level of quantization=8 (b) level of quantization=32 . . . . .	44
3.6	Performance evaluation in terms of probability of detection and probability of false alarm for two quantization levels (a) level=8 (b) level=32	45
3.7	Mutual information of echoes with two different condition (a) good signal (b) poor signal . . . . .	46
3.8	Entropy of echoes in RSN with K-L based weighting. Clear target is visible around sample 13900 . . . . .	47
3.9	Mutual information of echoes in RSN with K-L based weighting. Clear target is visible around sample 13900 . . . . .	48
3.10	Performance evaluation in terms of probability of detection versus probability of false alarm (ROC) for(a) without (b) with KL divergence.	49
4.1	Block diagram of centralized fusion for target detection . . . . .	51
4.2	Block diagram of centralized fusion with preprocessing on each branch	52
4.3	Block diagram of hybrid fusion for target detection . . . . .	52
4.4	Detailed block diagram of the three step information fusion for target detection . . . . .	53
4.5	Bayesian network for Target Detection . . . . .	61
4.6	Probability of target present after decision fusion. Target is detected with certainty . . . . .	61
4.7	Performance evaluation in terms of probability of detection for high conflict in three different methods: (a)D-S, (b)PCR5 and (c) Bayesian not considering Zadeh's paradox . . . . .	62

4.8	Performance evaluation in terms of probability of detection for high conflict using D-S, considering Zadeh’s paradox . . . . .	63
4.9	Performance evaluation in terms of probability of detection for high conflict using PCR5 considering Zadeh’s paradox . . . . .	63
4.10	Performance evaluation in terms of probability of detection for high conflict with Bayesian Network considering Zadeh’s paradox . . . . .	64
5.1	Detailed block diagram for information theory based opportunistic sensing in Radar Sensor Network . . . . .	67
5.2	Clutter distribution in the farfield for the last 5000 samples collected by 9 different radars with bin 20 bin . . . . .	70
5.3	Clutter distribution in the far-field for the last 5000 samples collected by 9 different radars with 100 bin . . . . .	71
5.4	Probability of error versus number of sensors, with 16 level of quantization . . . . .	74
5.5	Chernoff Information versus radar in nine different positions . . . . .	75
5.6	Entropy based Target detection with five sensors(position 3,4,5,6,9) selected by Chernoff Information with 16 level quantization. Target is detected . . . . .	76
5.7	Entropy based Target detection with three sensors(position 3,4,5) selected by Chernoff Information with 16 level quantization. Target is detected . . . . .	76
5.8	Entropy based Target detection with one sensor(position 4) selected by Chernoff Information with 16 level quantization. Target is detected . . . . .	77
5.9	Entropy based Target detection without OS . . . . .	77
6.1	P220 in monostatic mode . . . . .	80
6.2	TM-UWB Transceiver block diagram . . . . .	81

6.3	A periodic pulse wave in time and frequency domain . . . . .	81
6.4	MSR analysis tool setup tab . . . . .	86
6.5	Window displaying a single raw scan . . . . .	86
6.6	Location of the Human target and UWB radar on different sides of a 1 ft thick Gypsum partition wall (a) human target and (b) UWB radar	88
6.7	Location of the brick wall and UWB radar on different sides brick wall (a) brick wall and (b) UWB radar . . . . .	89
6.8	Location of the Human target and UWB radar on different sides wooden door (a)UWB radar and (b) Human Target . . . . .	90
6.9	Human target detection using two step information fusion. Target is detected around sample 4200 . . . . .	91
6.10	Human target detection using two step information fusion. Target is detected around sample 5120 . . . . .	91
6.11	Human target detection using two step information fusion. Target is behind door and expected around sample 4800 . . . . .	92
7.1	Frequency domain distribution of primary and secondary user . . . . .	95
7.2	System model on wireless sensor network (WSN) aided Cognitive Radio Network. Each individual sensor working as energy detector sends the local decision to the Fusion centre (FC) . . . . .	96
7.3	Consecutive orthogonal sub-carriers in time domain . . . . .	100
7.4	Probability of detection versus SNR for three different sensing schemes	106
7.5	Capacity versus SNR for three different power allocation schemes . . .	107
7.6	Throughput versus sensing time for three different power allocation schemes . . . . .	108
7.7	Three dimensional representation of throughput as a function of SNR and sensing time . . . . .	109

## List of Tables

Table		Page
4.1	Combination Result for DS and PCR5 . . . . .	56
6.1	PulseOn 220 Specifications . . . . .	83



## Chapter 1

### Introduction

Target detection through foliage which is a subject of intense research due to the complexity of the environment. In order to deal with performance degradation, Radar sensor network (RSN) based detection with multi-step information fusion is proposed, which is shown in Fig. 1.1. In RSN, networks of multiple distributed radar sensors are arranged to survey a large area and observe targets from different angles. Information fusion and integration is the process to achieve result which is not possible by individual sensors operating independently. We focus to more challenging environment when the signal quality is poor and probability of detection is low. Traditionally, radars are bi-static and acts independently and they are processed by, cluster-heads which use time and spatial diversity to combine them. In our proposed method, we use information fusion based combinations to detect the target. For many years, management of sensors, was performed by human operator. Human brain is more capable to understand abstract goal and make dynamic decision which computer-based algorithm is unable to understand. However, many military applications are moving toward the autonomous operation of management to keep the soldiers away from harm.

Opportunistic Sensing (OS) refers to a paradigm for signal and information processing in which a network of sensing systems can automatically discover and select sensor platforms based on an operational scenario. It uses appropriate methods to fuse the data, resulting in an adaptive network that automatically finds scenario-dependent, objective driven opportunities with optimized performance. We tried to

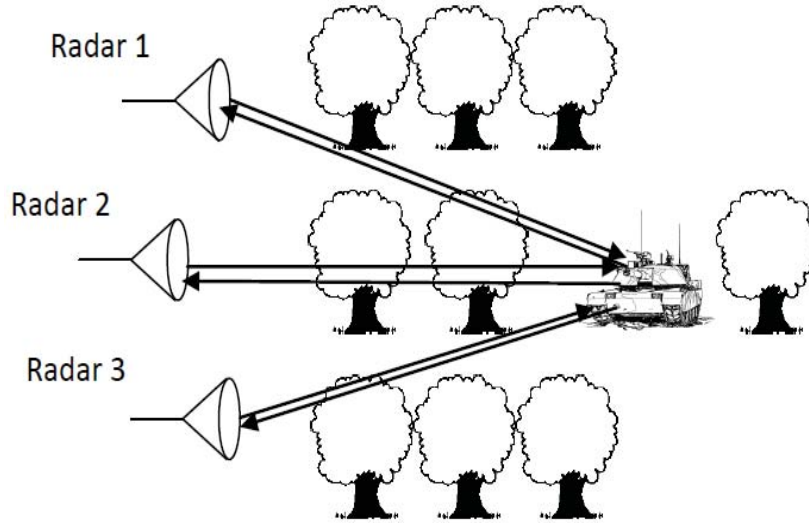


Figure 1.1. Target detection with Radar Sensor Network (RSN).

develop algorithm so that we can select the best sensor that will give us the best result.

A cognitive radio can sense the spectrum of the licensed user also known as primary user (PU) and identify the under-utilized spectrum known as white space or spectrum hole. Thus the reliability of the sensing scheme is crucial. However a single sensor is limited by path loss, shadowing and fading. In order to enhance the reliability of the detection a wireless sensor network (WSN), not necessarily embedded in cognitive receiver can be used. In this WSN, single sensor will make local decision and forward the decision to the fusion centre (FC). This sensor network will combat the fading through space diversity and will cover a large geographical area. There will be at least another sensor to detect the primary user which is far from a secondary user. Hence the two performance metrics of the sensing: 1) probability of detection and 2) probability of false alarm can be improved. The overall objective of CR is to increase the spectral efficiency and keeping the interference under

limit. However, as the sensing time is increased it can guarantee higher detection probability but the overall throughput goes down. The traditional optimization of throughput is achieved by water-filling power allocation. But water filling in CR is complex due to the added constraints of interference and false alarm. So we have three different metrics, we need to consider, sensing time, power and interference.

### 1.1 Preliminaries to UWB Based Detection

UWB communication is based on transmitting and receiving ultra short energy pulses with very high fractional bandwidth (greater than 0.2). In this definition, bandwidth means the difference between the highest and lowest frequencies of interest and contains about ninety five percent of the signal power [1],[2]. In 1995, James D. Taylor introduced UWB to engineers as a promising new concept for remote sensing [1]. In [3], Immoreev gave an overview on new practical applications of UWB radars. The primary advantages of UWB radar are very high bandwidth with exceptional good resolution, high power efficiency because of its low duty cycle, low probability of detection, low interference to legacy systems and ability to penetrate through material. UWB radars are used nowadays for different applications such as subsurface sensing, classification of aircrafts, collision avoidance, etc. In all of these applications the ultra-high resolution of UWB radars is essentially used.

In this dissertation we are particularly interested to use UWB radar to detect target in the forest because UWB has all the essential qualities needed for detection. However, signal radiated by narrow band has harmonics which makes them good candidates for match filtering and correlating with the reference. This does not work for UWB radar with heavy clutter and unknown target. We needed to further investigate to find the method that will combat the time varying channel we have in the forest.

## 1.2 Preliminaries to Target Detection Through Foliage

This dissertation deals with target detection through foliage which itself is a subject of intense research due to the complexity of the environment. The studies on foliage penetration can be categorized into two groups. One direction is to pursue the foliage clutter modeling [4], [5] and the second group centers on advanced signal processing [6], [7] and [8]. In [4], Liang applied two approaches to the wireless channel modeling: Saleh and Valenzuela (S-V) method for UWB channel modeling and CLEAN method for narrowband and UWB channel modeling. They validated that UWB echo signals (within a burst) do not hold self-similarity, which means the future signals cannot be forecasted based on the received signals and channel modeling is necessary from statistical point of view. In [5], Jing proved that the foliage clutter follows log-logistic model using maximum likelihood (ML) parameter estimation as well as the root mean square error (RMSE) on PDF curves between original clutter and statistical model data. In [6], Mayer performed whitening and dewatering to transform target signature. In [7], Nanis used adaptive filter to detect target in foliage. In [9], Jing proposed a differential based approach and in [10], she proposed short time fourier transform to detect target in foliage environment. In [11], Liang proposed a Discrete-Cosine-Transform (DCT)-based approach for sense-through-foliage target detection when the echo signal quality is good. They compared their approach against the scheme in which 2-D image was created via adding voltages with the appropriate time offset as well as the matched filter-based approach. They observed UWB channel has memory and matched filter-based approach couldnot work well.

As an alternative to these approaches information theory based target detection is emerging [12], [13], [14], [15], [16] and [17]. In [12], authors investigated a multi-target detector using mutual information for noise radar systems in low SNR regimes.

In [17], Aughenbaugh applied information theory for metric selection for information fusion. In [14], the authors studied target classification and detection with hidden Markov models. Entropy is used as a tool for detecting small target in sea clutter [18]. End point detection in speech signal can also be done by using entropy based method [19]. Entropy is also an established method in detecting the anomaly in data network traffic [20].

In this dissertation, we proposed to use entropy and mutual information based method to detect target in forest with good signal quality. Entropy is a measure of randomness which is capable of handling high amount of data and is real time efficient [21]. Mutual information tells us how much information one random variable has about another random variable [22]. Moreover, mutual information is insensitive to nonlinearities. Mutual information based target detection for random noise radar in low SNR region was already proposed [12]. However none of these studies used target obscured by foliage in poor signal quality. First we analyzed the data and came into conclusion that, targeted region is more random than the region without target. Two information theory based metrics, entropy and mutual information are proposed to detect the target. For entropy based detection based on Maximum entropy method, we proved that unless there is unique situation where each window has uniform distribution then entropy based target detection is possible using Maximum entropy method. The proposed algorithm is fundamentally different from the conventional wisdom, which assumes that we will have minimum information about the targeted region. It is nonconventional that from data analysis we found, uniform distribution of the targeted region, this will give higher entropy and lower conditional entropy, and will give higher mutual information in the targeted region. We also applied several quantization levels on the data for entropy based method and found best

result in 32 level of quantization. Results show that our approach can detect target successfully for good signal of real world data.

### 1.3 Preliminaries to Radar Sensor Network and Preprocessing

Networks of multiple distributed radar sensors, namely radar sensor networks (RSNs) can be utilized to combat the performance degradation [23]. RSN has attracted much interest in military and academia [24]. Some theoretical works on radar sensor network-based target detection were reported in [4], [25], [26] and [27]. A RSN not only provides spatial resilience for target detection and tracking compared to traditional radars, but also alleviates inherent radar defects such as the blind speed problem. This interdisciplinary area offers a new paradigm for parallel and distributed sensor research. In [24], Jing proposed both coherent and noncoherent RSN detection systems applying selection combination algorithm (SCA) performed by clusterhead to take the advantage of spatial diversity. Recently, the concept of MIMO radar have been proposed in [28] [29] and [30] motivated by the development in communication theory. Unlike the standard phased array radar that transmits scaled version of a single waveform, a MIMO radar can overcome radar cross section (RCS) scintillations by transmitting different signals due to the large spacing between the transmitting or receiving elements.

Information fusion and integration is being studied in several studies before. Varieties of technical perspective have been used to do the intelligent information fusion depending on the task [31], [32] and [33]. In our work, information fusion is done in three different steps, as categorized by Luo and Kay [35], [34], in different literatures. Broadly, the methods of estimation are applied in preliminary incoming signal at the first level, the classification methods are applied in medium level and inference methods are applied for decision making at a higher level. Preprocessing

is usually done by estimation. Popular recursive method of recursive estimation is, Kalman Filtering (KF). Although computationally efficient, KF assumes the linear Gaussian model. For target detection, we want to have a real time efficient non recursive algorithm. Two mostly used method of non recursive estimation are weighted average and least square estimation (LSE).

In this dissertation, we studied how to use UWB RSN and detect target in much challenging environment of forest. We employed a rake structure and pre-processed the data using information theory. In the first step a Kullback-Leibler (K-L) divergence based weighting is done to modify the histogram. K-L divergence maximized the information collected by multiple observations. Then two information theoretic metrics: entropy and mutual information are applied on the modified histogram. We also calculated the upper bound of the false alarm probability using another information theoretic criterion known as method of types.

#### 1.4 Preliminaries to Decision Fusion

Bayesian inference and Dempster and Shafer's reasoning are the two popular inference algorithms for decision fusion [36], [37], [38], [39], [40] and [41]. In our study, we use three different inference algorithms and compare their performances. The Dempster and Shafer (D-S) theory is a mathematical theory of evidence often used in sensor fusion [42]. It was first developed by Dempster and extended by Shafer. It can provide an optimal result from a set of options, without prior probability. D-S theory makes decision by independently judging all the hypotheses by its individual evidence [80]. Many researchers insist that normalization procedure in the DS combination rule involves counterintuitive result when there is high conflict in evidence. Several improved version have been proposed in literature as an alternative to DS theory [43], [44], [45], [46] and [47]. One of the popular modified rule is Proportional

Conflict Redistribution Rule 5 (PCR5). PCR5 is the most mathematically exact redistribution rule for conflicting mass than all other PCR methods.

Dempster-Shafer theory, deals with measures of belief as opposed to probability. In this dissertation, for our target detection algorithms, we have two different propositions: target present (t) and target not present respectively (nt). Entropy (E) and mutual information (MI) provides two different evidential sources  $m_1$  and  $m_2$ . We can find the belief function from the threshold value. The combined belief of target present can be calculated by using the Dempster's rule of combination. We also applied PCR5 rule in our study.

Bayesian network (BN), also known as belief networks, belongs to family of probabilistic graphical models (GMs). In our study we have a tree structured network with a root node T, which has no parent. T is the parent node with two children nodes  $E_h$  and  $MI_h$ , which represents high entropy and high Mutual information respectively. In this dissertation, among the decision fusion algorithms, Bayesian approach worked slightly better than PCR5 while combining evidential conflict. However PCR5 performed better than DS. Results show that accurate detection can be achieved by applying DS in case of low conflict.

## 1.5 Preliminaries to Opportunistic Sensing Using Chernoff Information

Major limitations of conventional approaches in RSN include inadequate performance for target recognition and huge processing load for big data. Opportunistic Sensing (OS) refers to a paradigm for signal and information processing in which a network of sensing systems can automatically discover and select sensor platforms based on an operational scenario. It uses appropriate methods to fuse the data, resulting in an adaptive network that automatically finds scenario-dependent, objective driven opportunities with optimized performance. In [48], detecting and eliminating



redundancy in a sensor network with a view to improving energy efficiency, while preserving the networks coverage was studied using Voronoi diagrams. In [49], Liang and Wang applied a singular-value decomposition (SVD)- QR algorithm to redundancy reduction for acoustic sensor networks. In [50] and [51], Liang applied rate distortion function for opportunistic sensing in RSN scenario.

The potential of Chernoff information is widely explored recently. A wide variety of information theoretic problems and communication problems deals with this new concept. Chernoff information was used in optimization of sensor network in distributed detection [52]. Error exponents in target class detection was investigated in [53]. It was used in UWB [54] and was also used in analysis of energy detectors of cognitive radio [55].

In this dissertation, we used UWB based RSN. There can be redundancy in the big data collected by various radars. Since it is possible that less sensors can achieve better performance, and less sensors can save the bandwidth, energy, memory and storage resource of sensor networks, its very desirable that principal sensors can be selected. Also the error probability associated with the detection is crucial in understanding the performance of the detection. Chernoff information gives the best error exponent in hypothesis testing, thus can be used as sensor selection scheme in fusion center. This OS reduces the processing load significantly and effectively utilize the sensing assets. In order to optimize the performance, data fusion is done based on Chernoff Stein Lemma.

## 1.6 Preliminaries to Human Detection

There have been several successful attempt to detect human using breathing motion [56], [57] and [58]. Staderini [57] has developed an UWB radar for non-intrusive breathing and heartbeat detection for medical purposes in LOS conditions.

Ossberger and al. [58] investigated feasibility of using UWB radar for through-wall detection of breathing persons. The experimental data used in this study was collected by [60], [59] and [61]. They applied several techniques such as short time fourier transform, singular value decomposition and doppler based detection to detect human target. As an alternative to these approaches we propose information theory based human detection.

In this dissertation, we propose to use information theory to UWB radar to detect human target. We applied relative entropy based preprocessing and entropy based detection. Various walls are investigated for their various electro-magnetic property.

## 1.7 Preliminaries to Capacity Analysis of Sensor Aided Cognitive Radio

Cognitive radio has the potential to solve the problem of spectrum [62] [63]. In literature the research in CR has two clear directions. One group of researchers investigated on different sensing schemes. And another group of researchers concentrated in power allocation scheme to optimize the throughput. In an effort to combine the power and sensing time there are very few literatures. The authors in [64], [65], [66] and [67] proposed energy efficient cooperative spectrum sensing in sensor aided CR. They take into account the optimal scheduling of the each sensor active time. The authors in [68] showed another interesting work on energy efficient detection. The authors in [69], investigated spectrum sensing towards ultra low overhead. In [70], Mosleh proposed the Bayesian network for the fusion centre of a distributed network in cognitive radio. The authors in [71], studied a cooperative spectrum sensing in multiple antenna based system. The authors in [72] propose power control schemes for secondary femto cells and that are upper- bounded by interference limits. Maximum capacity for MIMO-OFDM system is derived by [73]. Optimal and suboptimal

power allocation scheme in OFDM based CR was proposed by Bansal in [74]. In [75], Chai studied the power allocation scheme for Nakagami fading model. The authors in [76] showed trade-offs in cross layer approach to optimize the throughput. However they considered the single sensor embedded in the secondary user. Huang et al., [77] show joint detection and power allocation by alternating detection optimization (ADO). The authors in [78] proposed the wideband based spectrum sensing to optimize the sensing time and power allocation. The authors in [79] investigated on optimization of sensing throughput in UWB network. The authors in [80] studied on the low complexity algorithm of the cooperative resource allocation.

In this dissertation, we propose a sensor network aided cognitive radio system which will reduce the missed detection and reduce the interference. The non-convex optimization problem is divided in two separate sub problems and solved to get a suboptimal solution. Mathematical analysis shows that interference between primary and secondary depends on spectral distance, when the parallel channels are orthogonal like an OFDM based system. Results show that distance dependent modified water filling (DDMWF) scheme can achieve the higher data rate for the cognitive radio based secondary user.

## 1.8 Organization

The rest of this dissertation is organized as follows:

- *Chapter 2* applies information theory based scheme for target detection through foliage. It presents data analysis for the data collected by AFOSR. It applies various quantization level and applies Maximum entropy method and mutual information based method in target detection.
- *Chapter 3* applies ultra wide-band (UWB) radar sensor network (RSN) based Information fusion. It combines data from several radar sensors after applying

Kullback-Leibler (K-L) divergence based weighting which can generate a modified histogram. Then it applies Maximum Entropy Method (MEM) and mutual information based detection.

- *Chapter 4* introduces Dempster and Shafer (D-S) theory of evidence for decision. It also introduces the improved version of D-S theory for conflicting evidence and compares the performance with D-S and Bayesian network. Dempster-Shafer theory deals with measures of belief as opposed to probability. Results show that among the decision fusion algorithms, Bayesian approach worked slightly better than PCR5 while combining evidential conflict. Accurate detection can be achieved by applying DS in case of low conflict.
- *Chapter 5* applies Chernoff information to find the best error exponent in Bayesian approach of hypothesis testing. Chernoff information finds the best radar sensor and minimizes the processing load. As an alternative to Bayesian approach, we can minimize one of the errors subject to the constraint of the other error, which is known as Chernoff-Stein Lemma. Simulation results show that our approach can work successfully with real world data. Using this novel approach we could significantly reduce the number of radars from 9 to 1 while maintaining good performance. This new scheme of Opportunistic sensing (OS) not only ensures effective utilization of sensing assets but also provides optimal performance.
- *Chapter 6* modifies the algorithm developed in chapter 3 and chapter 2 for single radar, and applies in sense through wall human detection. Results show that with this novel approach, accurate detection can be achieved when human is hidden behind the gypsum wall. This method could also detect human hidden behind the brick wall.

- *Chapter7* applies, a sensor network aided cognitive radio system which will reduce the missed detection and reduce the interference. In sensor network multiple sensors will individually sense the channel and send their decision to the fusion center. We investigate the performance of various sensing and power allocation schemes for cognitive radio system. We formulate an optimization problem to design the optimal sensing time and transmit power to maximize the throughput. The non-convex optimization problem is divided in two separate sub problems and solved to get a suboptimal solution. Mathematical analysis shows that interference between primary and secondary in depends on spectral distance, when the parallel channels are orthogonal like an OFDM based system. Results show that distance dependent modified water filling (DDMWF) scheme can achieve the highest data rate for the cognitive radio based secondary user and then the optimal sensing time can be designed to maximize the throughput.
- *Chapter8* summarizes the dissertation and indicates the future direction.

## Chapter 2

### Information Theory Based Target Detection

#### 2.1 Introduction

Time varying and rich scattering complex environment of forest makes target detection through foliage an ongoing challenge. However, forest provides safe harbor to hostile forces and their malicious activities where war fighter has poor sensing capabilities. Our purpose is to find a method for Target detection using Ultra-wideband (UWB) radar sensor network(RSN) that is real time efficient, compact and easily deployable in the forest. Signal radiated by narrow band has harmonics, which makes them good candidates for match filtering and correlating with the reference [2]. This does not work for UWB radar with heavy clutter and unknown target. The ultra short energy pulses of UWB radar have very high bandwidth with exceptional good resolution, high power efficiency, low probability of detection, low interference to legacy systems and ability to penetrate through material. We can formulate the target detection as a hypothesis testing to choose between the null ( $H_0$ ), when the target is not present and the alternative hypotheses ( $H_1$ ), when the target is present. However to apply the Bayesian detection, accurate statistical information is necessary for this decision making problem. However, in many situations of practical interest we do not know the statistics of the probability of the target present  $P(H_1)$  or it might be very small. Also the distribution of foliage clutter is important. In general, the behavior of random process is governed by, Gaussian distribution. Since radar signal is the sum of independent reflections from uneven surface, it is tempting to invoke central limit theorem to justify the Gaussian clutter model. However it

is shown that the foliage clutter behaves dynamically and it is impulsive in nature [5]. Which also makes this classical theory of detection not appropriate for target detection. The challenges that are unique for this study are:

- Foliage clutter is dynamic and impulsive.
- The prior statistical information about the target presence is unknown.
- UWB signal shape changes many times during radar viewing. So conventional matched filters or correlators are unsuitable for target detection[2].

To deal with this problem we do the data analysis and introduce information based target detection.

## 2.2 Data Measurement and Analysis

### 2.2.1 Data Measurement

In this section we provide an overview of the experimental and measurement effort. Our work is based on the sense-through-foliage data from Air Force Research Lab [81]. In our work we use the frequency range between 300 MHz to 3 GHz. This has exceptional quality of good resolution and ground penetration. The foliage penetration measurement effort began in August and continued through December. This effort takes into account the late summer, fall and winter forest. Late summer has decreased water content whereas fall and winter has defoliated but dense forest. The measurements were taken on the grounds of virtual machine company of Holliston, Massachusetts. The target is a trihedral reflector with a slant length of 1.5 as shown in Fig. 2.1. This kind of reflector is used to represent metallic military equipment under foliage cover. The target was located 300 feet away from the lift where the entire measurement equipment was located as shown in Fig. 2.2. The foliage exper-

iment was constructed on a seven-ton man lift. The principal pieces of equipment secured on the lift include

1. HP signal Generator
2. Custom RF switch
3. Power supply
4. A Barth - pulsar
5. Tektronix model
6. 7704 B oscilloscope
7. Dual antenna mounting stand
8. Two antennas
9. Rack system
10. IBM laptop and
11. Weather shield (small hut)

The pulse generator uses a coaxial reed switch to discharge a charge line for a very fast rise time pulse-outputs.

The model 732 pulse-generator provides pulses of less than 50 picoseconds (ps) rise time, with amplitude from 150 V to greater than 2 KV into any load impedance through a 50 ohm coaxial line. The generator is capable of producing pulses with a minimum width of 750 ps and a maximum of 1 microsecond. This output pulse width is determined by charge line length for rectangular pulses, or by capacitors for 1/e decay pulses. Transmit and receive antennas required two degrees of rotational freedom to permit accurate pointing at the metallic target. The antennas could be adjusted during the course of experiment if they are misaligned. By policy, for purposes of safety and data quality, no measurement was taken where the wind gusts were more than 40 mph. The man lift was a 4-wheel drive diesel platform that was driven up and down in graded track 25 meters long with an experimental



lengthy of 10 meter. This track served as strip map of the radar track and extra 5 meters accommodate the length of the lift. Additional alignment was required at each position on the track to maintain pointing accuracy. The goal of the alignment procedure was to keep the antennas remained in a correct horizontal position aimed at the direction of the target. In order to assure that, a parallel line was set up to the desired line of antenna (string line) and a plumb line was established at the each end of the antenna mount. When the plumb lines were at equal distance from the string line the antennas were aligned in the proper direction relative to the strip map. An additional check was made in the lift to determine that the lift platform had remained in the horizontal position.



Figure 2.1. Target (A Trihedral Reflector) is shown 300 feet away.

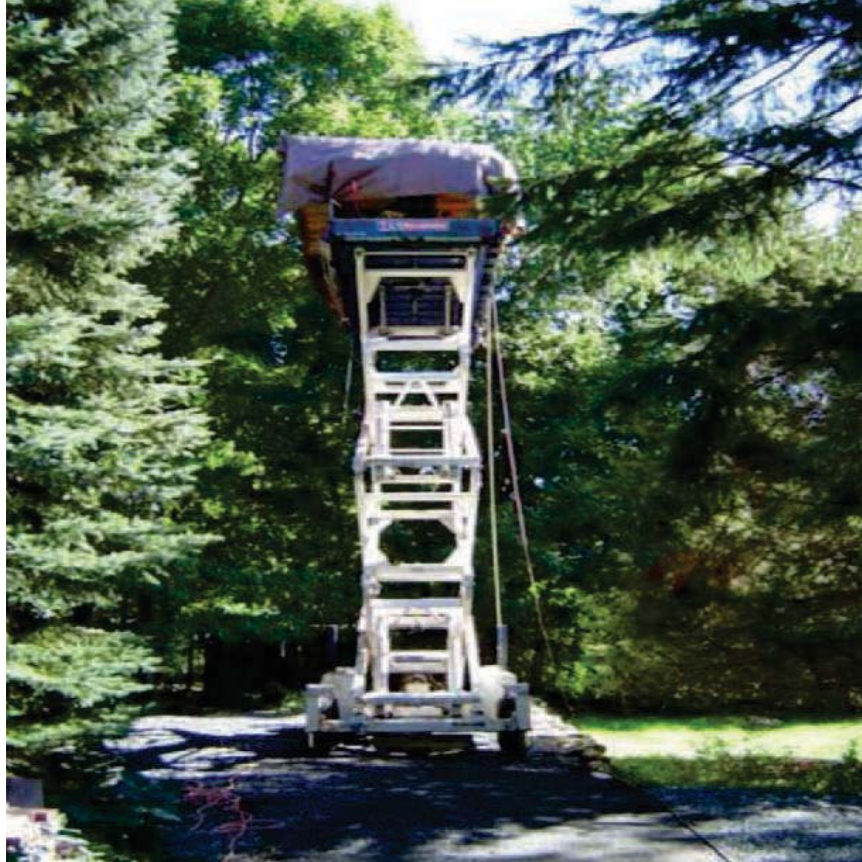


Figure 2.2. This figure shows the lift of the experiment.

### 2.2.2 Data Analysis

Our work is based on the sense-through-foliage data from Air Force Research Lab [81]. Our purpose is to find the target when the signal quality is not good. Each sample is spaced at 50 picoseconds interval, and 16,000 samples were collected for total time duration of 0.8 microseconds at a rate of approximately 20 Hz. The target was a trihedral reflector which was placed 300 feet away from the radar. The target should then be located around sample 13900. Initially, the Barth pulse source was operated at lower amplitude and 35 pulses of signals were obtained. This collection is referred to as "poor" data. The integration of these 100 pulses with higher amplitude is referred to as "good" data. The window size was used as 50. In Fig. 2.3 we provide

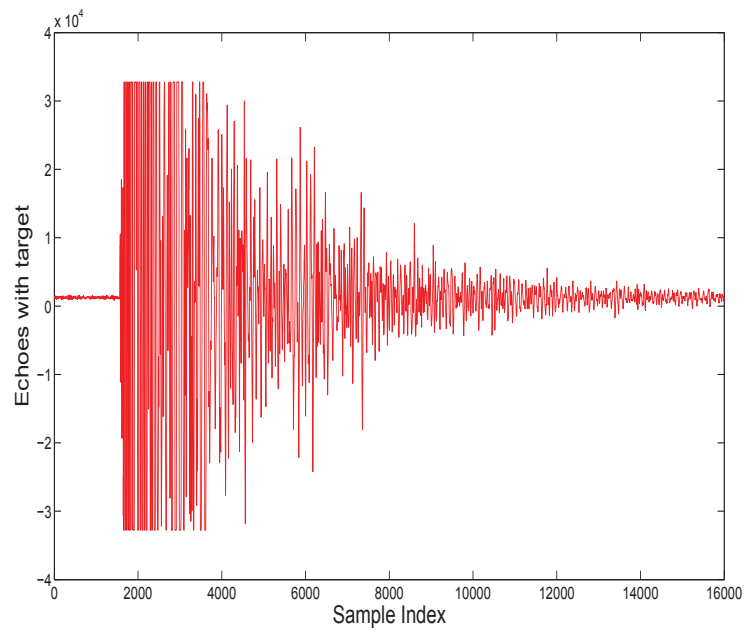
the full reflected echoes for two different cases, with target and without target. We provide expanded views of traces (with target) from sample 13,001 to 15,000 for two collections of data without target and with target in Figs. 2.4(a) and 2.4(b). The target response will be the echo difference between Fig. 2.4(a) and 2.4(b).

The echo difference for good signal is shown in Fig. 2.5 and the echo difference of poor signal is shown in Fig. 2.6. Clearly the signature of target is not detected around sample 13900 with poor signal. Fig. 2.7 is the representation of the average no of transition between the states. In order to find the general tendency of the echoes, we quantized the received echoes in 4 different states primarily. In Fig. 2.7, x and y axis represent four different possible states of echoes. Axis z represents the transition of states, which represent, what is the probability that an echo in time index t will go to the four possible sates in the time index t+1 and it can have 16 different values.

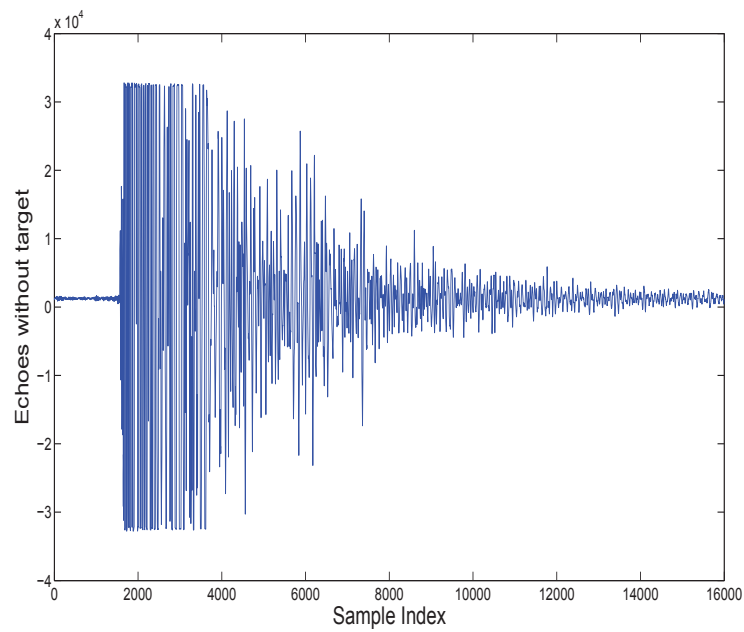
After careful analysis of the Figs. 2.4, 2.6 and 2.7 three important observations are made:

- 1) Observe Fig. 2.4(a) and Fig. 2.4(b), echoes in the target region is more random than echoes without the target.
- 2) Observe Fig. 2.6, when the signal quality is poor the difference of echoes does not give signature of target.
- 3) Observe Fig. 2.7, when x and y have same dimensions, we have got the highest value. In other words, number of samples, which are in a particular state remained in that state for the next sample index, most of the time. That means smaller number of echoes are changing their state, from one to another frame, when target is not present.

These observations gave the important reason to choose information theory based target detection. From observations 1 and 3, it is clear that the entropy that will measure the uncertainty will provide higher values in the targeted region.

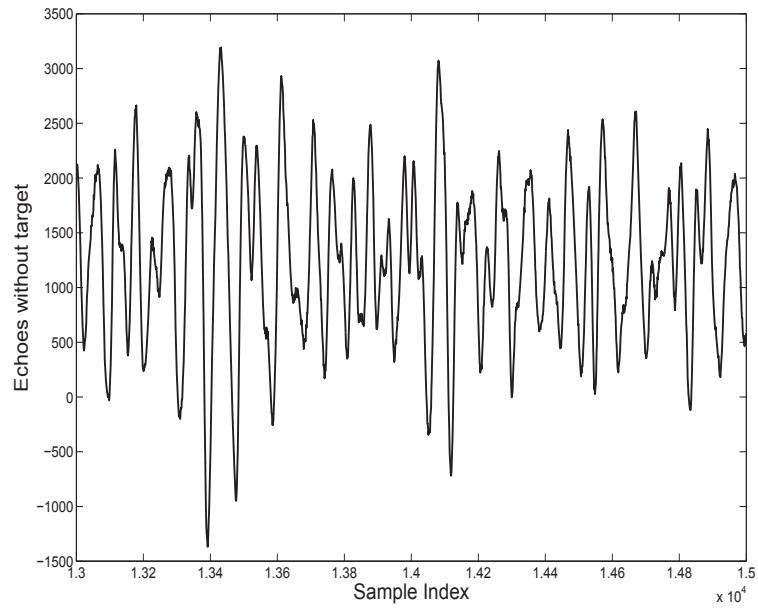


(a)

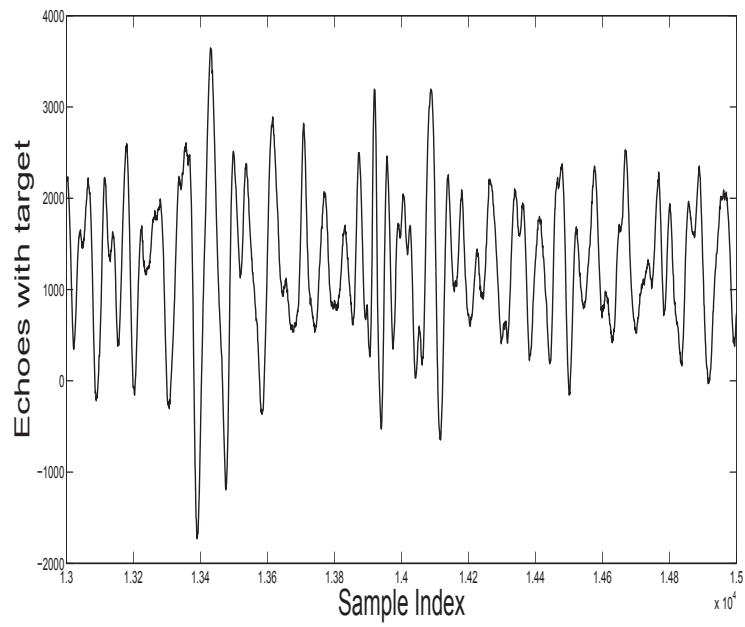


(b)

Figure 2.3. Reflected echoes for two different cases: (a) no target (b) with target .



(a)



(b)

Figure 2.4. Reflected echoes of sample index 13001 to 15000 for two different cases: (a) no target (b) with target .

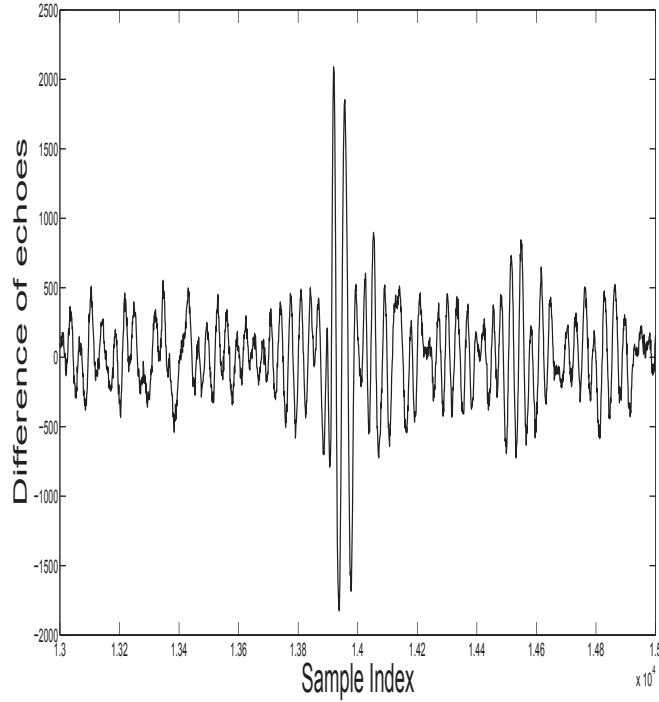


Figure 2.5. Expanded view of the echo difference. Signature of the target is detected around sample 13900.

However from observation 2, we conclude that entropy alone is not sufficient for poor signal quality. We propose to use Mutual information also to detect the target. Also due to the dynamic nature of the environment, it is possible that both entropy and mutual information might not be able to detect the target all the time. In order to make the inference, without a prior distribution, we might need to a solution for decision fusion.

### 2.3 Information Theory Based Detection

In this stage we perform the real target detection by two different methods. We found that smaller numbers of echoes are changing states and echoes are more random in targeted region. Based on this analysis, we have chosen two information

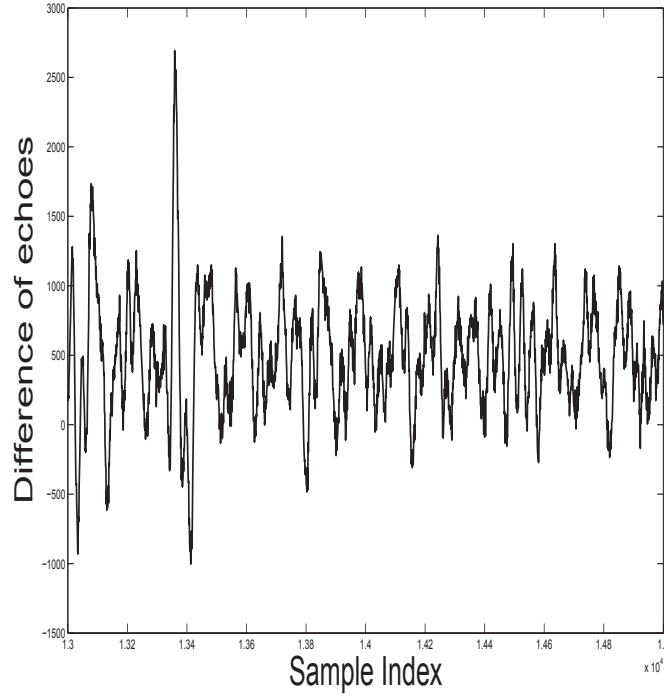


Figure 2.6. Expanded view of the echo difference. Signature of the target is not detected around sample 13900.

theoretic criterion: namely entropy and mutual information to detect the target. Since entropy is the measure of the randomness, echoes in targeted region should have higher entropy. We also need to calculate the mutual information of the subsequent radar return as second method of detection.

### 2.3.1 Maximum Entropy Method Based Target Detection

Entropy is a measure of uncertainty of a random variable [22]. Let  $X$  be a discrete random variable with alphabet  $X$  and probability mass function (pmf) as  $p(x)$ , then the entropy  $H(X)$  of the discrete random variable is,

$$H(X) = - \sum_{i=1}^n p(x_i) \log_2 p(x_i) \quad (2.1)$$

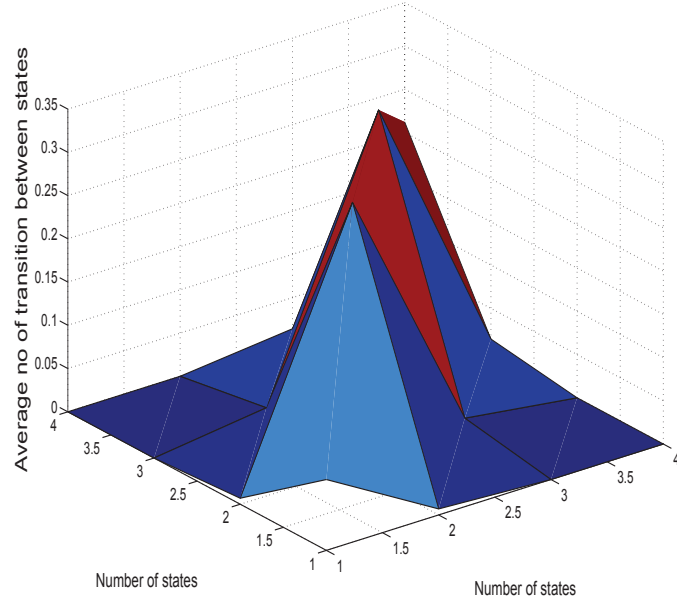


Figure 2.7. 3-D representation of the transition of the echoes in different state.

Maximum entropy method (MEM) finds the distribution which maximizes the entropy. Let assume the alphabet size of  $X$  is  $n$ , so  $X = \{x_1, x_2, \dots, x_n\}$ . PMF  $p(x_i)$  with maximum entropy is the one that does not introduce any additional assumption. Then  $p(x_i)$  must satisfy the following constraints [22]:

$$p(x_i) \geq 0 \quad (2.2)$$

$$\sum_{i=1}^n p(x_i) = 1 \quad (2.3)$$

$$\sum_{i=1}^n p(x_i) r_k(x_i) = \alpha_k \quad (2.4)$$

this is for  $k \leq m$  and  $p_i$  satisfies certain moment constraints  $\alpha_1, \alpha_2, \dots, \alpha_m$ , and  $r_k(x_i)$  is the  $k^{th}$  order power of  $x_i$ .



Now we can form the equation for the distribution that can achieve maximum entropy,

$$J(p(x_i)) = - \sum_{i=1}^n p(x_i) \ln p(x_i) + \lambda_0 \left(1 - \sum_{i=1}^n p(x_i)\right) + \sum_{k=1}^m \lambda_k \left(\alpha_k - \sum_{i=1}^n p(x_i) r_k(x_i)\right) \quad (2.5)$$

where  $\lambda_k (k = 0, 1, 2, \dots, m)$  are Lagrange multipliers. Now differentiating (2.5) with respect to  $p(x_i)$ ,

$$\frac{\delta J}{\delta p(x_i)} = -\ln p(x_i) - 1 + \lambda_0 + \sum_{k=1}^m \lambda_k r_k(x_i) \quad (2.6)$$

Setting (2.6) equals to zero we find the distribution of MEM

$$p(x_i) = e^{\{-1 + \lambda_0 + \sum_{k=1}^m \lambda_k r_k(x_i)\}} \quad (2.7)$$

If we do not have any constraints then from, (2.3) and (2.7) we obtain,

$$\sum_{i=1}^n e^{(\lambda_0 - 1)} = 1 \quad (2.8)$$

which yields,

$$\lambda_0 = 1 - \ln \frac{1}{n} \quad (2.9)$$

Substituting (2.9) in (2.7) we can conclude that,

$$p^*(x_i) = \frac{1}{n} \quad (2.10)$$

which is a constant. For discrete domain we can have various cases. Two particular cases we are going to discuss based on the given constraints.

*Case 1:* Let  $X = 1, 2, 3, 4, 5, 6, 7, 8$ . The distribution without constraints that maximizes the entropy is uniform distribution,

$$p_i = \frac{1}{8} \quad (2.11)$$

Case 2: Let expectation of  $X$  is defined as,  $E(X) = \sum ip(x_i) = \alpha$ . Then the distribution that maximizes the entropy is,

$$p^*(x_i) = \frac{e^{\lambda_i}}{\sum_{i=1}^8 e^{\lambda_i}} \quad (2.12)$$

where  $\lambda$  is chosen so that  $\sum ip(x_i) = \alpha$  [22].

This gives us the idea of determining the threshold and upper bound of the Entropy based target detection. Since the echoes in the foliage do not have any constraint [21], we consider case 1. In that way, we can conclude, unless we have a unique distribution that some other windows might have uniform distribution then target detection by entropy based method is possible.

### 2.3.2 Mutual Information Based Target Detection

Mutual information (MI) is a measure of the amount of information that one random variable contains about another random variable. Mutual information between two random variables  $X$  and  $Y$  with joint probability mass function  $p(x,y)$  and marginal probability mass function  $p(x)$  and  $p(y)$  is defined as,

$$MI(X; Y) = \sum \sum p(x, y) \log \frac{p(x, y)}{p(x)p(y)} \quad (2.13)$$

This can be further simplified as,

$$MI(X; Y) = H(X) - H(X|Y) \quad (2.14)$$

where  $H(X)$  is the entropy of  $X$  and  $H(X|Y)$  is the conditional entropy of  $X$  given  $Y$ . In our method, we have to find the  $MI(Q_k; Q_{k-1})$  from (2.14), where  $Q_k$  is the quantized received echoes and  $k$  denotes the current sample index and  $k - 1$  denotes the previous sample index. The proposed algorithm is fundamentally different from the conventional wisdom, which assumes that we will have minimum information

about the targeted region. It is nonconventional that from data analysis we found uniform distribution of the targeted region, this will give higher entropy and lower conditional entropy, and will give higher mutual information in the targeted region as shown in (2.14). The entropy and mutual information based target detection can be summarized in the next section.

### 2.3.3 Algorithm for Information Theory Based Target Detection

The target detection by maximum entropy method and mutual information which are discussed in previous section is summarized as follows:

- (1) Let  $Q$  be the non-uniform quantized received signal with a particular code-book and partition. Since the calculation of mutual information involved the processing in the  $O(n^2)$  when  $n$  is the quantization level, we try not to quantize too much.
- (2) A threshold value  $T$  that is less than  $\log_2 n$  is taken.
- (3) Let  $N = [N_1, N_2, N_3, \dots, N_M]$  set of windows. Let  $L$  is the length of the signal and  $s$  is the size of the window, then,  $M$  is  $L/s$ .
- (4) The probability mass functions of the echoes,  $p^j(Q)$  for quantized received echoes is calculated for each window,  $j$ . Entropy  $H^j(Q)$  is calculated for all  $j = 1 : M$ .
- (5) The conditional pmf of the echoes  $p^j(Q_k|Q_{k-1})$  for subsequent radar return is calculated. Here  $k$  is the sample index that will vary between  $1 : s$ . Conditional entropy,  $H^j(Q_k|Q_{k-1})$  is calculated for all  $j = 1 : M$ .
- (6) Mutual information of subsequent radar return,  $MI(Q_k; Q_{k-1})$  is calculated according to for all  $j = 1 : M$ .
- (7) If  $MI^j(Q_k; Q_{k-1}) > T$  then target is detected.
- (8) If  $H^j(Q) > T$  then target is detected.

## 2.4 Simulation Results

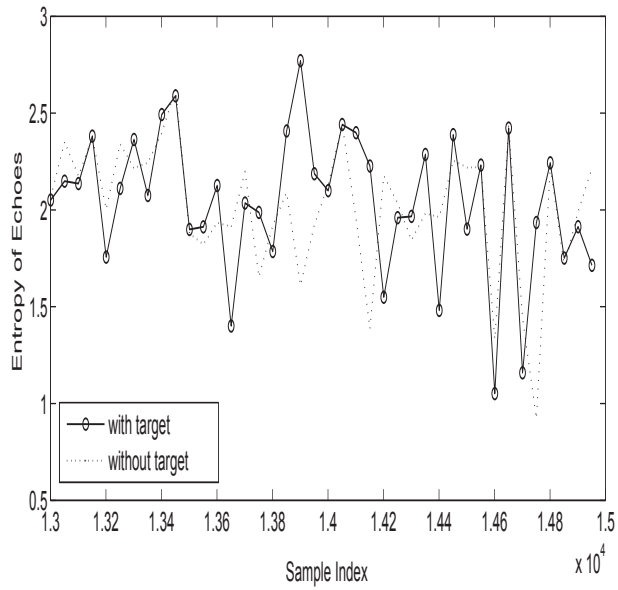
In this section, we will discuss the simulation result we found in this chapter. As already mentioned each sample of data is spaced at 50 picoseconds interval, and 16,000 samples were collected for total time duration of 0.8 microseconds at a rate of approximately 20 Hz. We expect the target at sample no 13900. Initially, the Barth pulse source was operated at lower amplitude and 35 pulses of signals were obtained. This collection is referred to as "poor" data. The integration of these 100 pulses with higher amplitude is referred to as "good" data. The window size was used as 50.

In Fig. 2.8 performance of entropy based target detection with a single radar are presented for two different cases: Fig. 2.8(a) is for good quality data and Fig. 2.8(b) is for poor quality data. In this case signals were quantized before entropy were calculated. At this stage, we applied 8 level of quantization. Single radar with entropy based method could detect target for good signal quality but was unable to detect target with poor signal quality as shown in Fig. 2.8(b).

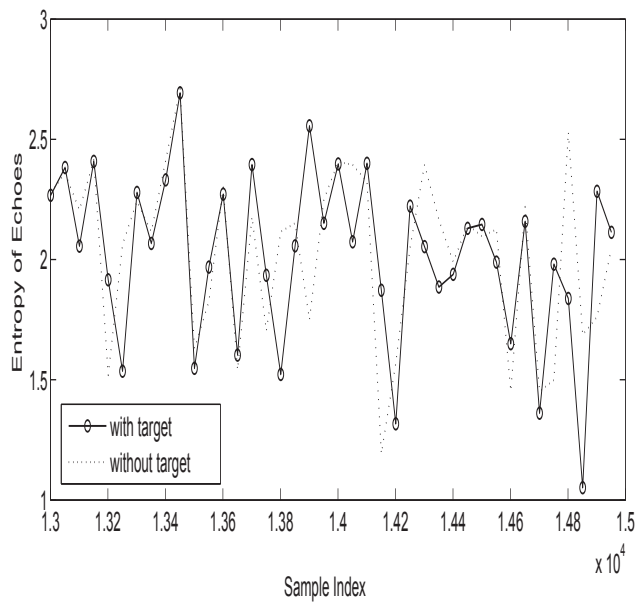
Fig. 2.9 shows the signature of the target after quantization. It proves that even after quantization the signature of target is visible.

Fig. 2.10 shows the conditional entropy when the background is given. The interesting observation we can make here is that the conditional entropy is the lowest at the targeted region. It emphasize that mutual information will also be higher in the targeted region.

To demonstrate the performance of the mutual information we represent the simulation in Fig. 2.11. Fig. 2.11(a) is the detection of the signal with single radar. Fig. 2.11(b) is the mutual information with poor quality signal. It shows that with poor quality data MI alone is unable to detect the target without significant false alarm. Comparing the figure 2.8 and 2.11 we can say that entropy is more efficient to detect target with poor quality data.



(a)



(b)

Figure 2.8. Entropy of reflected echoes collected by single Radar for two different cases: (a) good signal (b) poor signal .

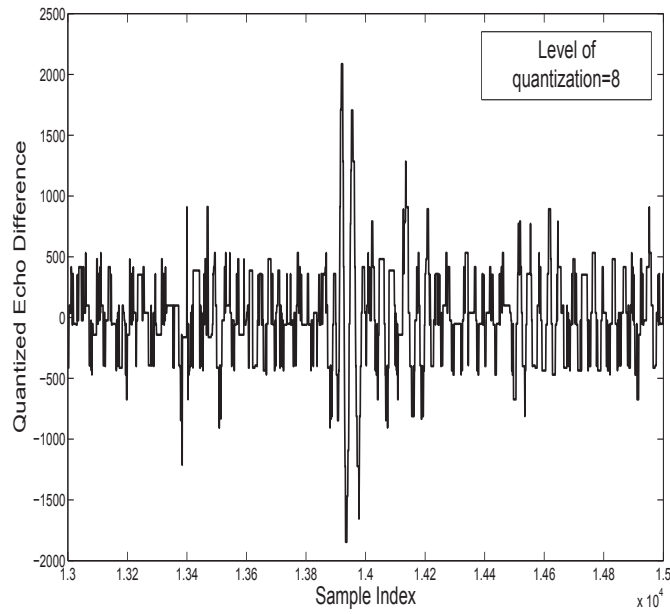


Figure 2.9. Quantized signature of target.

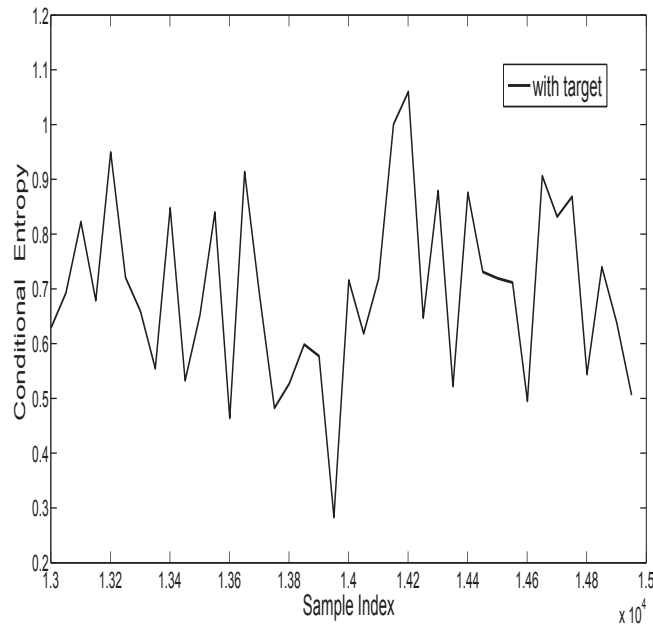
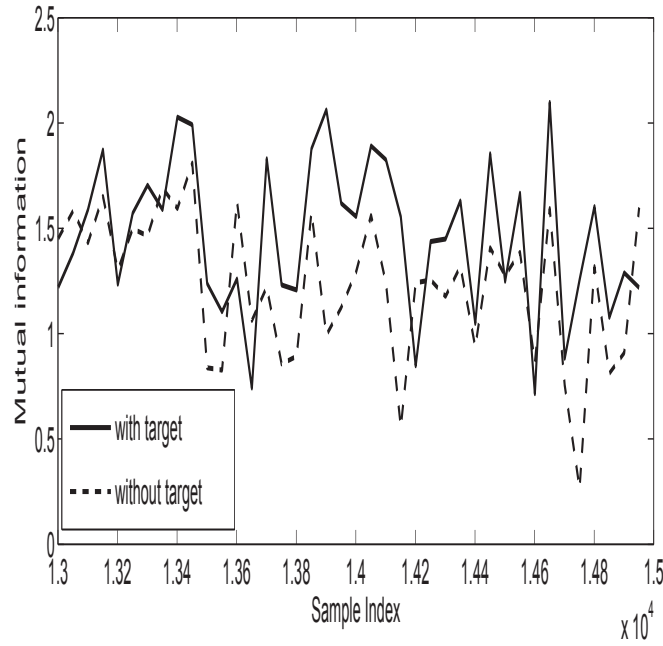
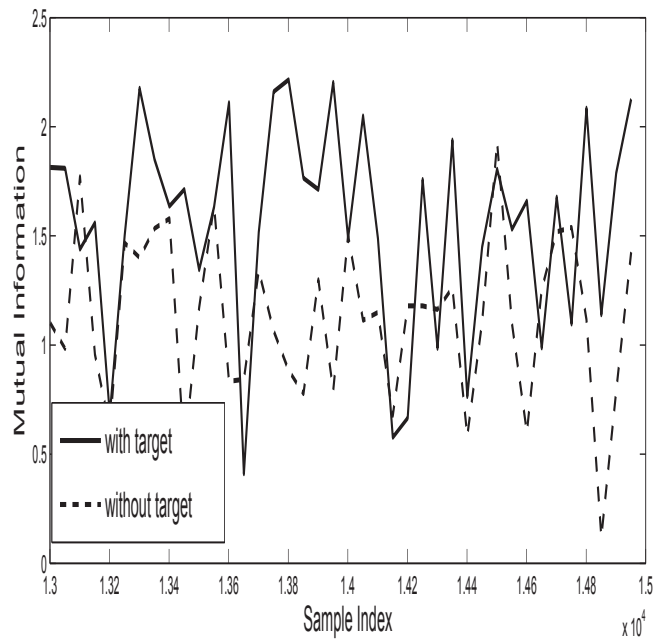


Figure 2.10. Conditional entropy given the background.



(a)



(b)

Figure 2.11. Mutual information of echoes with two different condition (a) good signal (b) poor signal .

## 2.5 Conclusion

In this chapter we propose a new scheme for target detection using information theory. Dynamic nature of the foliage imposes lot of challenges to detect target, without statistical information. To enhance the performance of the poor signal we apply information theory to UWB radar. This work is based on sense through foliage data collected by AFOSR. First we analyzed the data and came into conclusion that, targeted region is more random than the region without target. Two information theory based metrics, entropy and mutual information are proposed to detect the target. For entropy based detection we proved that unless there is unique situation where each window has uniform distribution then entropy based target detection is possible using Maximum entropy method. Results show that our approach can detect target successfully from real world data. However entropy is more efficient in target detection than mutual information.



## Chapter 3

### Radar Sensor Network and KL Based Preprocessing

#### 3.1 Introduction

When the pulse to pulse variability is high and the amplitude of the signal is low, then single radar is unable to detect the target as shown in Fig. 3.1. In order to deal with performance degradation, Radar sensor network (RSN) based detection with multi-step information fusion is proposed. In order to get better performance, we need to do some preprocessing. At first we used simple weight preprocessing and then we use K-L divergence based weighted average as fusion technique. Kullback-Leibler (K-L) divergence based weighting is done to modify the histogram. K-L divergence maximized the information collected by multiple observations. Then two information theoretic metrics: entropy and mutual information are applied on the modified histogram.

#### 3.2 Preprocessing

##### 3.2.1 Simple Weight Preprocessing

RSN and rake structure that we employ in our work has 9 different radars each collected 35 reading. These radars are mono-static and independent. RSN provides better signal quality if they are spaced sufficiently far apart since two radars will not experience deep fading at the same time. Also the collections of the reading from different positions of the radar were not taken at the same time. This guarantees the time as well as spatial diversity in the proposed RSN. Information collected by indi-

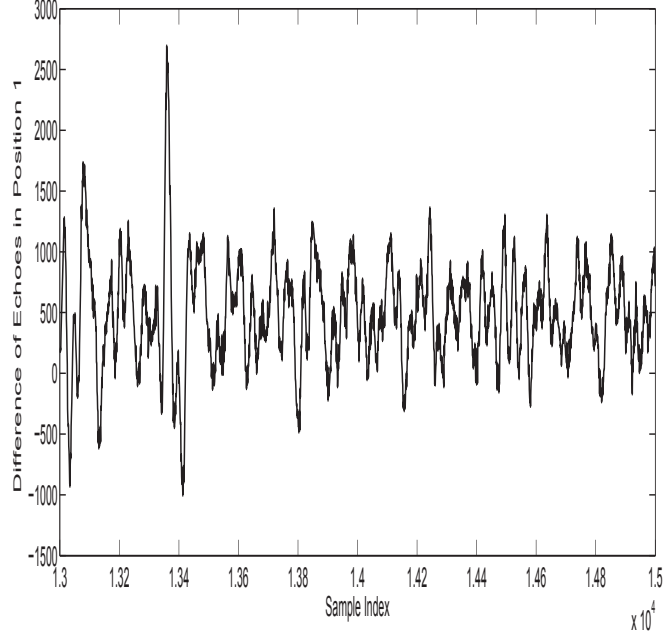


Figure 3.1. Reflected echo difference on a single radar in position 1.

vidual radars, are combined by the fusion center by using the weighted average. The power based weighting,  $w_r$  for each radar of the RSN can be given by the following,

$$w_r = \frac{E(Q_r^2)}{\sum_{r=1}^9 E(Q_r^2)} \quad (3.1)$$

$$E(Q_r^2) = \text{var}(Q_r) + [\text{mean}(Q_r)]^2 \quad (3.2)$$

where  $Q_r$  is the quantized received echoes for the  $r^{\text{th}}$  radar. We applied this weighting scheme in “good” signal quality and could detect the target. However in case of poor signal quality we were unable to detect. So we change in preprocessing is incorporated with a different technique based in relative entropy or KL distance.

### 3.2.2 Information Fusion by Information Theory

In order to improve the simple weight preprocessing, we propose to use information theory based information fusion. To explain the foundation of the information

fusion based on information theory, we need to introduce an information theoretic concept known as Method of types. It is a powerful procedure in which we consider the sequences that has the same empirical distribution [22]. With this restriction, we can derive strong bounds on the number of sequences with a particular empirical distribution and the probability of each sequence in this set. It is then possible to derive strong error bounds in target detection problem when target detection is done using information theoretic method like entropy which depends only on empirical distribution.

*Theorem 1: False alarm probability is lower when the relative entropy or KL divergence has higher value.*

*Proof:* Let R number of radar sensors are collecting independent observations  $\mathbf{s} = S_1, S_2, \dots, S_n$ . Let the observed echoes generated by each of this radar,  $\mathbf{s}$  has n symbols from an alphabet  $S = \{a_1, a_2, \dots, a_{|S|}\}$ . The type  $Q_{\mathbf{s}}(a)$  (empirical probability distribution) of sequence is the relative proportion of occurrences of each symbol of  $S$  and can be written as [22],

$$Q_{\mathbf{s}}(a) = N(a|\mathbf{s})/n, \quad \forall a \in S \quad (3.3)$$

where  $N(a|\mathbf{s})$  denotes the number of occurrences of the symbols a in the sequence. Let  $Q_n$  denote the set of types with denominator n. For example if  $S = \{1, 2, 3\}$ , the set of possible types with denominator n is,

$$\begin{aligned} Q_n = & \{(Q(1), Q(2), Q(3)) : (\frac{0}{n}, \frac{0}{n}, \frac{n}{n}), (\frac{0}{n}, \frac{1}{n}, \frac{n-1}{n}) \\ & \dots (\frac{n}{n}, \frac{0}{n}, \frac{0}{n})\} \end{aligned} \quad (3.4)$$

There are  $|\mathcal{S}|$  components in the vector that specifies the types. The numerator on each component can take only  $n + 1$  values. So we can write,

$$|Q_n| \leq (n + 1)^{|\mathcal{S}|} \quad (3.5)$$

The exact size of type class  $T(Q)$  for any type  $Q \in Q_n$  is a combinatorial problem which is,

$$|T(Q)| = \binom{n}{nQ(a_1), nQ(a_2), \dots, nQ(a_{|\mathcal{S}|})} \quad (3.6)$$

The most interesting thing we need to observe is that there are only a polynomial number of types of length  $n$ . In order to derive the probability of a particular sequence that belongs to the target when generated by another distribution, we can use this valuable concept. And this is related to entropy and relative entropy or KL distance. For target detection using information theory, we need to calculate the entropy related with the radar observations [88]. Entropy is a measure of uncertainty of a random variable [22]. Let  $\mathbf{S}$  be a sequence with  $n$  number of samples collected by each radar and it has empirical distribution  $q_i$ , then the entropy of  $\mathbf{S}$  of this sequence is,

$$H(\mathbf{S}) = - \sum_{i=1}^m q_i \log_2 q_i \quad (3.7)$$

The KL divergence or relative entropy for probability mass functions of  $p_i$  and  $q_i$  can be calculated as,

$$D_{KL}(p_i || q_i) = \sum_{i=1}^m p_i \log_2 \frac{p_i}{q_i} \quad (3.8)$$

here  $p_i$  is pmf related with the sequence with target and  $q_i$  is related with the target not present. Here  $m$  in (3.7) and (3.8) depends on the quantization level.

If  $X_1, X_2, \dots, X_n$  are drawn i.i.d. according to  $Q(x)$ , the probability of  $\mathbf{x}$  depends on its type. Since all sequence in the same type has the same probability,  $Q^n(x^n) = \prod_{i=1}^n Q(x_i)$ , denotes the product distribution according to the distribution  $Q$ . [22],

$$\begin{aligned}
Q^n(\mathbf{x}) &= \prod_{i=1}^n Q(x_i) \\
&= \prod_{a \in X} Q(a)^{N(a|\mathbf{x})} \\
&= \prod_{a \in X} Q(a)^{nP_{\mathbf{x}}(a)} \\
&= \prod_{a \in X} 2^{nP_{\mathbf{x}}(a)\log Q(a)} \\
&= \prod_{a \in X} 2^{n(P_{\mathbf{x}}(a)\log Q(a) - P_{\mathbf{x}}(a)\log P_{\mathbf{x}}(a) + P_{\mathbf{x}}(a)\log P_{\mathbf{x}}(a))} \\
&= 2^{n \sum_{a \in X} (-P_{\mathbf{x}}(a)\log \frac{P_{\mathbf{x}}(a)}{Q(a)} + P_{\mathbf{x}}(a)\log P_{\mathbf{x}}(a))} \\
&= 2^{-n(H(P_{\mathbf{x}}) + D(P_{\mathbf{x}}||Q))}
\end{aligned} \tag{3.9}$$

From (3.9) and (3.5) for any  $P \in P_n$  and any distribution  $Q$  the probability of any type class  $T(P)$  under  $Q^n$  is  $2^{-nD(P||Q)}$  to first order in the exponent [22],

$$\frac{1}{(n+1)^{|S|}} 2^{-nD(P||Q)} \leq Q^n(T(P)) \leq 2^{-nD(P||Q)} \tag{3.10}$$

From this observation it is obvious that, when there is no target present the sequence of reflected echoes can still have a chance to generate the sequence related with target present which is given in (3.9) and (3.10). This is related with the false alarm probability.

Based on theorem 1, we develop our information fusion algorithm. We can apply our algorithm in several steps as shown in Fig.3.2

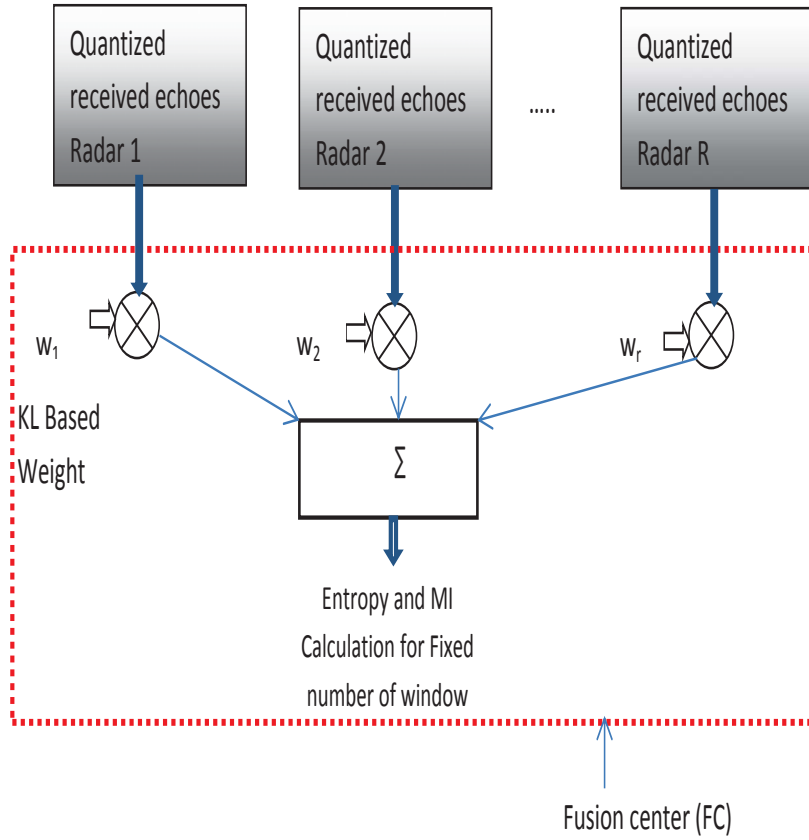


Figure 3.2. Block diagram of multi-step information fusion.

*Step1:* We create two  $n \times R$  matrix " $T_w$ " and " $T_o$ ". Here " $T_w$ " represents the radar collection with target and " $T_o$ " represents the radar collection without target,

$$T_w = \begin{vmatrix} Radar1 & Radar2 & Radar3 & \dots & RadarR \\ sample1 & sample1 & sample1 & \dots & sample1 \\ sample2 & sample2 & sample2 & \dots & sample2 \\ \vdots & \vdots & \vdots & \vdots & \vdots \\ samplen & samplen & samplen & \dots & samplen \end{vmatrix}$$

$$T_0 = \begin{pmatrix} Radar1 & Radar2 & Radar3 & \dots & RadarR \\ sample1 & sample1 & sample1 & \dots & sample1 \\ sample2 & sample2 & sample2 & \dots & sample2 \\ \vdots & \vdots & \vdots & \vdots & \vdots \\ samplen & samplen & samplen & \dots & samplen \end{pmatrix}$$

here R is the number of radars and n is the number of samples collected by each radar.

*Step 2:* Then the K-L divergence based weighting,  $w_r$  for each column can be calculated as,

$$w_r = \frac{D_r}{\sum_{r=1}^R D_r} \quad (3.11)$$

and

$$D_r = D_{KL}(p_r||q_r) \quad (3.12)$$

here  $p_r$  be the pmf of the quantized echoes of the  $r_{th}$  column of the  $T_w$  matrix and  $q_r$  be pmf related with the quantized echoes of the  $r_{th}$  column of the  $T_o$  and  $D_{KL}$  is the divergence calculated from the (3.8). The returned echoes are quantized and pmf are calculated before applying (3.11).

*Step3:* Each column of  $T_w$  is multiplied by the corresponding weight  $w_r$ . After performing the transpose of the matrix, we can calculate the summation of the matrix. We can name that Matrix as P.

*Step4:* Let  $W = [W_1, W_2, W_3, \dots, W_M]$  set of windows present with M number of windows. Here M is  $n/k$ , and k is the size of the window. The probability mass functions of the echoes,  $p^j(P)$  for quantized received echoes is calculated for each window, j. Entropy  $H^j(P)$  is calculated for all  $j = 1 : M$ .

*Step5:* Threshold value T is chosen based on the ROC curve for a particular probability of detection and for a particular probability of false alarm. If  $H^j(P) > T$

then target is detected. For entropy based detection,  $T < \log_2 m$ , should also be considered, when  $m$  is the quantization level.

### 3.2.3 False Alarm Rate for Continuous Case

*Lemma1:* If target has a type P which follows  $\mathbf{U}(a, b)$  and the clutter Q follows  $\mathbf{N}(\mu, \sigma)$ , then the false alarm probability of target detection  $P_{FA}$  can be expressed as,

$$P_{FA} \leq 2^{-n(-\ln(b-a) + \ln\sqrt{2\pi}\sigma + \frac{\mu}{6\sigma^2}(b^2 + ab + a^2) - \frac{\mu}{4\sigma^2}(b+a) + \frac{\mu^2}{2\sigma^2})} \quad (3.13)$$

*Proof:* Foliage environment differs from indoor and we plotted the histogram of the clutter in the far field which follows the Gaussian Distribution as shown in Fig. (3.3) and (3.4). Also in Chapter2 we saw that targeted region is almost uniform.

Now KL distance for the continuous case can be written as

$$D(p(x)||q(x)) = \int_0^\infty p(x) \ln \frac{p(x)}{q(x)} dx \quad (3.14)$$

For our case  $p(x)$  follows  $\mathbf{U}(a, b)$  and  $q(x)$  follows  $\mathbf{N}(\mu, \sigma)$  can be expressed as,

$$p(x) = \frac{1}{b-a} \quad (3.15)$$

and

$$q(x) = \frac{1}{\sqrt{2\pi}\sigma} e^{-\frac{(x-\mu)^2}{2\sigma^2}} \quad (3.16)$$

KL distance between a uniform distribution  $p(x)$  and Gaussian distribution  $q(x)$  is,

$$D(p(x)||q(x)) = \int_a^b \frac{1}{b-a} \ln \left( \frac{\frac{1}{b-a}}{\frac{1}{\sqrt{2\pi}\sigma} e^{-\frac{(x-\mu)^2}{2\sigma^2}}} \right) dx \quad (3.17)$$



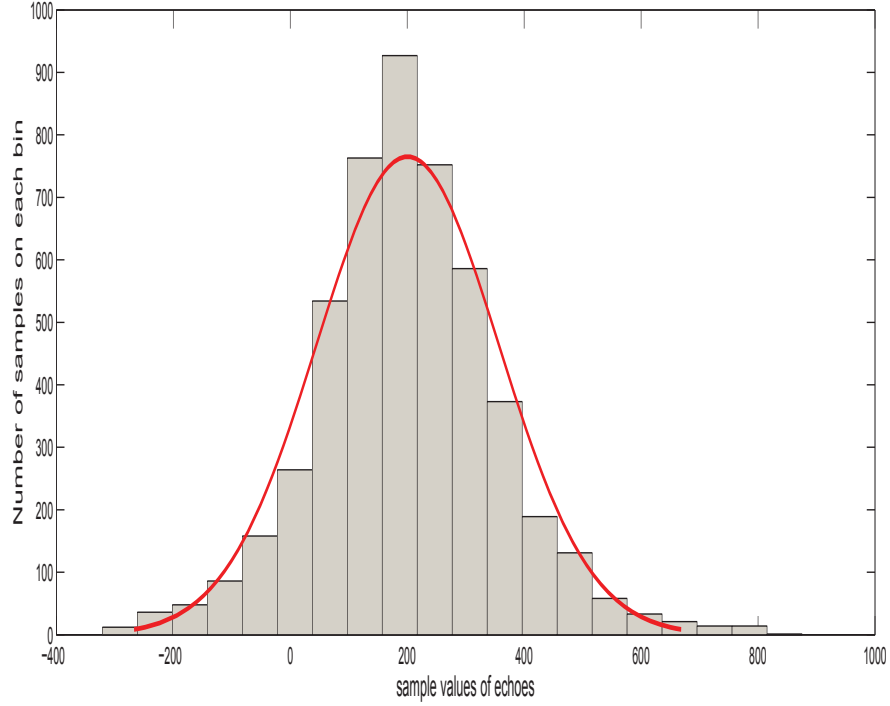


Figure 3.3. Clutter distribution in the farfield for the last 5000 samples collected by 9 different radars with 20 bin.

After simplification this can be written as,

$$\begin{aligned}
 D(p(x)||q(x)) &= \frac{1}{b-a} \int_a^b -\ln(b-a) dx \\
 &+ \frac{1}{b-a} \int_a^b \ln \sqrt{2\pi} \sigma dx \\
 &+ \frac{1}{b-a} \int_a^b \frac{\{x-\mu\}^2}{2\sigma^2} dx
 \end{aligned}
 \tag{3.18}$$

This can be further simplified as,

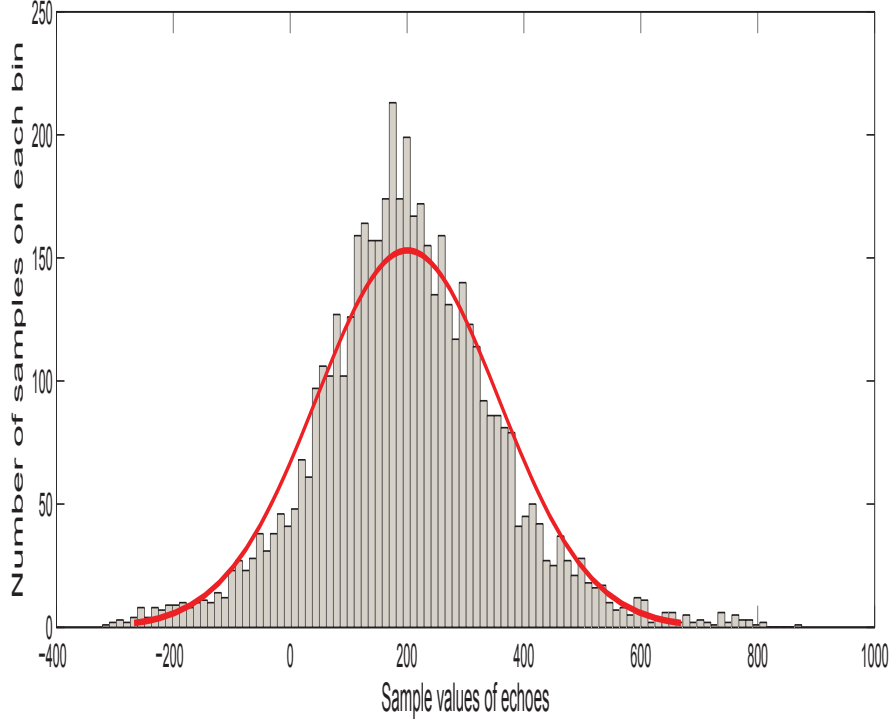


Figure 3.4. Clutter distribution in the farfield for the last 5000 samples collected by 9 different radars with 100 bin.

$$\begin{aligned}
 D(p(x)||q(x)) &= -\ln(b-a) + \ln\sqrt{2\pi}\sigma \\
 &+ \frac{\mu}{6\sigma^2}(b^2 + ab + a^2) \\
 &- \frac{\mu}{4\sigma^2}(b+a) + \frac{\mu^2}{2\sigma^2}
 \end{aligned} \tag{3.19}$$

Now replacing (3.19) in (3.10), we can find the Lemma 1.

### 3.3 Simulation Results

To demonstrate the performance of RSN based target detection using weight based weighting and entropy we performed simulation for different quantization lev-

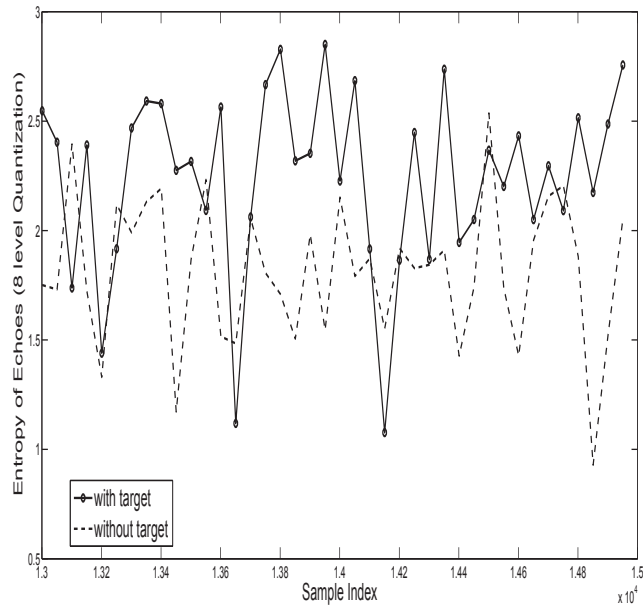
els. Level of quantization was varied between 8 and 32 as shown in Figs. 3.5(a), and 3.5(b). Target is detected more clearly for higher level of quantization as shown in Fig. 3.5(b).

The performance evaluation in terms of the false alarm and probability of detection is given in Fig. 3.6(a) and 3.6(b). Here the x axis correspondence various threshold value. It is important to note that level of quantization plays an important role. Comparing the Figs. 3.6(a) and 3.6(b), it is clear that false alarm is never zero for 100 percent detection probability. However, in Fig. 3.6(b), when threshold is 4.25 to 4.5, result indicates 100 percent detection.

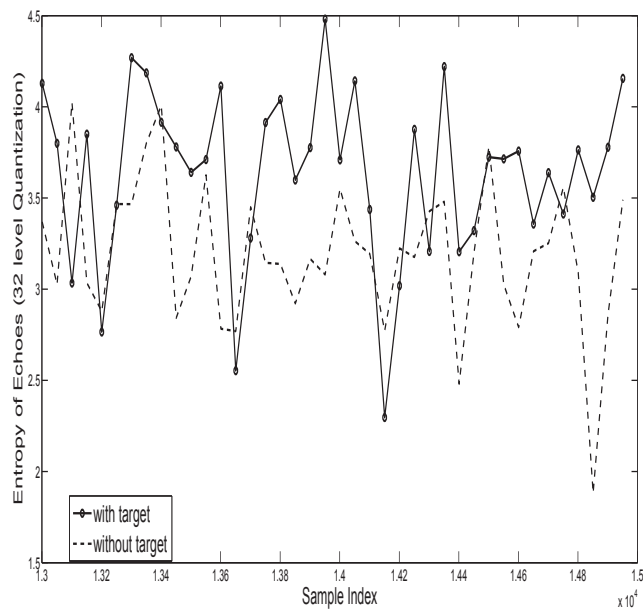
To demonstrate the performance of the mutual information we represent the simulation in Fig. 3.7. Fig. 3.7(a) is the detection of the signal with single radar. Fig. 3.7(b) is the mutual information of RSN with poor quality signal. It shows that with poor quality data RSN alone is unable to detect the target without significant false alarm. Comparing the figure 3.5(b) and 3.7(b) we can say that entropy is more efficient to detect target with poor quality data.

Figs. 3.8 and 3.9 illustrate two-step information fusion with K-L based weighting with entropy and mutual information respectively. We can see the RSN with two-step information fusion can clearly detect the target with the target as the highest point around sample13900 with much more certainty. It is clear both entropy and mutual information with K-L distance based weighting in Fig. 3.8 and Fig. 3.9 gave significant performance improvement than the traditional power based weighting from the previously illustrated results in Figs. 3.5 and 3.7. This significant performance improvement is the vital achievement of this paper.

Another way of representing this performance improvement is through ROC curves as shown in Fig. 3.10. ROC represent the probability of detection versus probability of false alarm for different threshold value. Fig. 3.10 (a) represents the

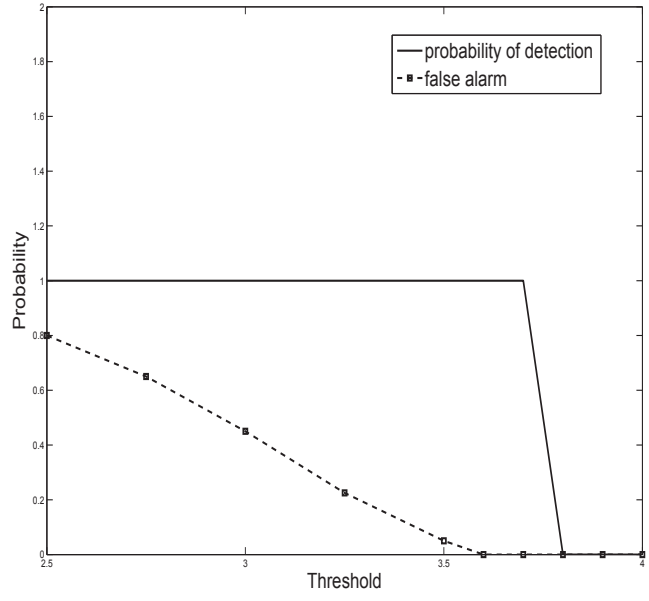


(a)

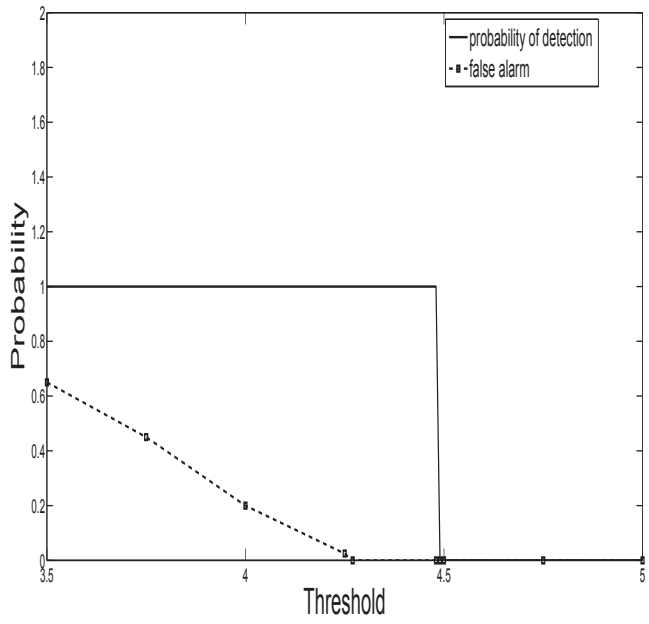


(b)

Figure 3.5. Entropy of echoes of poor signal with power based weighted RSN for two quantization level: (a) level of quantization=8 (b) level of quantization=32.

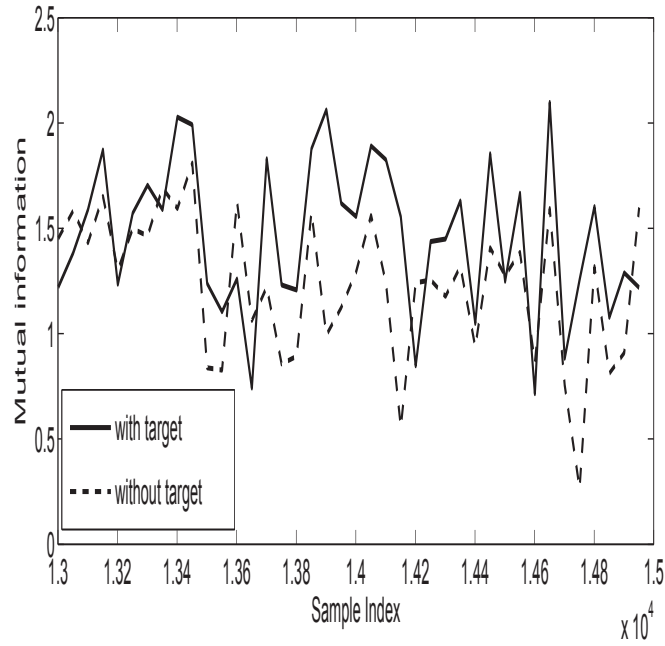


(a)

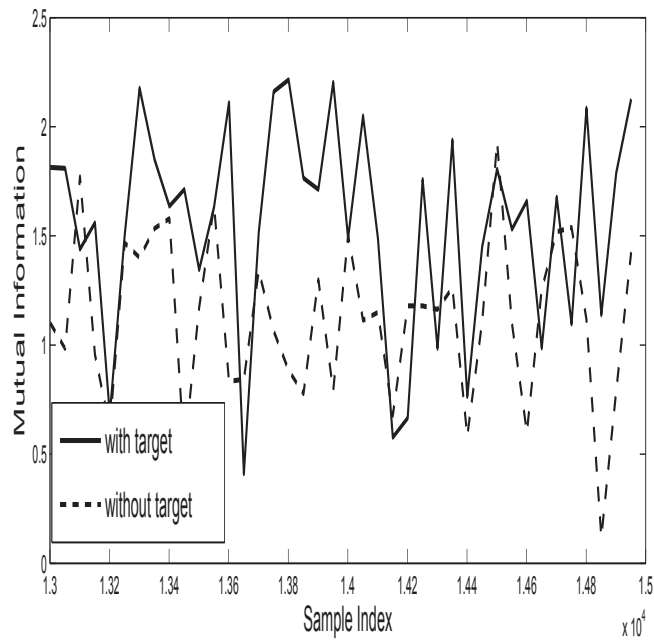


(b)

Figure 3.6. Performance evaluation in terms of probability of detection and probability of false alarm for two quantization levels (a) level=8 (b) level=32.



(a)



(b)

Figure 3.7. Mutual information of echoes with two different condition (a) good signal (b) poor signal .

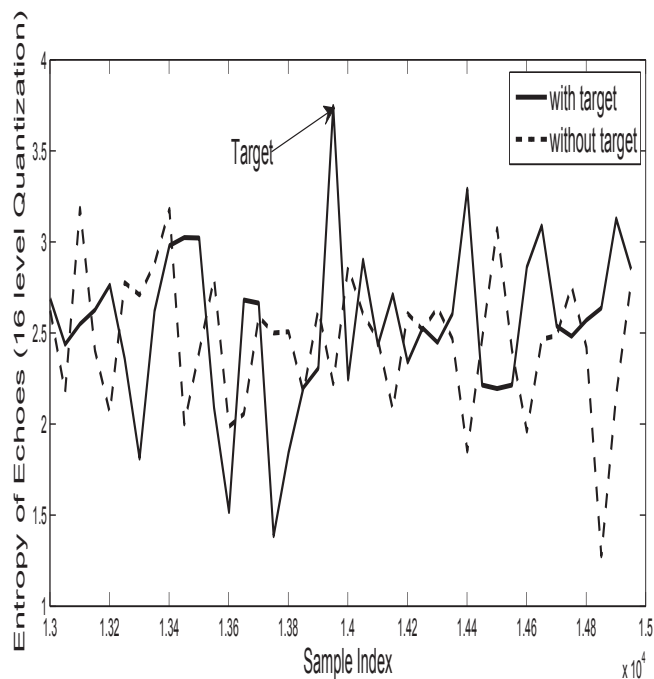


Figure 3.8. Entropy of echoes in RSN with K-L based weighting. Clear target is visible around sample 13900.

ROC with entropy with 8 level of quantization with power based weighting. However, with two step K-L weighting improved the detection and ROC moved toward the upper left corner, as shown in Fig. 3.10(b).

### 3.3.1 Computational Complexity

Computational complexity of this algorithm is fairly low. There is no computationally exhaustive process such as FFT or JPD involved. From MATLAB profiler it was checked that the complexity was in the  $O(N)$  where  $N$  is the data size. All other target detection algorithm where signal processing is involved is highly dependent on FFT, complex multiplication, matrix multiplication and can have very high computational load.

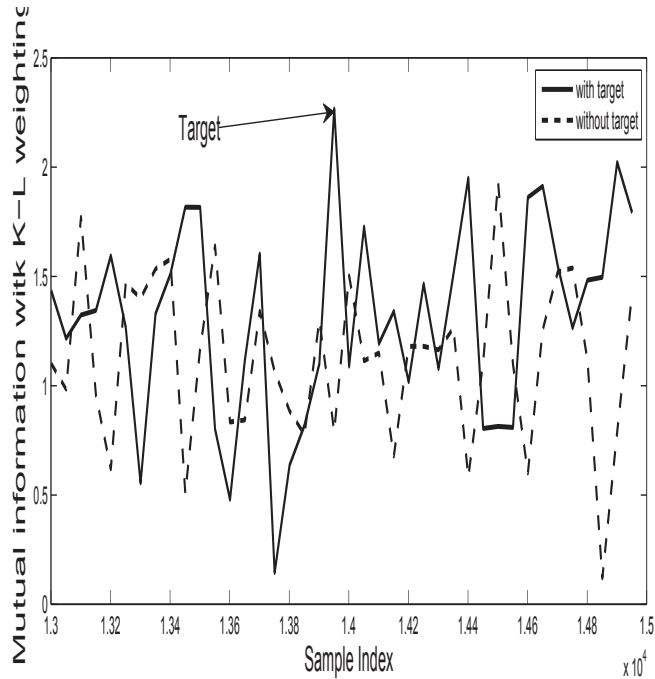
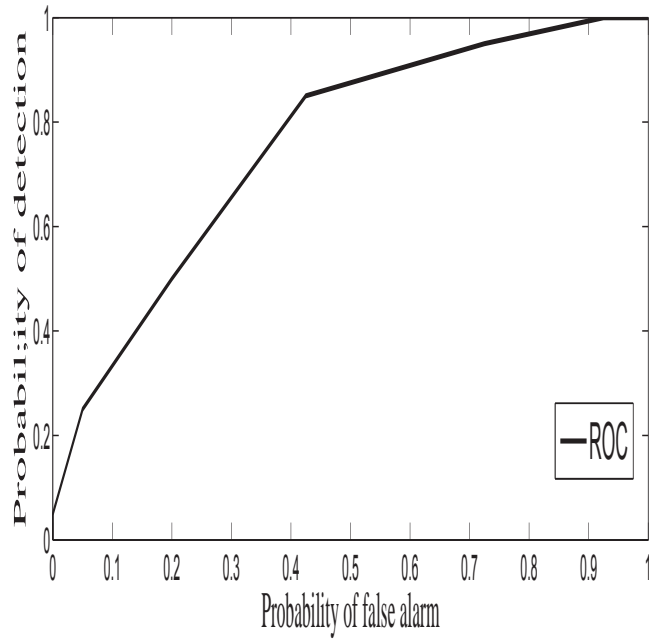


Figure 3.9. Mutual information of echoes in RSN with K-L based weighting. Clear target is visible around sample 13900.

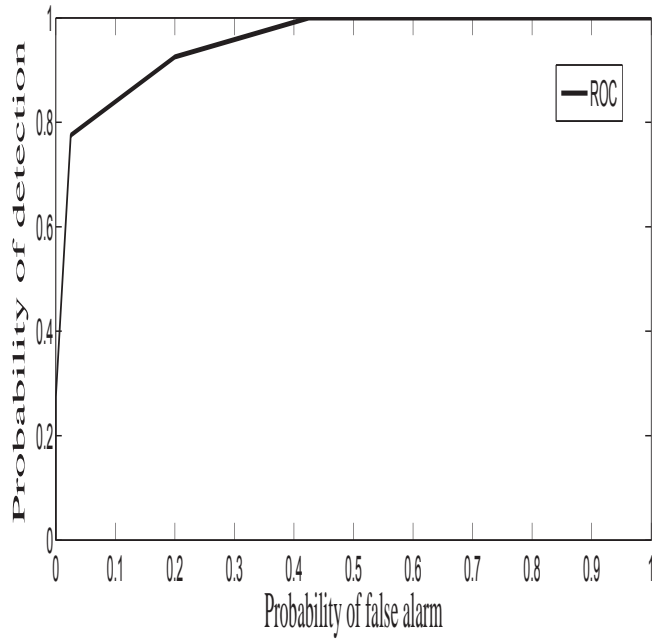
### 3.4 Conclusion

In this chapter, we propose to use information fusion scheme for target detection through foliage using ultra wide-band (UWB) radar sensor networks (RSN). We proposed to use relative entropy or KL based weighting on each branch of the radar sensor. The performance of the algorithm was evaluated, based on real world data. Results show that our algorithm does provide huge improvement while it is compared with the existing method of power based weighting. This method can be an excellent alternative to signal processing based methods as it is computationally efficient and it has less processing load. In future this algorithm can be applied to big data scenario. It can also be applied to human detection. We can also collect more data and apply it to multi-target environment.





(a)



(b)

Figure 3.10. Performance evaluation in terms of probability of detection versus probability of false alarm (ROC) for(a) without (b) with KL divergence..

## Chapter 4

### Decision Fusion Based on Dempster Shafer's Theory and Bayesian Network

#### 4.1 Introduction

By Decision Fusion, we need to achieve decision that are not possible by individual radars operating individually. In our method, radars in RSN are not collecting the information at the same time and place. It is possible that decision based on entropy and mutual information can be different. We want to resolve the conflict of decision by applying different methods. Bayesian inference and Dempster and Shafer's reasoning are the two popular inference algorithms for decision fusion [35][80][39][40] and [41]. In our study, we use three different algorithms and compare their performances. We used Dempster and Shafer's theory and Bayesian network to diffuse the decision. We also introduce the improved version of D-S theory known as Proportional conflict redistribution rule-5(PCR-5) for conflicting evidence and compared the performance with D-S and Bayesian network.

Two of the main philosophies or paradigms of Decision Fusion are Bayes theorem and Dempster and Shafer theory. One advantage of using one approach over the other is the extent to which prior information is available. The oldest paradigm, and the one with the strongest foundation, is Bayes theory, which deals with probabilities of events. Dempster-Shafer theory, deals with measures of belief as opposed to probability. While probability theory states whether something is or is not true, Dempster-Shafer theory allows for more nebulous states of a system (or really, our knowledge), such as unknown. Both theories have a certain initial requirement. Dempster-Shafer theory requires masses to be assigned in a meaningful way to the

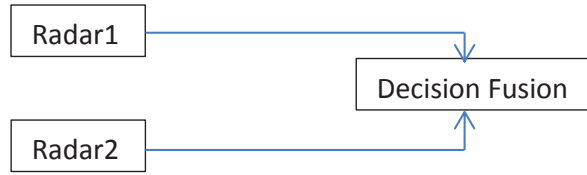


Figure 4.1. Block diagram of centralized fusion for target detection.

various alternatives, including the unknown state; whereas Bayes theory requires prior probabilities, the alternatives to which they are applied are all well defined. Although Dempster-Shafer theory does not need prior probabilities to function, it does require some preliminary assignment of masses that reflects our initial knowledge of the system. A further paradigm which is not discussed in this Chapter is fuzzy logic.

Figs. 4.1, 4.2 and 4.3 depicts several ways to fuse data from several sensors. Figs. 4.1 shows centralizing the fusion and combines all of the raw data from the sensors in one main processor. In principle this is the best way to fuse in the sense that nothing has been lost in preprocessing; but in practice centralised fusion leads to a huge amount of data traversing the network, which is not necessarily practical or desirable. Fig. 4.2 shows preprocessing the data at each sensor which reduces the amount of data flow needed, while in practice the best setup might well be a hybrid of these two types as shown in Fig. 4.3. We chose to use the preprocessing on each radar as shown in Fig.4.2

## 4.2 Block Diagram

The block diagram of the multi-step information fusion based target detection is shown in Fig. 4.4. The first step of the information fusion is done by K-L divergence

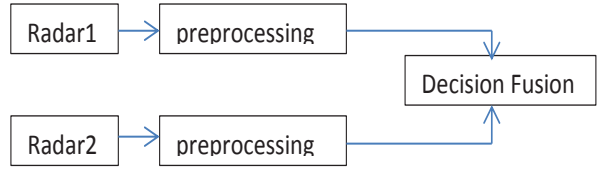


Figure 4.2. Block diagram of centralized fusion with preprocessing on each branch.

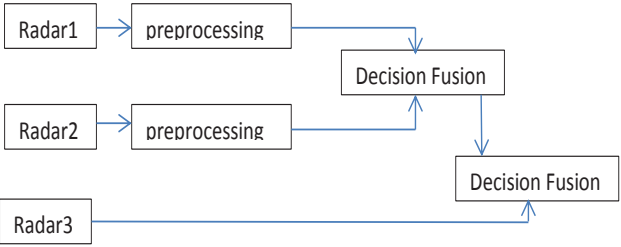


Figure 4.3. Block diagram of hybrid fusion for target detection.

and is clearly explained in Chapter 3. The second stage of the processing is explained in chapter 2 and the last stage of the decision fusion will be explained in this Chapter. The numerical values of the BBA are given in the simulation result part of this Chapter which is calculated based on the threshold values. It is important to note that we have to quantize the received echoes before we apply our method. These echoes are collected by nine different radars and each collected 35 different readings. These collections were summed before the quantization takes place.

### 4.3 Decision Fusion

#### 4.3.1 DS Theory

The Dempster and Shafer (D-S) theory is a mathematical theory of evidence often used in sensor fusion [42]. It was first developed by Dempster and extended by Shafer. It can provide an optimal result from a set of options, without prior

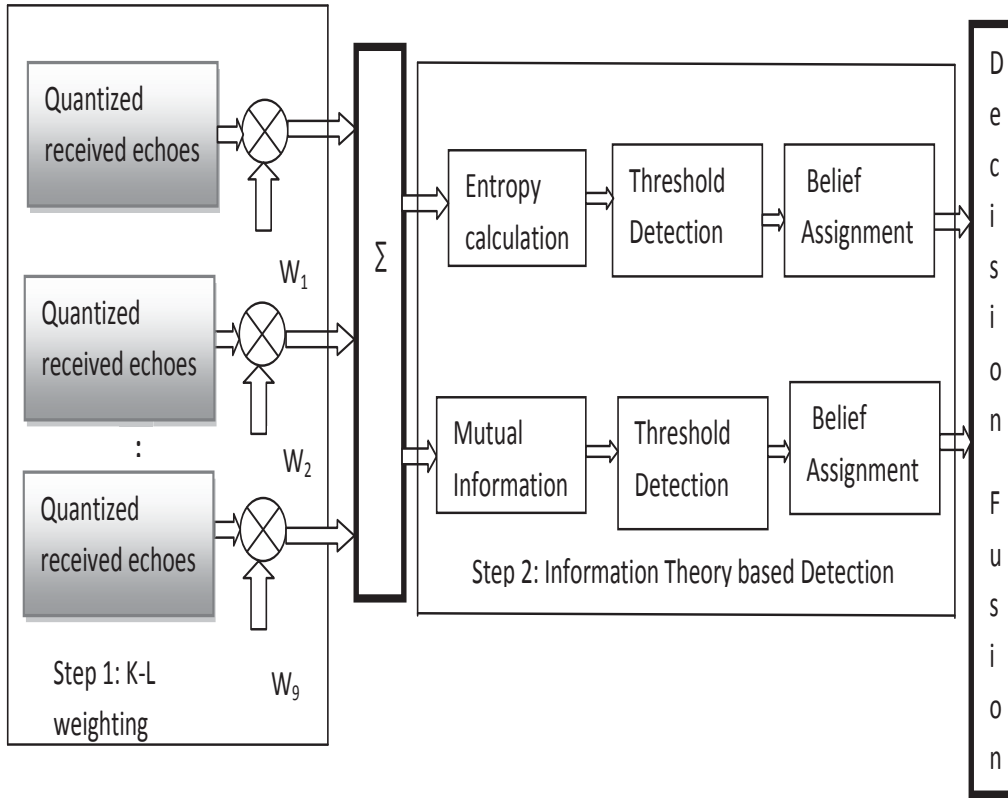


Figure 4.4. Detailed block diagram of the three step information fusion for target detection.

probability. D-S theory makes decision by independently judging all the hypotheses by its individual evidence [80]. This section provides some brief overview of the Evidence theory.

Definition1: Let  $U$  be a finite set of mutually exclusive proposition commonly known as frame of discernment. The power set of  $2^U$  is the set of all subsets, including the null set  $\phi$  and itself. Each subset in the power set is called the focal element. A value between  $[0, 1]$  is given to each focal element, which is based on the evidence. Basic belief assignment (BBA) is also known as the mass function( $m$ ) of

the individual proposition. It is assigned to every subset of the power set, satisfying the following:

$$\begin{aligned} m(\emptyset) &= 0 \\ \sum_{A \subseteq U} m(A) &= 1 \end{aligned} \tag{4.1}$$

where  $m(A)$  can be considered as the accurate belief degree of proposition  $A$ .

Definition2: Two other functions are also associated with the  $m(A)$  are belief function  $Bel(A)$  and the plausibility function  $Pl(A)$ . The belief and plausibility functions are derived from the value of  $m(A)$ , where belief is the lower bound of the probability  $P(A)$  and the plausibility is the upper bound of the  $P(A)$ . The belief is the global measure that the hypotheses is true, while  $Pl(A)$  may be viewed as the amount that could be potentially be placed. The definition of these two quantities are given below,

$$Bel(A) = \sum_{B \subseteq A} m(B), \forall A \subseteq U \tag{4.2}$$

$$Pl(A) = \sum_{B \cap A = \emptyset} m(B), \forall A \subseteq U \tag{4.3}$$

*Rule of combination:* Dempster's rule of combination combines two independent sets of mass assignments by orthogonal sum. If  $m_1$  and  $m_2$  are two BBAs pertaining to two different evidential sources, the combined basic belief assignments is obtained via Dempster's rule of combination as follows:

$$(m_1 \oplus m_2)(C) = \frac{\sum_{B \cap A = C} m_1(A) \times m_2(B)}{1 - \sum_{B \cap A = \emptyset} m_1(A) \times m_2(B)} \tag{4.4}$$

This rule ignores the conflict of evidence by a normalizing factor  $K$ , while  $K$  is given by the following,

$$K = \sum_{A \cap B = \emptyset} m_1(A) \times m_2(B) \tag{4.5}$$

In our study we have frame of Discernment as

$$U = \{t, nt\} \tag{4.6}$$

Two different propositions are target present (t) and target not present respectively(nt). Entropy (E) and mutual information (MI) provides two different evidential sources  $m_1$  and  $m_2$ . We can find the belief function from the threshold value. The combined belief of target present can be calculated as follows,

$$(m_1 \oplus m_2)(t) = \frac{m_1(t) \times m_2(t)}{1 - m_1(nt) \times m_2(t) - m_2(nt) \times m_1(t)} \tag{4.7}$$

#### 4.3.2 Proportional Conflict Redistribution Rule 5

Many researchers insist that normalization procedure in the DS combination rule involves counterintuitive result when there is high conflict in evidence. A lot of modified rule that can solve the problem are proposed. One of the popular one is Proportional Conflict Redistribution Rule 5 (PCR5)[37]. PCR5 is the most mathematically exact redistribution rule for conflicting mass than all other PCR methods [37]. We saw several successful use of PCR5 in sensor simulations in various literatures [44], [45] and [46].

For our frame of discernment as given by 4.6 the PCR5 rule will be

$$(m_1 \oplus m_2)(t) = m_1(t) \times m_2(t) + \frac{m_1^2(t) \times m_2(nt)}{m_1(t) + m_2(nt)} + \frac{m_2^2(t) \times m_1(nt)}{m_2(t) + m_1(nt)} \tag{4.8}$$

The details for more than two pieces of evidence combining can be referred to [37].

A numerical example can be presented here to compare the combination of the two

rules. A body of evidence (BOE) is the set of all the focal elements,  $(\mathfrak{R}, m) = (\{\{A\}, m(A)\} | A \subset P(U), m(A) > 0\}$ ; here  $P(U)$  is the power set of frame of discernment,  $U$ . Three body of evidence are showed as follows:

$$(\mathfrak{R}_1, m_1) = (\{\{t\}, .8\}, \{\{nt\}, .2\}); \quad (4.9)$$

$$(\mathfrak{R}_2, m_2) = (\{\{t\}, .7\}, \{\{nt\}, .3\}); \quad (4.10)$$

$$(\mathfrak{R}_3, m_3) = (\{\{t\}, .0\}, \{\{nt\}, 1\}); \quad (4.11)$$

Table I shows the comparison of the calculation for the DS and PCR5 method. From Table I it is clear, when there is less conflict, DS and PCR-5 give similar results, as shown in combining  $m_1$  and  $m_2$ . But when the conflict is high PCR5 gives better result than DS as shown by the last column while combining  $m_1$  and  $m_3$ . This kind of conflicting situation is also known as ‘Zadeh’s Paradox’ [43].

Table 4.1. Combination Result for DS and PCR5

Rule	combination	$m_1 \oplus m_2$	$m_1 \oplus m_3$
DS rule	m(t)	.903	0
	m(nt)	.097	1
PCR5 rule	m(t)	.843	.356
	m(nt)	.157	.644

### 4.3.3 Bayesian Network

Bayesian network (BN), also known as belief networks, belongs to family of probabilistic graphical models (GMs). BN correspond to another GM structure known as a directed acyclic graph (DAG). BN represents a Joint probability distribution (JPD) over a set of random variables. The nodes of the DAG represent the random variables. The graph encodes independence assumption, by which each



variable is independent of its non-descendants, given its parent is in DAG. Thus a BN can represent a JPD in factored form by conditional probability table (CPT). Consider the case where we have  $n$  no of evidential sources  $S_1, S_2, S_3, \dots, S_n$  for a particular node  $D$ . We can write Bayes' theorem as,

$$P(D|S_1, S_2, S_3, \dots, S_n) = \frac{P(D) \times P(S_1, S_2, \dots, S_n|D)}{P(S_1, S_2, \dots, S_n)} \quad (4.12)$$

If we make assumption as sources are independent given  $D$  then we can write,

$$P(S_1, S_2, \dots, S_n|D) = P(S_1|D) \times P(S_2|D) \times \dots \times P(S_n|D) \quad (4.13)$$

The term  $P(S_1, S_2, \dots, S_n)$  can be eliminated by normalization.

In our study we have a tree structured network with a root node  $T$ , which has no parent.  $T$  is the parent node with two children nodes  $E_h$  and  $MI_h$ , which represents high entropy and high Mutual information respectively. This structure is shown in Fig. 4.5.  $T$  can have two different states,  $T=t$  or  $T=nt$ .  $T=t$  means target is present and  $T=nt$  means target is not present. Now as explained in (4.13), the conditional probability of target present with high entropy and mutual information can be calculated as,

$$P(T = t|E_h, MI_h) = \alpha \times P(T = t) \times P(E_h|T = t) \times P(MI_h|T = t) \quad (4.14)$$

here  $\alpha$  is the normalization constant. We assume  $E_h$  and  $MI_h$  is independent of each other and we also assume prior distribution is uniform and  $P(T = t) = .5$ . Details for this method can be referred to [38] [47].

#### 4.3.4 Computational Complexity

The computational complexity for the DS is related to the element in the frame of Discernment, which in our case is only two.

#### 4.4 Simulation Results

In this chapter, we want to combine the decision of two methods based on entropy and mutual information. It should also be noted that the level of quantization is also different for these two different methods, that is why we are unable to compare their performance in a single simulation and we use Dempster rule of combination to combine them.

Results we found in Figs. 3.8 and 3.9 are combined by (4.7),(4.8) and (4.14). Before applying (4.7), we need to assign our belief function for the evidential support. We consider ‘‘Zadeh’s paradox’’ [43] and applied a very small value instead of zero for small probability. The belief function of entropy,  $m_1(t)$  is assigned as shown by the following,

$$m_1(t) = \begin{cases} 0.8 & \text{when } H(Q) \geq 3 \\ 0.5 & \text{when } 2.5 \leq H(Q) < 3 \\ 0.01 & \text{when } H(Q) < 2.5 \end{cases} \quad (4.15)$$

where  $H(Q)$  is the entropy of the quantized received echoes in the  $k^{th}$  window after K-L distance based weighting. The belief function of mutual information,  $m_2(t)$  assigned is shown by the following,

$$m_2(t) = \begin{cases} 0.8 & \text{when } MI(Q_k : Q_{k-1}) \geq 2.1 \\ 0.5 & \text{when } 1.5 \leq MI(Q_k : Q_{k-1}) < 2.1 \\ 0.01 & \text{when } MI(Q_k : Q_{k-1}) < 1.5 \end{cases} \quad (4.16)$$

where  $MI(Q_K; Q_{k-1})$  is the mutual information of the quantized received echoes in the subsequent radar return in the window after K-L distance based weighting. The Dempster based combination successfully detects the target presence as shown in Fig. 4.6. It is important to note that three-step information fusion identifies the target with complete certainty.

However as we have already shown in Table I that D-S sometimes are not so efficient for high conflict. We select a set of data without K-L divergence, with 8 level of quantization and applied DS rule of combination. It gives several windows with higher values as shown in Fig. 4.7 (a). However this was resolved better by PCR5 as shown in Fig. 4.7(b). Here the conflicting windows lowered down. We also applied Bayesian network and it performed slightly better than PCR5 as shown in Fig. 4.7(c). In this figures we did not consider “zadeh’s paradox”. We consider “zadeh’s paradox” in Figs. 4.8, 4.9 and 4.10

#### 4.4.1 Conclusion

In this chapter, we propose three different schemes Dempster and Shafer (D-S) theory of evidence, proportional conflict redistribution rule 5(PCR) and Bayesian network for decision fusion. In previous chapters, we propose to use information theory and mutual information based method to be applied to RSN and preprocessed the data using KL. However due to the complexity of the environment it is possible we might get conflicting result. We want to resolve the conflict of decision by applying different methods. Dempster-Shafer theory, deals with measures of belief as opposed to probability. For our target detection algorithms, two different propositions are target present (t) and target not present respectively(nt). Entropy (E) and mutual information (MI) provides two different evidential sources  $m_1$  and  $m_2$ . We can find the belief function from the threshold value. The combined belief of target present

can be calculated by using the Dempster's rule of combination. Many researchers insist that normalization procedure in the DS combination rule involves counterintuitive result when there is high conflict in evidence. A lot of modified rule that can solve the problem are proposed. One of the popular one is Proportional Conflict Redistribution Rule 5 (PCR5). PCR5 is the most mathematically exact redistribution rule for conflicting mass than all other PCR methods. Bayesian network (BN), also known as belief networks, belongs to family of probabilistic graphical models (GMs). In our study we have a tree structured network with a root node T, which has no parent. T is the parent node with two children nodes  $E_h$  and  $MI_h$ , which represents high entropy and high Mutual information respectively. Among the decision fusion algorithms, Bayesian approach worked slightly better than PCR5 while combining evidential conflict. However PCR5 performed better than DS. Results show that accurate detection can be achieved by applying DS in case of low conflict.

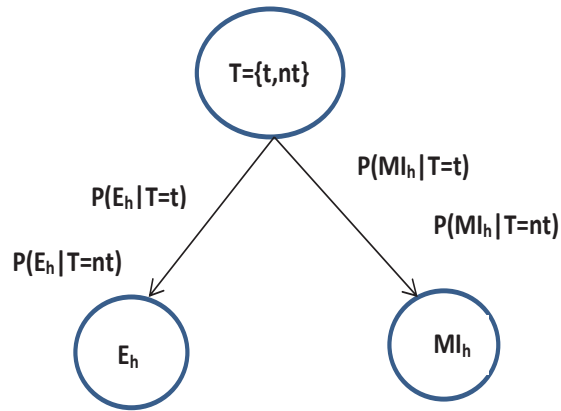


Figure 4.5. Bayesian network for Target Detection.

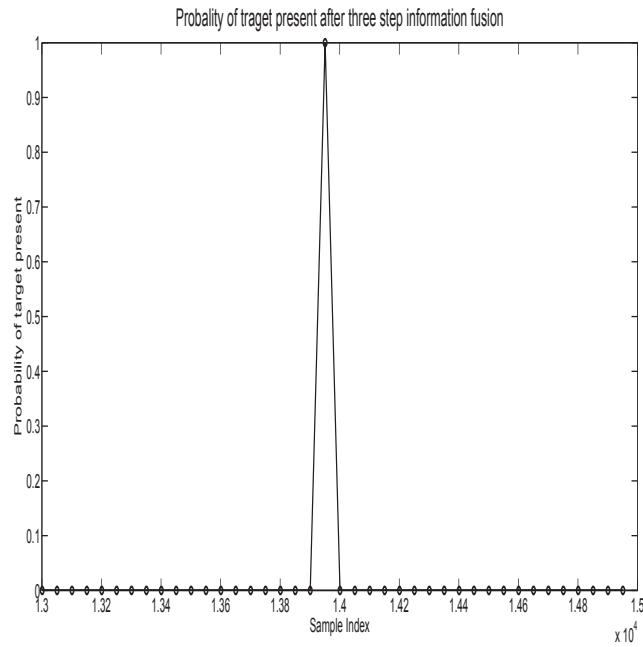
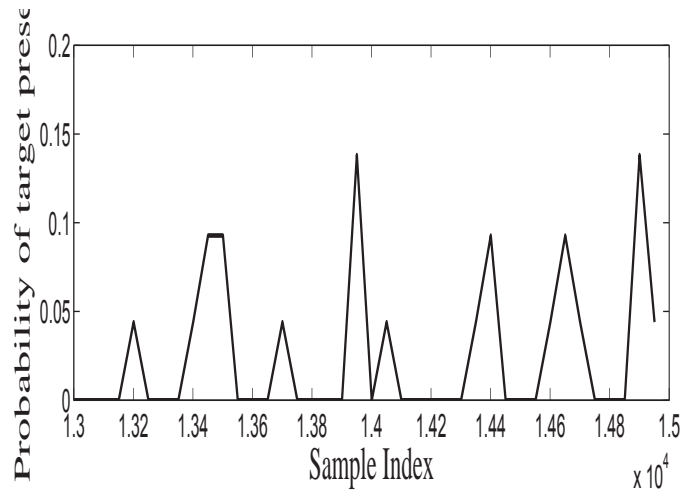
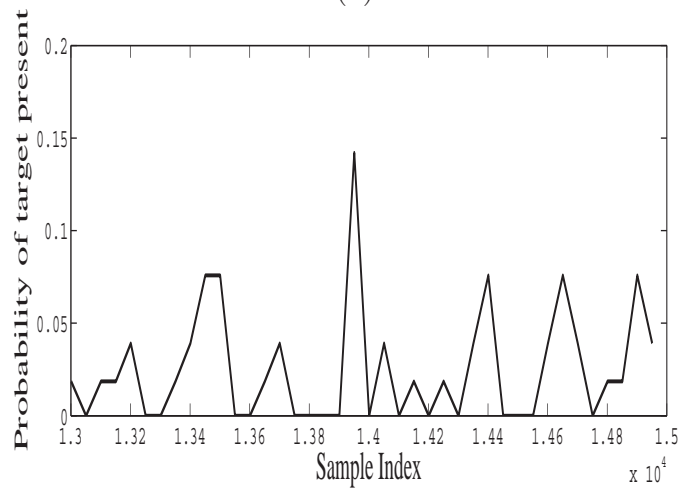


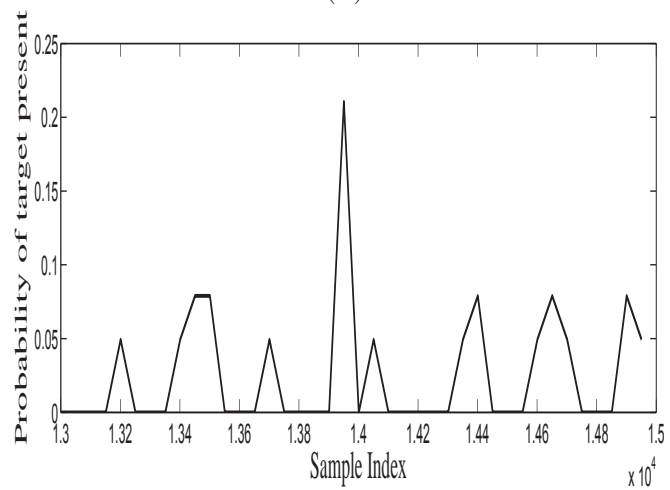
Figure 4.6. Probability of target present after decision fusion. Target is detected with certainty.



(a)



(b)



(c)

Figure 4.7. Performance evaluation in terms of probability of detection for high conflict in three different methods: (a) D-S, (b) PCR5 and (c) Bayesian not considering Zadeh's paradox.

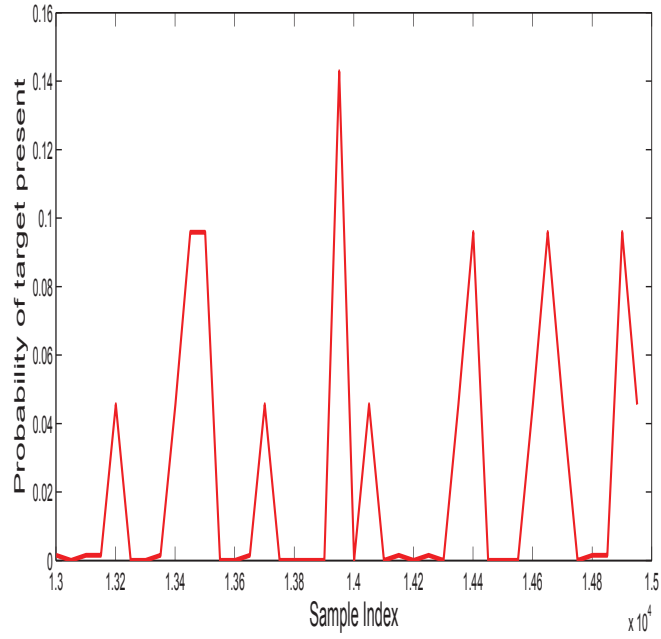


Figure 4.8. Performance evaluation in terms of probability of detection for high conflict using D-S, considering Zadeh’s paradox.

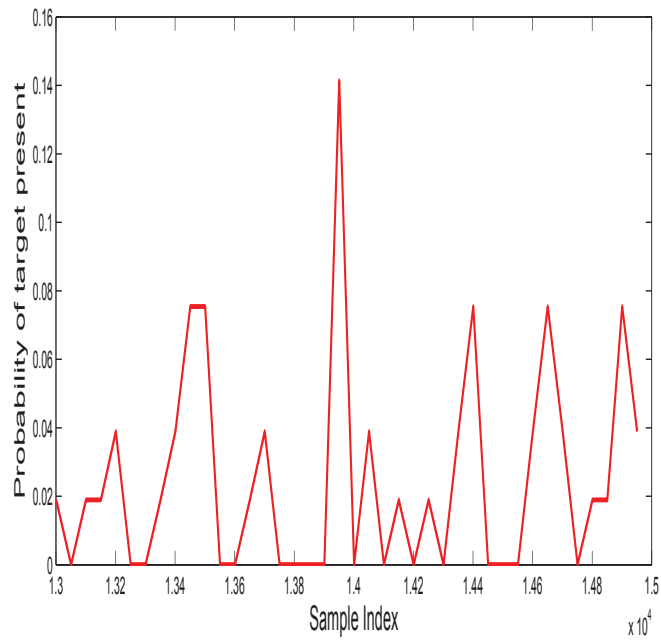


Figure 4.9. Performance evaluation in terms of probability of detection for high conflict using PCR5 considering Zadeh’s paradox.

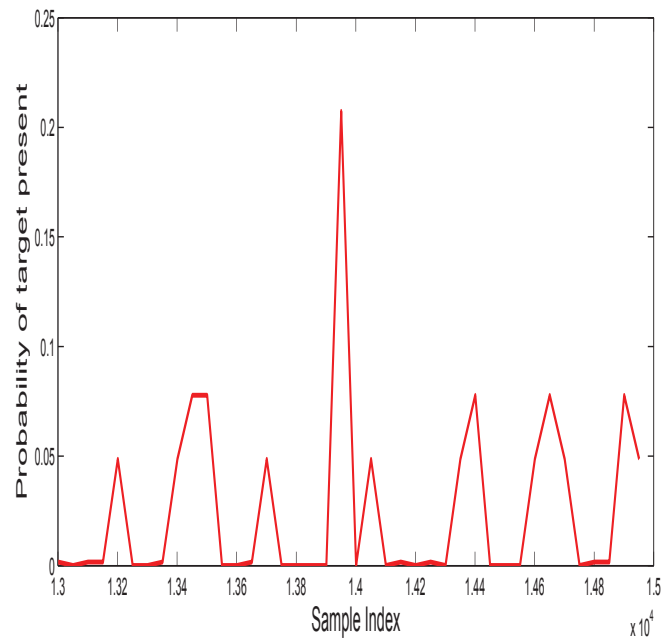


Figure 4.10. Performance evaluation in terms of probability of detection for high conflict with Bayesian Network considering Zadeh's paradox.



## Chapter 5

### Sensor Selection Based on Chernoff Information

#### 5.1 Introduction

In this chapter, we propose to use information theory to automatically select the best sensors in a Ultra Wide Band (UWB) Radar Sensor Network (RSN) to detect target in foliage environment. Information theoretic algorithms such as entropy and mutual information are discussed in Chapter 2 that can be applied to data collected by various sensors for target detection. However, the complexity of the environment possess uncertainty in fusion center and the big data collected by sensors can have huge processing load. In this chapter, we propose to use another information theoretical criterion known as Chernoff information that can provide the best error exponent of detection in Bayesian approach. We also used Chernoff Stein Lemma for fusing the data to optimize the performance. The performance of the algorithm was evaluated, based on real world data. Results show that our opportunistic sensing (OS) algorithm does efficient utilization of sensing assets and provide same performance while it is compared with the existing method without OS.

In Radar Sensor Network (RSN), multiple distributed radar sensors survey a large area and observe targets from different angles. Major limitations of such conventional approaches include inadequate performance for target recognition and huge processing load for big data. Opportunistic Sensing (OS) refers to a paradigm for signal and information processing in which a network of sensing systems can automatically discover and select sensor platforms based on an operational scenario. It uses appropriate methods to fuse the data, resulting in an adaptive network that au-

tomatically finds scenario-dependent, objective driven opportunities with optimized performance. From the experimental data collected by Air Force, it has been found that echoes with target are more random than the region without target. This finding leads us to use Maximum entropy Method (MEM) and mutual information as the target detection tool. However, there can still be redundancy in the big data collected by various radars. Since its possible that less sensors can achieve better performance, and less sensors can save the bandwidth, energy, memory and storage resource of sensor networks, its very desirable that principal sensors can be selected. Also the error probability associated with the detection is crucial in understanding the performance of the detection. Chernoff information gives the best error exponent in hypothesis testing, thus can be used as sensor selection scheme in fusion center. This OS reduces the processing load significantly and effectively utilize the sensing assets. In order to optimize the performance, data fusion is done based on Chernoff Stein Lemma.

The rest of the chapter is organized as follows. In Section 5.2, we describe the system model. In Section 5.3, we explain design and analysis of Chernoff information based sensing and Chernoff Stein Lemma based data fusion. In Section 5.4, we present the simulation results. We conclude this paper and propose some future research in Section 5.5.

## 5.2 System Model

RSN and rake structure that we employ in our work has nine different radars, each collected 35 reading as shown in Fig.5.1. These radars are mono-static and independent. Since two radars will not experience deep fading at the same time, RSN provides better signal quality when they are spaced sufficiently far apart. Also the collections of the reading from different position of the radar were not taken at

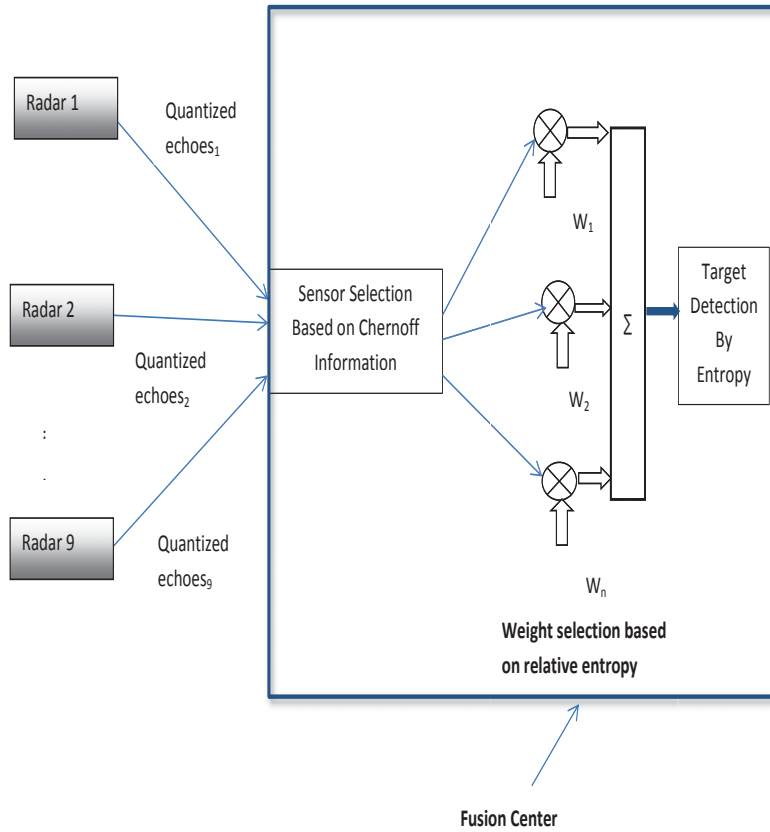


Figure 5.1. Detailed block diagram for information theory based opportunistic sensing in Radar Sensor Network.

the same time. This guarantees the time as well as spatial diversity in the proposed RSN. Information collected by individual radars are quantized and sent to fusion center to combine by using the weighted average. But before the weighted average is applied best sensors will be selected based on their Chernoff information. Also the weight will be applied based on Chernoff Stein Lemma. Detailed analysis of these theorems are discussed in the Section 5.3. Finally an information theoretic algorithm, Maximum entropy Method(MEM) is used to detect target.

### 5.3 Design and Performance Analysis Based on Chernoff Information and Chernoff Stein Lemma

Chernoff information gives best error exponent for hypothesis testing in Bayesian approach. The higher the Chernoff information the lower the probability of error in detection. In this chapter, we propose to use Chernoff information as sensor selection scheme. This will significantly reduce the processing delay and improves the performance as well.

If we assume the R radar sensors are independent and the observations of the sensors are i.i.d then; let  $X_1, X_2, \dots, X_n$  be i.i.d  $Q(x)$ ; let  $A_n \subseteq \chi_n$  is acceptance region for hypothesis  $H_1$ ; we can consider the two hypothesis as follows,

$$\begin{aligned} H_1 : \quad Q &= P_1 & \text{Target} & \text{present} \\ H_2 : \quad Q &= P_2 & \text{Target} & \text{absent} \end{aligned} \tag{5.1}$$

Consider the general decision function when  $g(X_1, X_2, \dots, X_n) = 1$  mean  $H_1$  is accepted and  $g(X_1, X_2, \dots, X_n) = 2$  means  $H_2$  is accepted. We can define the two probabilities of error, one is the missed detection  $\alpha_n$  and other is the false alarm  $\beta_n$ ,

$$\alpha_n = Pr(g(X_1, X_2, \dots, X_n) = 2 | H_1 \text{ true}) = P_1^n(A_n^c) \tag{5.2}$$

and

$$\beta_n = Pr(g(X_1, X_2, \dots, X_n) = 1 | H_2 \text{ true}) = P_2^n(A_n) \tag{5.3}$$

Now if we assume that  $Q = P_1$  with prior probability  $\pi_1$  and  $Q = P_2$  with prior probability  $\pi_2$ , the overall probability of error is,

$$P_e^{(n)} = \pi_1 \alpha_n + \pi_2 \beta_n \tag{5.4}$$

In order to get the minimum probability of error, in general we wish to minimize both error as expressed by (5.4). The probability of error in detection  $P_e$  asymptotically it holds that[22],

$$\lim_{n \rightarrow \infty} \frac{\log P_e}{n} = -CI^* \quad (5.5)$$

In other words for large n we obtain

$$P_e \approx \exp(-nCI^*) \quad (5.6)$$

here  $CI^*$  is the Chernoff information. The Chernoff information between two pmf p and q is defined as[22],

$$CI^* = C(p, q) = - \min_{0 \leq \lambda \leq 1} \log \sum_{k=1}^M p_k^\lambda q_k^{1-\lambda} \quad (5.7)$$

where M is related to quantization level.  $\lambda$  value should be chosen by the following,

$$D(p||\lambda) = D(q||\lambda) \quad (5.8)$$

Here D is defined by (3.8).

*Chernoff Stein Lemma* As an alternative to Bayesian approach, we can minimize one of the error subject to the constraint of the other error, which is known as Chernoff-Stein Lemma. In that case  $\alpha_n < \epsilon$ , and  $\beta_n$  for two distribution  $P_1$  and  $P_2$  can be expressed as,

$$\lim_{n \rightarrow \infty} \frac{1}{n} \log \beta_n^\epsilon = -D(P_1||P_2) \quad (5.9)$$

here  $\alpha_n$  and  $\beta_n$  is defined in (5.2) and (5.3), D is KL distance. From this we can say that the false alarm probability is inversely proportional to KL distance. This finding is consistent to Chapter 3, where we found the relation between false alarm and KL based on Method of types. In this section same can be explained with Chernoff Stein Lemma.

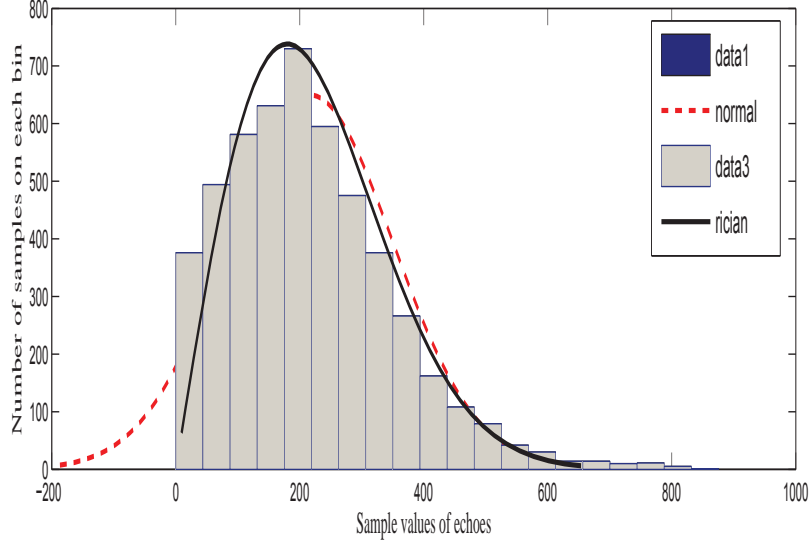


Figure 5.2. Clutter distribution in the farfield for the last 5000 samples collected by 9 different radars with bin 20 bin.

One of the popular indoor UWB channel model is S-V model. But the foliage environment differs from indoor and we plotted the histogram of the clutter in the far field which follows the Gaussian Distribution as shown in Figs. 3.3 and 3.4. Also in a previous paper, it has been shown that the outdoor UWB channel follows a Rician distribution [4], whereas the target region is uniform.

*Theorem2:* If target has a distribution which follows  $\mathbf{U}(a, b)$  and the clutter Q follows  $\mathbf{N}(\mu, \sigma)$ , then the probability of error in target detection  $Err_d$  can be expressed as,

$$Err_d \approx \exp(-n(C)) \quad (5.10)$$

where C can be denoted as,

$$C = -\lambda(b-a)\ln(b-a) - (1-\lambda)(b-a)\ln(\sqrt{2\pi}\sigma) - (1-\lambda) \left[ \left( \frac{b^3 - a^3}{6\sigma^2} \right) - \mu \left( \frac{b^2 - a^2}{2\sigma^2} \right) + \frac{\mu^2}{2\sigma^2}(b-a) \right] \quad (5.11)$$

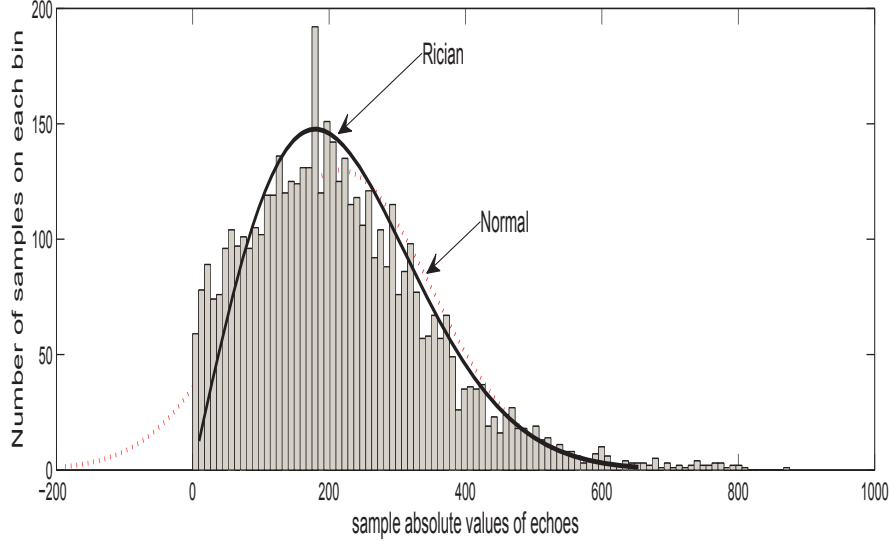


Figure 5.3. Clutter distribution in the far-field for the last 5000 samples collected by 9 different radars with 100 bin.

*Proof*

Chernoff information between a uniform density  $p(x)$  and Gaussian distribution  $q(x)$  can be written as,

$$\begin{aligned}
 CI &= C(p(x), q(x)) \\
 &= -\min_{0 \leq \lambda < 1} \ln \int_a^b \left[ \frac{1}{b-a} \right]^\lambda \left[ \frac{1}{\sqrt{2\pi}\sigma} e^{-\frac{(x-\mu)^2}{2\sigma^2}} \right]^{1-\lambda} dx
 \end{aligned} \tag{5.12}$$

Now denoting the natural log term as  $C(\lambda)$  this can be further simplified as

$$\begin{aligned}
 C(\lambda) &= -\lambda \int_a^b \ln(b-a) dx - (1-\lambda) \int_a^b \ln(\sqrt{2\pi}\sigma) dx \\
 &\quad - (1-\lambda) \int_a^b \frac{(x-\mu)^2}{2\sigma^2} dx
 \end{aligned} \tag{5.13}$$

$$\begin{aligned}
&= -\lambda(b-a)\ln(b-a) - (1-\lambda)(b-a)\ln(\sqrt{2\pi}\sigma) \\
&- (1-\lambda) \left[ \left(\frac{b^3-a^3}{6\sigma^2}\right) - \mu\left(\frac{b^2-a^2}{2\sigma^2}\right) + \frac{\mu^2}{2\sigma^2}(b-a) \right]
\end{aligned} \tag{5.14}$$

As the theoretical close form approximation of Chernoff information between a uniform and gaussian density can be expressed as (5.14), theorem 1 can be proved from (5.14) and (5.6).

Since Figs. (5.2) and (5.3) shows the Rician distributed clutter we calculated C for Rician distribution and is attached in Appendix B.

*Lemma 2:* If target has a distribution which follows  $\mathbf{U}(a, b)$  and the clutter Q follows  $\mathbf{N}(\mu, \sigma)$  and missed detection is fixed, the false alarm rate can be expressed as  $Err_f$  can be expressed as,

$$Err_f \approx \exp(-n(D(P||Q))) \tag{5.15}$$

where D can be denoted as,

$$\begin{aligned}
D(P||Q) = & -\ln(b-a) + \ln\sqrt{2\pi}\sigma + \frac{\mu}{6\sigma^2}(b^2 + ab + a^2) \\
& - \frac{\mu}{4\sigma^2}(b+a) + \frac{\mu^2}{2\sigma^2}
\end{aligned} \tag{5.16}$$

*Proof:* Proof is attached in Chapter 3.

Since Figs. (5.2) and (5.3) shows the Rician distribution, we calculated D for Rician distribution and attached in the appendix A.

## 5.4 Simulation Results

Our work is based on the sense-through-foilage data from Air Force Research Lab [81]. Initially, the Barth pulse source was operated at lower amplitude and 35



pulses of signals were obtained. This collection is referred to as “poor” data. The integration of these 100 pulses with higher amplitude is referred to as ”good” data, and some works have been done on target detection based on such data sets, such as DCT-based approach [9] and differential-based approach [11]. The window size was used as 50.

In Fig. 5.4, we assess the proposed method of target detection in terms of the probability of error for nine different radars, in 16 levels of quantization. To compare the performance in terms of probability of error in detection, we used three different methods, Chernoff Information, Chernoff Stein Lemma and the theoretical approximation of Chernoff Stein Lemma. Clearly the probability of error in detection decreases as number of radars increases. Between these methods Chernoff Information performs much better than Chernoff Stein Lemma. Chernoff information can achieve less than 0.1 of probability of error in detection with only 2 radars whereas Chernoff Stein Lemma needs at least 7 radars for achieving similar performance.

Fig. 5.5 shows the Chernoff information in various radar position. The purpose of this study is to apply OS so that we can utilize the sensing assets efficiently. We want to select the radars which will provide the highest Chernoff information as they will provide the lowest error in detection while hypothesis testing is done using Bayesian approach.

Fig. 5.6 shows the performance of an entropy based target detection using Chernoff information as sensor selection scheme. Here only five sensors are chosen with the highest Chernoff information. Clearly the position of the radar with highest Chernoff is selected as position 3,4,5,6,9. The target is detected around sample 13900.

Fig. 5.7 shows the performance of an entropy based target detection while only three radars are chosen based on their Chernoff information. The target is detected around sample 13900.

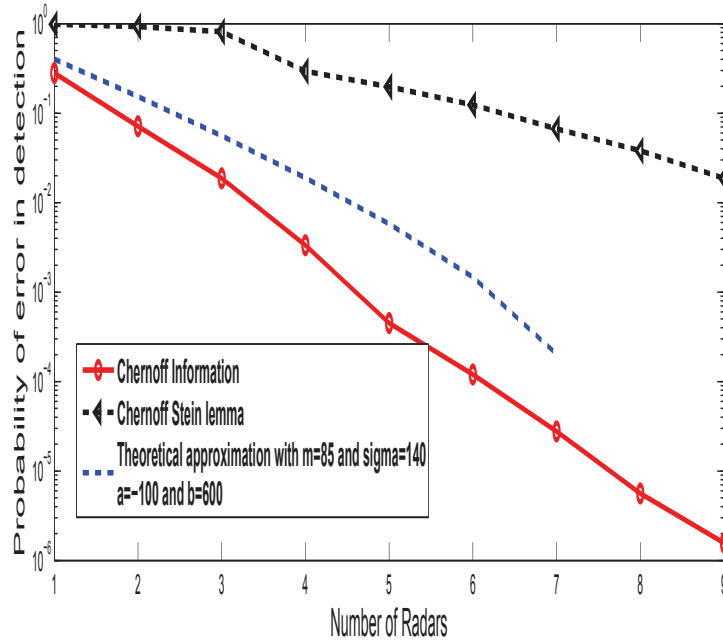


Figure 5.4. Probability of error versus number of sensors, with 16 level of quantization.

Fig. 5.8 shows the performance of an entropy based target detection while only one radar is chosen based on their Chernoff information. The target is detected around sample 13900. Fig. 5.9 shows the performance of the target detection algorithm without OS. If we compare the performance between Figs. 5.8 and 5.9, clearly the performance with OS is equally good as the performance without OS. This proves the effectiveness of our algorithm in detection while significantly reducing the huge processing load of the big data, collected by 9 different radars in 35 different position with 16000 sample. The reduction in processing load is 9:1.

## 5.5 Conclusion

We propose theory and algorithm for a new scheme of Opportunistic sensing(OS) that not only ensures effective utilization of sensing assets but also provides

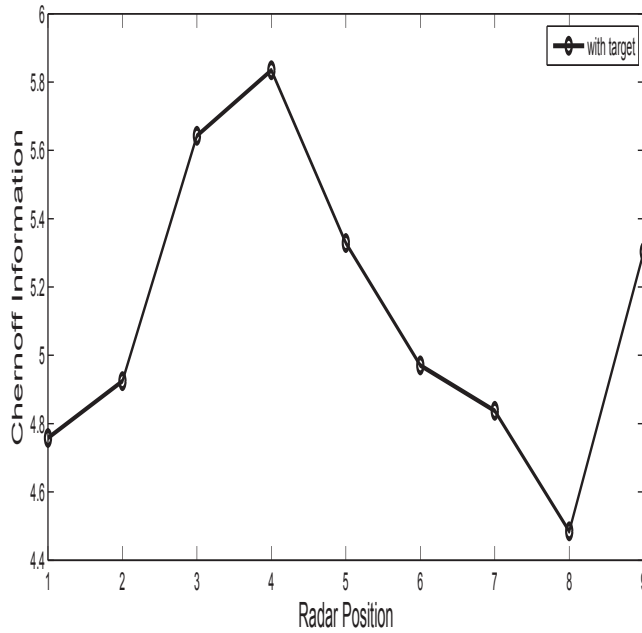


Figure 5.5. Chernoff Information versus radar in nine different positions.

optimal performance. We propose to use Chernoff information as sensor selection scheme and we also propose to use Chernoff Stein Lemma based information fusion in the fusion center. We derived the close form approximation for the Chernoff information and KL distance between uniform and Gaussian densities. This is a novel approach since it has not been investigated so far. Simulation results show that our approach can work successfully with real world data. Using this novel approach we could significantly reduce the number of radars from 9 to 1 while maintaining good performance. In future we shall acquire more data and apply this algorithm to multi-target detection.

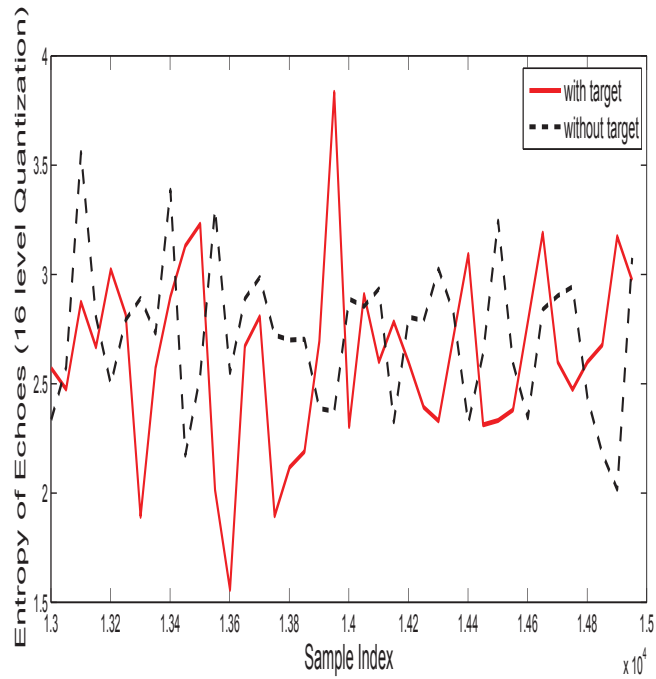


Figure 5.6. Entropy based Target detection with five sensors(position 3,4,5,6,9) selected by Chernoff Information with 16 level quantization. Target is detected.

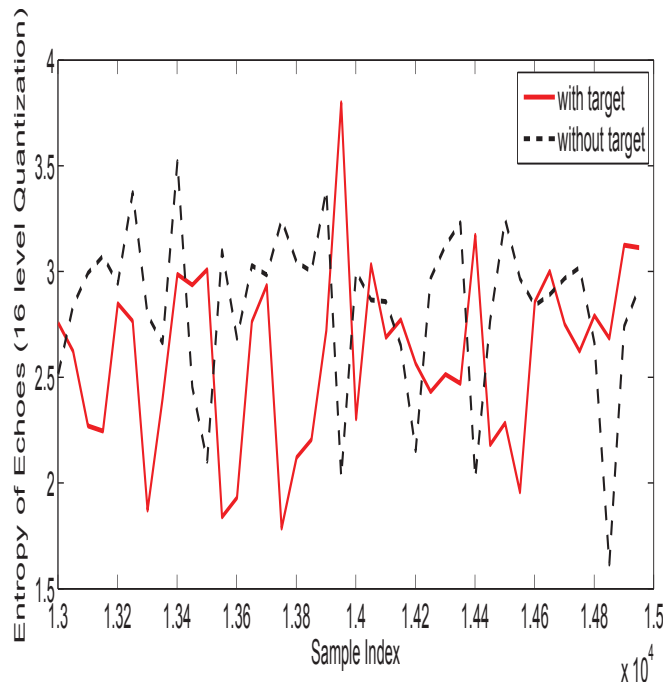


Figure 5.7. Entropy based Target detection with three sensors(position 3,4,5) selected by Chernoff Information with 16 level quantization. Target is detected.

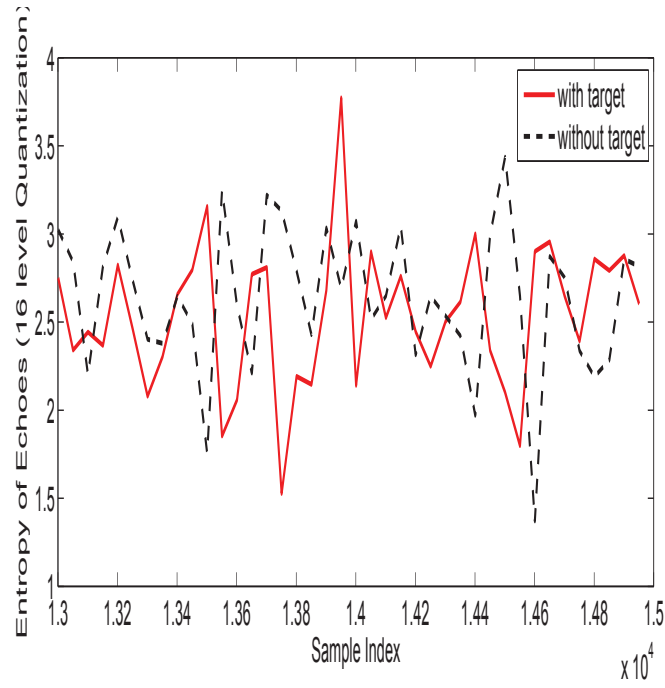


Figure 5.8. Entropy based Target detection with one sensor(position 4) selected by Chernoff Information with 16 level quantization. Target is detected.

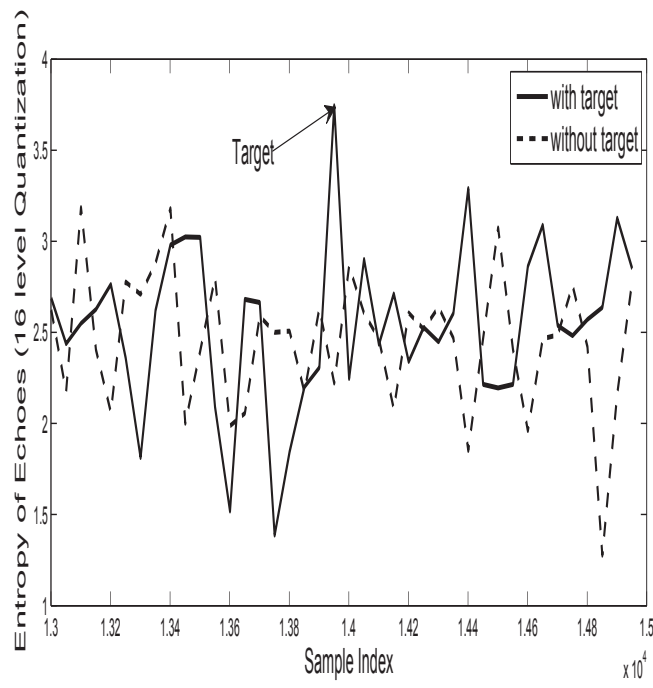


Figure 5.9. Entropy based Target detection without OS.

## Chapter 6

### Human Detection Based on Information Theory

#### 6.1 Introduction

The detection of human hidden by walls are of interest for rescue, surveillance and security operations. The problem of rescuing people from beneath the collapsed buildings does not have an ultimate technical solution that would guarantee efficient detection and localization of victims. Due to the ability to penetrate through typical building materials, UWB radar is considered as preferred tool for detection. Detection of human beings with radars is based on movement detection such as respiratory motions and movement of body parts. These motions cause changes in frequency, phase, amplitude and time-of-arrival as scattered pulses come from the target. In this study, we implemented an information theory based human detection using UWB radar. We applied relative entropy based weighting for preprocessing and in second step we calculated the entropy for several fixed window.

In Chapter 2 we proposed entropy based method to detect target in forest with good signal quality. The current scenarios are different as human target behaves differently than the metallic target. Human body has complex shape and spatial extent of human body is larger than the transmitted UWB pulse. Returned UWB signals are consists of multipath components as signals, returned from different body parts, are scattered independently. Even the dielectric of the wall will have significant effect on detection. Antenna coupling with the wall and multiple reflections from the wall will further deteriorate the performance. In order to reduce the performance

degradation we, propose to use relative entropy based weighting after the clutter reduction on several scans collected from the same radar.

The rest of the Chapter is organized as follows: Data collection is described in Section 6.1.1. Two step information theory based detection is discussed in Section 6.2. In Section 6.3, we present the simulation results. We conclude this paper and propose some future research in Section 6.4.

### 6.1.1 Measurement Setup

This study considers PulseON P220 UWB radar, developed by time domain, in monostatic mode. Here waveform pulses are transmitted from a single Omni-directional antenna and the scattered waveforms are received by a collocated Omni-directional antenna as shown in Fig.6.1 [82] [83] [84]. It has a center frequency of 4.3 GHz. An Ethernet cable is used to connect the radio to the PC and radar can be controlled using application software provided with the radios. Extremely low power, spectral efficiency, immunity to interference and excellent wall penetration characteristics make this radar suitable for indoor human detection. In general, UWB signal is noise-like due to the low energy density. Random noise waveform is inherently low probability of intercept (LPI) and low probability of detection (LPD). The large bandwidth along with discontinuous transmission makes UWB signal resistant to severe multi-path interference and jamming. Thus, it is an ideal candidate to work as a sensor for obscured regions in hostile environments [85].

Fig. 6.2 shows high-level block diagram of a TM-UWB transceiver [82]. It can be seen that the transmitter does not contain a power amplifier. Instead a pulse generator generates the transmission pulse at requisite power. A vital part of the pulse generation circuit is the antenna, which acts as a filter. The architecture of receiver resembles the transmitter, except that the pulse generator feeds the multiplier



Figure 6.1. P220 in monostatic mode.

with a template waveform within the correlator. Also, baseband signal processing must extract the modulation and control signal acquisition and tracking. TM-UWB transmitters emit very short duration Gaussian monocycles with tightly controlled pulse-to-pulse intervals. The pulse-to-pulse intervals are relatively long. Thus, the short duration pulse leads to wide band signal and long pulse-to-pulse interval leads to low duty cycle. Time Domain UWB products have monocycle pulse widths of between 0.20 and 1.50 nanoseconds and pulse-to-pulse intervals of between 25 and 1000 nanoseconds [82], [86]. Pulse position modulation (PPM) scheme is used in the systems and pulse-to-pulse interval is varied on a pulse-by-pulse basis in accordance with two components: an information signal and a channel code. A single bit of information is transmitted using multiple pulses. The PulseON systems use long sequences of monocycles for communications instead of single monocycles. Based on the information signal and channel code, PPM is used to vary the pulse-to-pulse intervals. When the sequences of monocycles are sent, it is important to ensure the spectral quality integrity.

Few important related parameters related to radio configuration are important in analyzing captured scans. These are hardware and software integration, window



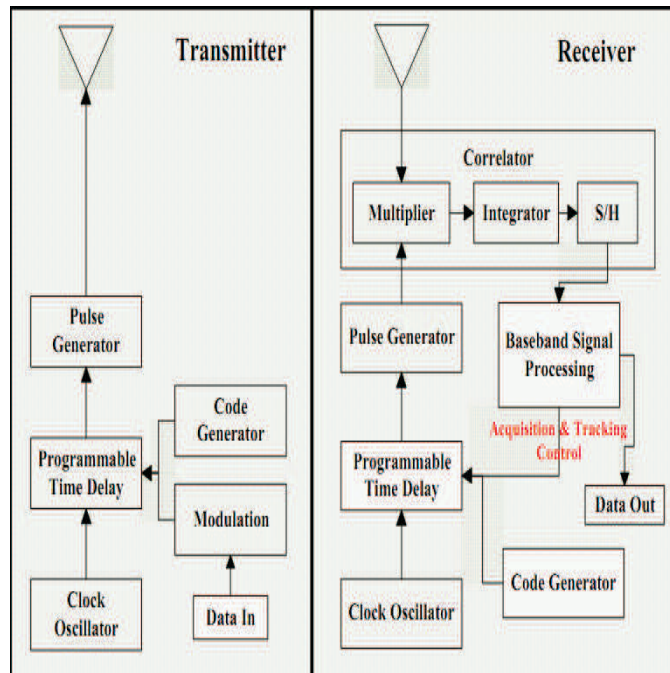


Figure 6.2. TM-UWB Transceiver block diagram.

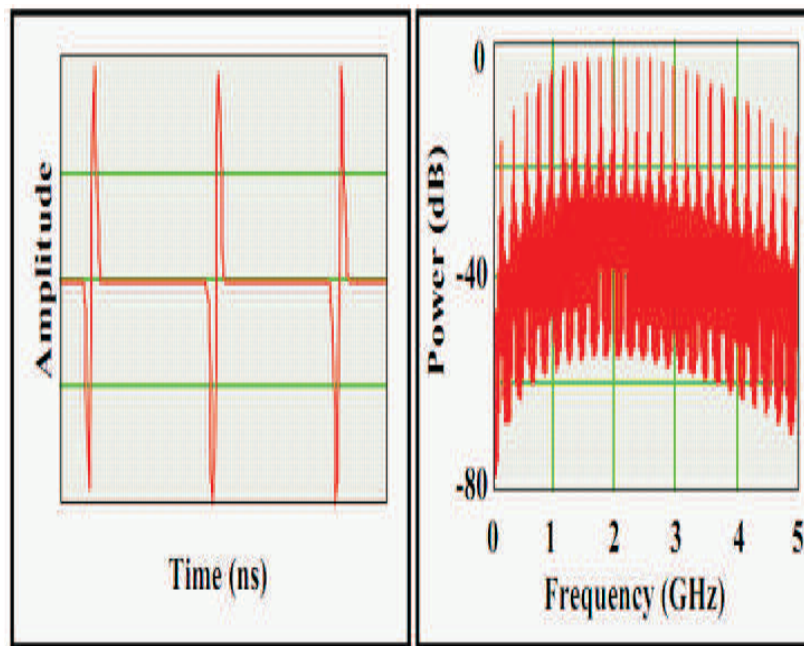


Figure 6.3. A periodic pulse wave in time and frequency domain.

size, number of pulses per scan, number of sample per scan, pulse rate and scan rate. Integration is the number of radio pulses that radar combines to increase the signal-to-noise ratio. There are two types of integration. Hardware integration is performed by the radios hardware. Software integration is performed by the radios kernel software and occurs after hardware integration. The total integration is the total number of UWB pulses per waveform sample, and is found by multiplying hardware and software integration. Window Size (ft) is the difference between stop position and the start position. Pulses per waveform is the number of UWB radio pulses required for the entire waveform (single scan). If we denote number of sample point per scan as  $nsample$ , then

$$nsample = \frac{2 * window\ size * .3048}{c * step\ size} \quad (6.1)$$

Now number of pulses per scan can be denoted as  $npulse$  and can be calculated as,

$$npulse = hi * si * nsample \quad (6.2)$$

here  $hi$  is hardware integration and  $si$  is software integration. Thus the scan rate can be calculated as follows,

$$ScanRate = \frac{npulse}{pulserate} \quad (6.3)$$

$$Totalscan = Scanrate * data - collecton - time \quad (6.4)$$

From the above expressions we can see that increasing the scan Window Size or Integration size increases the scan time and thus reduces the Scan Rate. However increasing the Step Size increases the Scan Rate. The specifications for PulseOn P220 is given in Table 6.1.

Table 6.1. PulseOn 220 Specifications

Parameter	PulseOn set up
Center freq	4.3 GHz
Bandwidth (percentile)	53.4
10 dB Bandwidth	2.3 GHz
Pulse type	Gaussian monocycle
pulse duration	4.3 ps
resolution	6.5 cm
pulse repetition frequency	9.6 MHz
EIRP	-12.8 dBm

## 6.2 Four Step Method

In this chapter, we use two information theoretic criterion entropy and relative entropy to detect human in indoor environment. In our previous study, we have successfully applied our algorithm in sensing through foliage for metallic target, in UWB Radar Sensor Network. The current scenario is totally different from our previous study. Here the target is human, the environment is indoor and the human is behind three different kind of wall; gypsum wall, brick wall and wooden door. Also here we have single radar collecting multiple scans in contrast with Radar Sensor Network.

We have already define entropy and relative entropy or KL divergence in (2.1) and in (3.8) respectively. Since entropy measure the randomness in Chapter 2 for detecting the target with maximum entropy method, we assume the targeted region is more random and has more uniform distribution than the clutter. However, we need to do the preprocessing to make the detection more effective. For preprocessing, we generally use the methods of estimation. Two mostly used method of non recursive estimation are weighted average and least square estimation (LSE)[35]. In this study we use relative entropy or K-L divergence based weighted average as fusion technique

and the foundation of this is in information theory. In Chapter 3, it is shown that the KL divergence can detect the change in histogram quickly and can be used for the weighting. Breathing motion in human will cause periodic changes in the received signal at a distance where target is located. We can apply our algorithm in several steps.

*Step1:*In order to reduce the clutter in the environment we need to take the difference in multiple scans. For that purpose we create two  $N \times M$  matrix “A1” and “A2” with and without target, which is constructed using  $M = 100$  scans, each of length  $N = 6400$ ,

$$A = \begin{pmatrix} scan1 & scan2 & scan3 & \dots & scanM \\ sample1 & sample1 & sample1 & \dots & sample1 \\ sample2 & sample2 & sample2 & \dots & sample2 \\ \vdots & \vdots & \vdots & \vdots & \vdots \\ sampleN & sampleN & sampleN & \dots & sampleN \end{pmatrix}$$

Two other matrix C1 and C2 can be constructed, where difference is taken between successive columns of the matrix A1 and A2, which captures changes from one scan to another and helps to suppress the static clutter signal. The matrix construction for the difference matrix C is shown below:

$$C = \begin{pmatrix} scan1 - scan2 & scan2 - scan3 & scan3 - scan4 & \dots & scan(M - 1) - scan(M) \\ sample1 & sample1 & sample1 & \dots & sample1 \\ sample2 & sample2 & sample2 & \dots & sample2 \\ \vdots & \vdots & \vdots & \vdots & \vdots \\ sampleN & sampleN & sampleN & \dots & sampleN \end{pmatrix}$$

*Step2:*We transpose that difference matrix C and construct two  $C_{inv}$  matrices for with target and without target.

*Step 3:* We applied relative entropy based weighting on each of this row. Now the matrix  $C_{inv}$  is a  $(M - 1) \times N$  matrix. Now each row corresponds to the number of scans and weight is applied on each row based on their KL divergence.  $s_i$  be the pmf of the quantized echoes of the  $i_{th}$  row of the  $C_{inv}$  matrix and  $b_i$  be pmf related with the quantized echoes of the  $i_{th}$  row of the  $C_{inv}$  without target then the K-L divergence based weighting,  $w_i$  for each row of can be applied by the following,

$$w_i = \frac{D_i}{\sum_{i=1}^{M-1} D_i} \quad (6.5)$$

and

$$D_i = D_{KL}(s_i || b_i) \quad (6.6)$$

where  $D_{KL}$  is the divergence calculated from the (3.8). The returned echoes are quantized and pmf are calculated before applying (6.5).

*Step 4:* After this each row is multiplied by the corresponding weight, we take the summation of the matrix  $C_{inv}$ . Then we applied our second step and applied entropy based detection with 16 level of quantization. Now we can calculate the entropy for fixed number of window.

### 6.3 Simulation Results

After configuring the radio as shown in Table 6.1, the radar starts scanning. Fig. 6.4 shows the monostatic radar analysis tool. The hardware integration was 512 and software integration was 2. Pulse repetition frequency was 9.6 MHz, step size was 1 bin and window size was 10 feet. Fig. 6.5 shows one single raw scan. For each measurement set, scans were acquired for duration of around 1 minute. The number of scans acquired depends on the scan rate which in turn depends on the waveform scan resolution, the window size, and the Integration size.

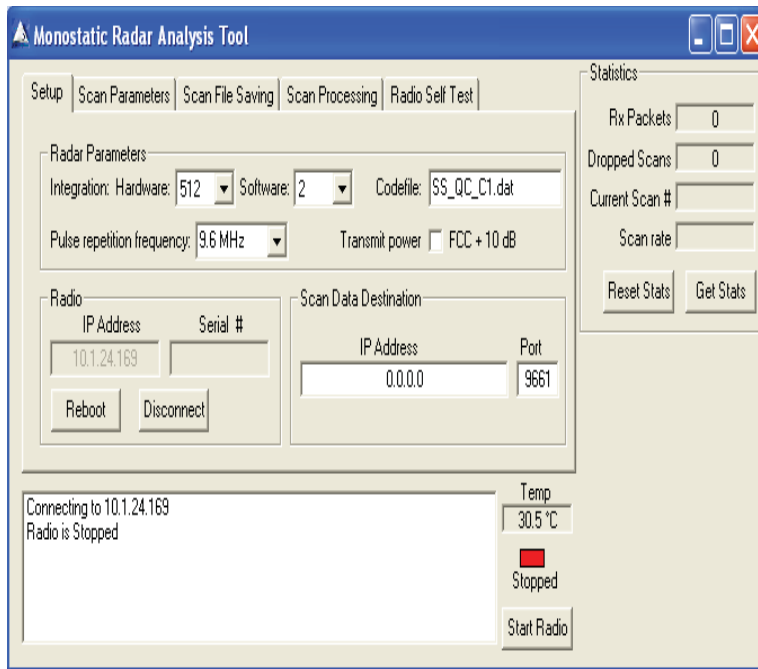


Figure 6.4. MSR analysis tool setup tab.

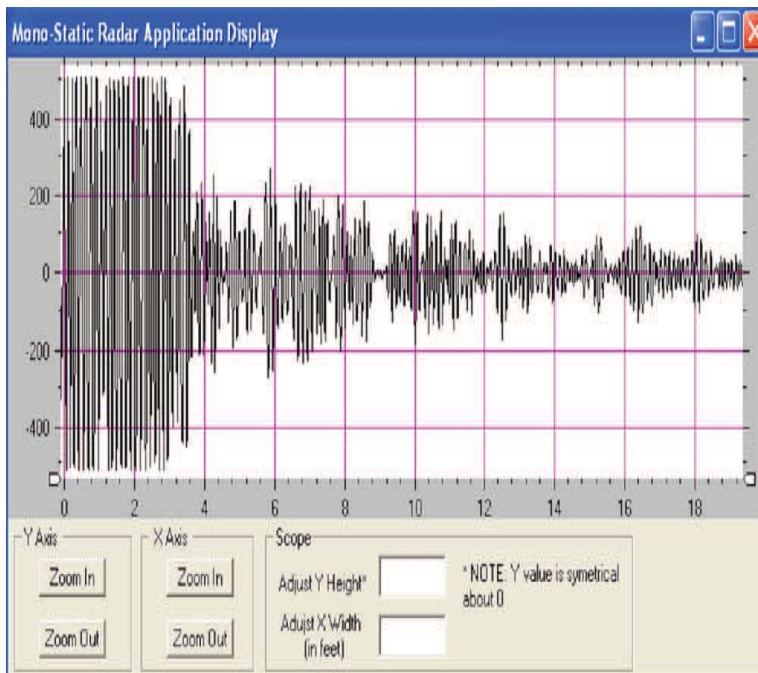


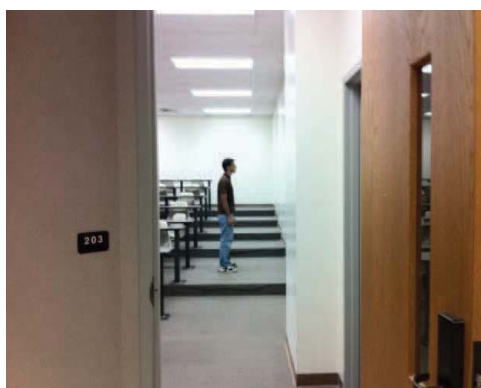
Figure 6.5. Window displaying a single raw scan.

In this study we considered the measurement taken at three different positions: behind gypsum wall, behind brick wall and behind wooden door. Fig. 6.6 shows the location of the radar and human target on different sides of a 1 ft thick Gypsum partition wall. Person is at a distance of 6.5 ft from the radar on the other side of the wall and the height of the antennas from ground is 3 feet 4 inches. Fig. 6.7 shows the location of the radar in one sides of a 12 cm Brick wall. Person is standing at a distance of 8 from the radar on the other side of the door. Fig. 6.8 shows the location of the radar and Human target on different sides of a 4 cm wooden door. Person is standing at a distance of 7.5 feet from the radar on the other side of the door.

Fig. 6.9 shows the entropy based target detection when human is behind the gypsum wall. In this case matrix A is constructed using 100 scans captured at scan rate of 0.6827 scans/sec for total time duration of 68 sec. Total number of sample was 6400. We applied our algorithm and calculated entropy for 128 different window with 50 size of samples on each. Human was detected around sample 4200 as shown in Fig. 6.9.

Fig. 6.10 shows the entropy based target detection when human is behind the brick wall. After applying our algorithm we can see in Fig. 6.10 that there is a pick around the 5120 sample. Since human was located about 8 feet away from the wall, it was expected in the range.

Fig. 6.11 shows the entropy based target detection when human is behind the wooden door. For this particular case human was around sample 4800. In Fig. 6.11, we can see a pick around sample 4800, however that is not the highest point. In that case this algorithm is not suitable for wooden door.



(a)



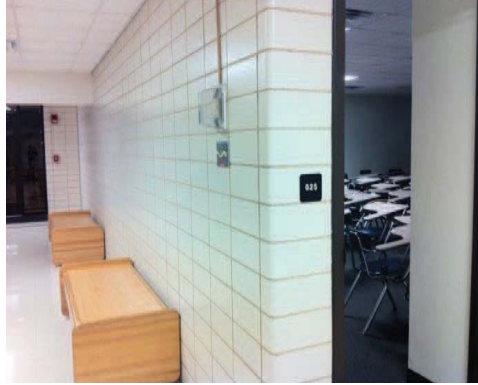
(b)

Figure 6.6. Location of the Human target and UWB radar on different sides of a 1 ft thick Gypsum partition wall (a) human target and (b) UWB radar.

#### 6.4 Conclusions

Detection of human hidden behind the walls is a challenging task. In this study, we propose to use information theory to UWB radar to detect human target. We applied relative entropy based preprocessing and entropy based detection. Results show that with this novel approach, accurate detection can be achieved when human is hidden behind the gypsum wall. This method could also detect human hidden behind the brick wall. However this method did not work for detecting human behind the wooden door.





(a)



(b)

Figure 6.7. Location of the brick wall and UWB radar on different sides brick wall (a) brick wall and (b) UWB radar.

An important parameter that affects through-wall sensing is the Wall Dielectric Constant. The frequencies used are less than 960MHz or between 1.99GHz to 10.6 GHz as per the FCC regulations. Metal walls are fully reflective and thus detection through such walls is impossible using radar. However, most wall materials in use are wood, concrete, glass, and stone. Although these are low loss dielectric materials, there may be situations where the transmission loss through walls may be high at specific frequencies or frequency bands. Examples include wave propagation through concrete walls containing reinforced bars or moist concrete . The transmission of electromagnetic waves through the wall causes decrease in velocity due to the



(a)



(b)

Figure 6.8. Location of the Human target and UWB radar on different sides wooden door (a)UWB radar and (b) Human Target.

dielectric constant of the wall. Higher the dielectric constant and more the thickness of the wall, larger will be the delay. This results in the targets behind the wall to appear farther away than they actually are [87]. To overcome the attenuation in frequency bands, wide-band signal ensures that at least some of the energy will get through the wall and permit the processing of the target-reflected signals.

In future, we can acquire data on multi position of the radar and apply our method in Radar Sensor Network. We can also consider the posture of the human and conduct study for various position of human such as standing, sitting or facing the wall.

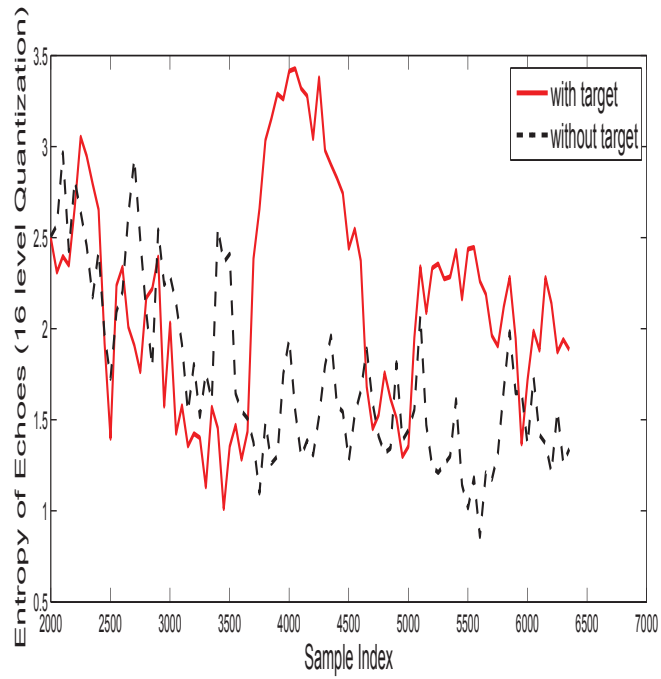


Figure 6.9. Human target detection using two step information fusion. Target is detected around sample 4200.

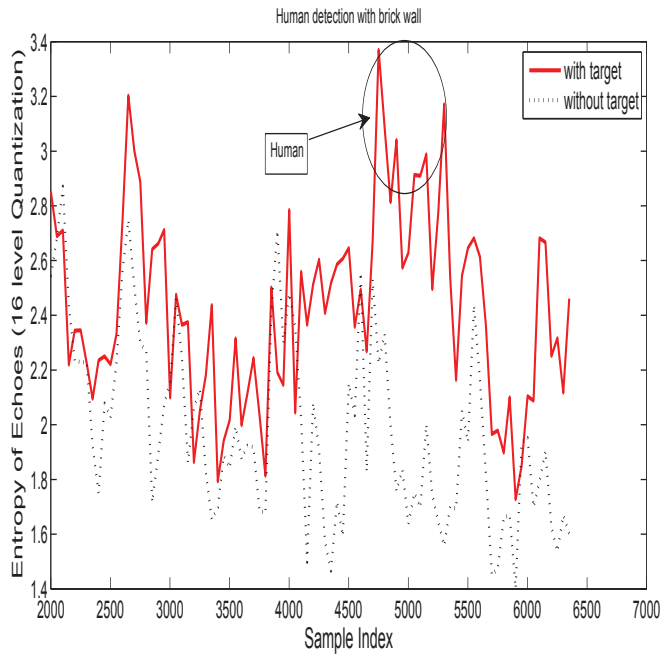


Figure 6.10. Human target detection using two step information fusion. Target is detected around sample 5120 .

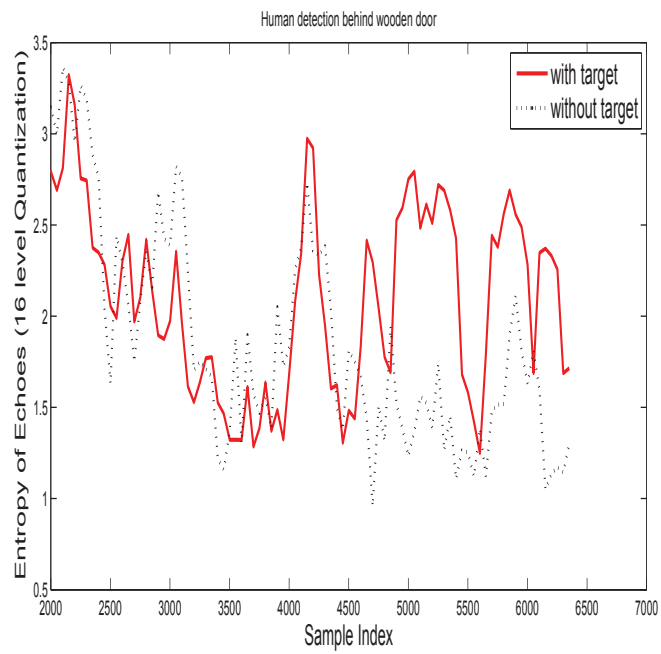


Figure 6.11. Human target detection using two step information fusion. Target is behind door and expected around sample 4800.

## Chapter 7

### Throughput Optimization of Cognitive Radio Using Sensor Network and Power Allocation

Federal Communications Commission report has shown that most of the spectrum that is statically assigned to licensed users is heavily underutilized [62]. Cognitive Radio (CR) solves the scarcity of spectrum for wireless communication by opportunistically using the under-utilized spectrum. A cognitive radio can sense the spectrum of the licensed user also known as primary user (PU) and identify the under-utilized spectrum known as white space or spectrum hole. Thus the reliability of the sensing scheme is crucial. However a single sensor is limited by path loss, shadowing and fading. In order to enhance the reliability of the detection a wireless sensor network (WSN), not necessarily embedded in cognitive receiver can be used [63]. In this WSN, single sensor will make local decision and forward the decision to the fusion centre (FC). This sensor network will combat the fading through space diversity and will cover a large geographical area. There will be at least another sensor to detect the primary user which is far from a secondary user. Hence the two performance metrics of the sensing: 1) probability of detection and 2) probability of false alarm can be improved. The overall objective of CR is to increase the spectral efficiency and keeping the interference under limit. However, as the sensing time is increased, it can guarantee higher detection probability but the overall throughput goes down. The traditional optimization of throughput is achieved by water-filling power allocation. But water filling in CR is complex due to the added constraints of

interference and false alarm. So we have three different metrics, we need to consider, sensing time, power and interference.

## 7.1 System Model

In this chapter, we consider a communication system based on OFDM. Orthogonality of the OFDM system allows high spectral efficiency and guarantees less cross talk between the sub-carriers. It simplifies the equalizer and it does not need guard interval between the carriers. The whole bandwidth is divided into  $N$  no of sub-carriers and each subcarrier is having the bandwidth as  $\Delta f$ . In frequency domain we consider the unoccupied bands are located on each side of PU as shown in Fig. 7.1. Secondary users (SU) are sparsely located and there exist a WSN to assist the secondary transmitter in spectrum sensing. Each nodes of the WSN are energy detectors that will locally made decision based on the local observation and pass the decision to the Fusion centre for the decision fusion. Fusion centre can apply different decision fusion algorithm such as OR logic, majority rule or log likelihood to make the final decision. Then after the necessary spectrum allocation, power control will be applied for throughput optimization. We assume there are three instantaneous fading gains that are known to the transmitter of the SU. The fading gain between SU transmitter and SU's receiver for the  $n_{th}$  carrier is denoted as  $h_n^{ss}$ , the gain between the SU's transmitter and the  $m_{th}$  PU receiver is denoted as  $h_m^{sp}$  and the gain between the  $m_{th}$  PU's transmitter and SU's receiver denoted as  $h_m^{ps}$ . It is assumed that each sub-carrier transmits in Raleigh fading channel and the channels are estimated by channel estimation mechanism before the transmission. The system model is shown in Fig. 7.2.

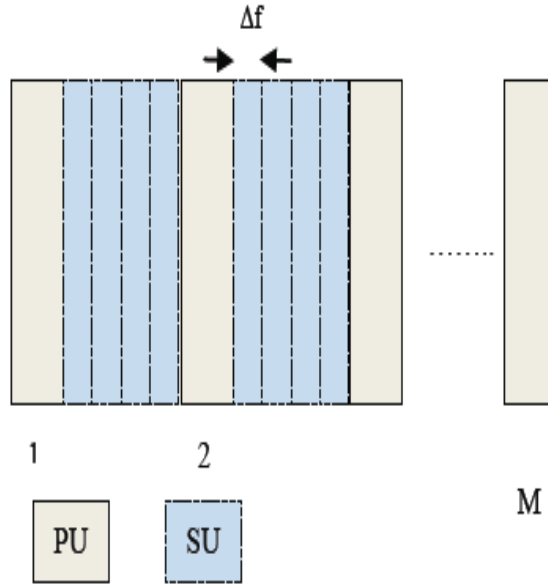


Figure 7.1. Frequency domain distribution of primary and secondary user.

## 7.2 WSN Based Spectrum Sensing

In this chapter, the wireless sensor network is responsible for sensing the spectrum and allocating the sub-carriers to the secondary system. During the sensing the CRs are not transmitting. The sensors in the WSN are energy detectors.

The binary hypothesis testing for spectrum detection at a certain subcarrier  $n$  is given as follows:

$$\begin{aligned}
 R_n = Z_n & : H_0 & \text{PU absent} \\
 R_n = \zeta_n H_n + Z_n & : H_1 & \text{PU present}
 \end{aligned} \tag{7.1}$$

where  $\zeta_n$  is the received signal of the  $n^{th}$  subcarrier at the  $i^{th}$  sensor and  $R_n$  is the signal transmitted by the PU at the  $n^{th}$  subcarrier and the  $Z_n$  is the normally

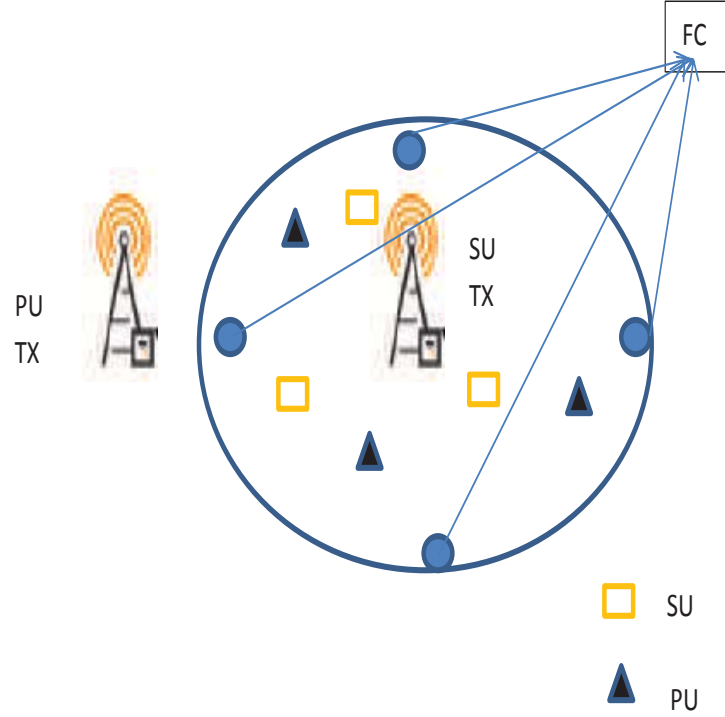


Figure 7.2. System model on wireless sensor network (WSN) aided Cognitive Radio Network. Each individual sensor working as energy detector sends the local decision to the Fusion centre (FC).

distributed noise with zero mean and  $\sigma_n^2$  is the variance. For each subcarrier  $L$  no of samples are being collected and the test statistics of the energy detector is given by:

$$E_n = \frac{1}{L} \sum_{l=1}^L |R_n|^2 \quad (7.2)$$

where  $E_n$  follow chi-square distribution with  $2L$  degrees of freedom, if the signal is complex or  $L$  degrees of freedom if it is non-complex. Based on the probability distribution function of the test statistics, the detection probability,  $P_d^i$  and the false alarm  $P_{fa}^i$ , of the  $i^{th}$  sensor can be approximated by [76],

$$P_d^i = Pr\{E_n \geq \eta_i | H_1\} = Q[\{\eta_i - \gamma_i - 1\} \sqrt{\frac{L}{2\gamma_i + 1}}] \quad (7.3)$$

$$P_{fa}^i = Pr\{E_n \geq \eta_i | H_0\} = Q[\{\eta_i - 1\} \sqrt{L}] \quad (7.4)$$



where  $\eta_i$  is the detection threshold and  $\gamma_i$  is the SNR for the  $i_{th}$  sensor. Now, we can replace the L values as the multiplication of sensing time with sampling frequency. Then the sensing time  $\tau$  can be expressed in term of the of the targeted detection probability,  $P_d^{tar}$  and targeted false alarm probability  $P_{fa}^{tar}$ . The expressions are,

$$\tau = \frac{1}{f_s} \left\{ \frac{Q^{-1}(P_{fa}^{tar})}{\eta_i - 1} \right\}^2 \quad (7.5)$$

$$\tau = \frac{2\gamma_i + 1}{f_s} \left\{ \frac{Q^{-1}(P_d^{tar})}{\eta_i - \gamma_i - 1} \right\}^2 \quad (7.6)$$

where  $\tau$  is the sensing time and  $f_s$  is the sampling frequency. The local decision based on the single sensor will need a low bandwidth control channel and will be passed to the FC. We will discuss three different method of decision fusion in the FC.

### 7.2.1 Decision Fusion by OR Logic

It is already been shown [70] that the OR based decision for the decision fusion at the fusion center can detect the spectrum hole. If the sensor network has D no sensors the OR based decision can be applied in the fusion center as follows:

$$P_D = 1 - \prod_{i=1}^D (1 - P_d^i) \quad (7.7)$$

$$P_{FA} = 1 - \prod_{i=1}^D (1 - P_{fa}^i) \quad (7.8)$$

However this is always not the best method as shown in literature.

### 7.2.2 Majority rule

In this rule the local sensing is fused in one bit binary decision rule based on the following,

$$q_i = \left\{ \begin{array}{ll} 1, & E_n \geq \eta_i \\ 0, & E_n < \eta_i \end{array} \right\} \quad (7.9)$$

Now the one bit decision will be fused together so that if more than half of the sensors are voting for PU presence the FC will make the decision as PU present. The fusion decision can be shown by the following,

$$Y = \sum_{i=1}^D q_i = \begin{cases} \geq [\frac{D}{2}], & H_1 \\ < [\frac{D}{2}] & H_0 \end{cases} \quad (7.10)$$

Now if we assume all the sensors are employing the same detection threshold then the detection probability and the probability of the false alarm can be given by,

$$P_D = Pr\{H_1|H_1\} = \sum_{i=[\frac{D}{2}]^+}^D \binom{D}{i} P_d^i (1 - P_d)^{D-i} \quad (7.11)$$

$$P_{FA} = Pr\{H_1|H_0\} = \sum_{i=[\frac{D}{2}]^+}^D \binom{D}{i} P_{fa}^i (1 - P_{fa})^{D-i} \quad (7.12)$$

### 7.2.3 Log Likelihood Ratio

In this rule we can assume that the single bit decision  $q_i$  is kept in a decision vector  $\bar{q} = (q_1, q_2, \dots, q_D)^T$ . The decision at the fusion centre will be taken by the following log likelihood ratio [70],

$$L(\bar{q}) = \frac{Pr\{\bar{q} | H_1\}}{Pr\{\bar{q} | H_0\}} = \prod_{i=1}^D \frac{Pr\{q_i | H_1\}}{Pr\{q_i | H_0\}} \stackrel{H_1}{\leq}_{H_0} \zeta \quad (7.13)$$

Also it is defined that,

$$P(q_i|H_1) = \begin{cases} P_d^i & q_i = 1 \\ 1 - P_d^i & q_i = 0 \end{cases} \quad (7.14)$$

Here if  $D=2$ , then  $q$  will have four different values. If  $q_4$  is  $[1, 1]^T$ ,  $q_3$  is  $[1, 0]^T$ ,  $q_2$  is  $[0, 1]^T$  and  $q_1$  is  $[0, 0]^T$  then,

$$L(\bar{q}) = \begin{cases} \frac{P_d^1 P_d^2}{P_{fa}^1 P_{fa}^2}, & q_4 \\ \frac{P_d^1 (1 - P_d^2)}{P_{fa}^1 (1 - P_{fa}^2)}, & q_3 \\ \frac{1 - P_d^1 P_d^2}{(1 - P_{fa}^1) P_{fa}^2}, & q_2 \\ \frac{(1 - P_d^1)(1 - P_d^2)}{(1 - P_{fa}^1)(1 - P_{fa}^2)}, & q_1 \end{cases} \quad (7.15)$$

However this might take lots of processing time.

### 7.3 Throughput Analysis with Sensing Time and Interference Constraint

In this section, we formulate the throughput as a function of the sensing time and power allocation. Our objective is to optimize the throughput of the CR, while taking the interference to the PU as one of the major consideration. The CR user tries to find the spectrum holes that are not being used by the PU. When the energy detectors are sensing the spectrum, four different scenarios can happen. If we consider the same hypothesis as shown in (7.1), the scenarios can be illustrated as follows:

$$\begin{aligned} S1 &= Pr\{H_0|H_0\} \\ S2 &= Pr\{H_0|H_1\} \\ S3 &= Pr\{H_1|H_1\} \\ S4 &= Pr\{H_1|H_0\} \end{aligned} \quad (7.16)$$

If we want to further illustrate, S1 and S3 are the correct decisions. Here only S1 is the desirable correct decision, in CR's point of view. S2 represent the scenario when the PU is active however the decision of the sensor network is wrong. This missed detection will be the major reason for the interference. Scenario 4 is another incorrect decision that will generate the false alarm, further degrading the spectrum usage. Two kinds of interferences are introduced in OFDM system. One is introduced by

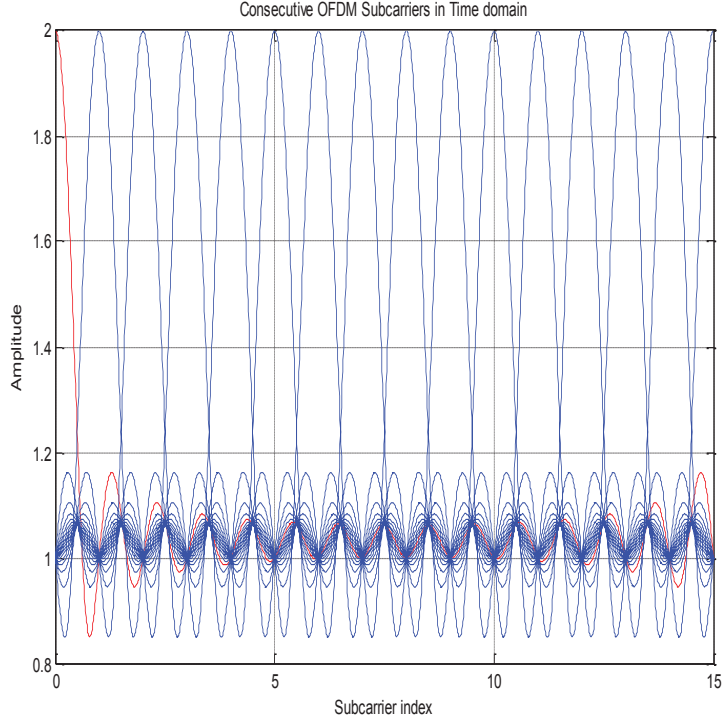


Figure 7.3. Consecutive orthogonal sub-carriers in time domain.

the SU to the PU which is due to the situation S2. The other is the interference introduced by the primary user to the  $n_{th}$  subcarrier of the secondary user. Both of them depend on the spectral distance and transmit power. The power density spectrum assuming the nyquist pulse can be written as [74],

$$\Phi_n(f) = P_n T_s \left( \frac{\sin \pi f T_s}{\pi f T_s} \right)^2 \quad (7.17)$$

where  $T_s$  is the symbol duration and  $P_n$  is the transmit power allocated to the  $n^{th}$  subcarrier. Fig. 7.3 shows the orthogonal subcarrier generated in OFDM based system. The interference that will be introduced to the PU is the integration of the Power density spectrum across the PU band. This can be expressed as,

$$I_{SU}^{(n)}(d_{nm}, P_n) = |h_n^{sp}|^2 P_n T_s \int_{d_{nm}-B_M/2}^{d_{nm}+B_M/2} \left( \frac{\sin \pi f T_s}{\pi f T_s} \right)^2 df \quad (7.18)$$

where  $d_{nm}$  represents the distance in frequency between the  $n_{th}$  subcarrier and  $m_{th}$  PU band and  $BM$  is the band width of the  $m_{th}$  primary. The interference introduced by the  $m_{th}$  PU to the  $n_{th}$  subcarrier, will be the integration of the power density spectrum of the PU signal across the  $n_{th}$  subcarrier can be written as,

$$I_{PU} = |h_n^{sp}|^2 P_n T_s \int_{d_{nm}-\Delta F/2}^{d_{nm}+\Delta F/2} E\{I_N(\omega)\} d\omega, \quad (7.19)$$

where,  $EIN(w)$  can be written as,

$$EI_N(\omega) = \frac{1}{2\pi s} \int_{-\pi}^{\pi} \Phi PU(e^{j\omega}) \left( \frac{\sin(\omega - \psi)s/2}{\sin(\omega - \psi)s/2} \right)^2 d\omega \quad (7.20)$$

is the power density spectrum of the PU after S FFT process. Here  $w$  represents the frequency normalized to the sampling frequency.

Now if we assume the interference between the secondary users is negligible due to the orthogonality of the OFDM system, throughput of the CR network in  $N$  no of carrier can be expressed as,

$$C = \left[ \sum_{n=1}^N \left( \frac{T-\tau}{T} \right) \Delta f Pr\{H_0\} (1 - P_{FA}^n) \log_2 \left( 1 + \frac{P_n |h_n^{ss}|^2}{\sigma_n^2} \right) \right] + \left[ \sum_{n=1}^N \left( \frac{T-\tau}{T} \right) \Delta f Pr\{H_1\} (1 - P_D^n) \log_2 \left( 1 + \frac{P_n |h_n^{ss}|^2}{I_{PU} + \sigma_n^2} \right) \right] \quad (7.21)$$

where  $T$  is the total frame time and  $I_{PU}$  can be calculated from (7.19),  $P_{fa}^n$  and  $P_D^n$  is the decision feed back from the FC for the  $n_{th}$  carrier and they are function of sensing time,  $\tau$ . However we know that in the design of the CR, the interference that is introduced by the secondary user to the PU has a threshold that we need to maintain.

Our objective is to optimize the throughput considering all the constraints. So we can do the problem formulation of the optimization as follows,

$$\begin{aligned} & \max_{P_n, \tau} C \\ & s.t. \sum_{m=1}^M \sum_{n=1}^N I_{SU}^{(n)}(d_{nm}, P_n) \leq I_{th} \end{aligned} \quad (7.22)$$

$$P_n \geq 0 \quad \forall n = 1, 2, \dots, N \quad (7.23)$$

$$P_{FA}(\tau) = \sum_{i=\frac{D}{2}}^D \binom{D}{i} P_{fa}^i (1 - P_{fa}^i)^{D-i} \leq \alpha \quad (7.24)$$

$$\sum_{n=1}^N P_n \leq P_T \quad (7.25)$$

This problem is non convex and the constraint in (7.24) is non convex too. Thus finding the optimal solution is difficult. In order to find the suboptimal solution we can divide the problem in two sub-problems and find the optimal power and sensing time.

## 7.4 Power Control and Sensing Time Design

### 7.4.1 Power Allocation

In order to allocate the power to the user by relaxing the sensing time constraint, we can easily apply the waterfilling algorithm with interference constraint. Then  $P_n$  optimal can be written as [74]

$$P_n^* = \max \left\{ 0, \frac{1}{\lambda \sum_{m=1}^M Q_n^{(m)}} - \frac{\sigma^2 + I_{PU}}{|h_{nSS}|^2} \right\} \quad (7.26)$$

where  $\lambda$  is the Lagrange multiplier for the inequality, where  $Q_{nm}$  can be expressed as,

$$Q_n^{(m)} = |h_m^{sp}|^2 T_s \int_{d_{nm}-B_M/2}^{d_{nm}+B_M/2} \left( \frac{\sin \pi f T_s}{\pi f T_s} \right)^2 df \quad (7.27)$$

From (7.26) we can conclude

$$\sum_{m=1}^M \sum_{n=1}^N Q_n^{(m)} \max \left\{ 0, \frac{1}{\lambda \sum_{m=1}^M Q_n^{(m)}} - \frac{\sigma^2 + I_{PU}}{|h_{nSS}|^2} \right\} \leq I_{th} \quad (7.28)$$

The objective of water filling is to achieve maximum data rate while exploiting the varying channel gain. The channel with better channel gain is allocated higher power so that better data rate is achieved. For the Cognitive radio the optimized power allocation is achieved by (7.26). Since the calculation of  $\lambda$  value is quiet complicated and required several steps, we try to avoid this optimal solution. If we ignore the second term in (7.26) the power is inversely proportional to the  $Q_n$  which depends on the spectral distance between primary and secondary. Then we can apply distant dependent modified water filling (DDMWF) where the initial water line is achieved by allocating the power in step method.

We consider five sub-carriers where the middle one will be given the highest power considering that it is furthest from the primary. Two of the subcarrier will be given the medium step power and two of them will be given the lowest power as they are closest. The total power is still remain constant and depend on the given SNR. Then we repeat this allocation for three different blocks and total fifteen sub-carriers are considered on both sides of the PU. Let  $P_T$  denotes total power, sc is no of subcarrier per block and l is the no of block, for our particular case we divide the steps of the waterline, by the following: 1. If we have sc=5 per block, then three strong sub-carriers in three different block has initial power allocation as

$$P_i = \frac{P_t}{3 \times l} \quad (7.29)$$

2. If we have sc=5, then six of the sub-carriers can have the initial power as

$$P_i = \frac{P_t}{6 \times l} \quad (7.30)$$

3. If we have  $sc=5$ , six of the sub-carriers can be given the initial power as,

$$P_i = \frac{P_t}{9 \times l} \quad (7.31)$$

After the initial power allocation the water line will be updated and sub-optimal solution will be found by the iterative process. Finally the capacity of the secondary user is measured. We made the assumption that since the sub-carrier that is spectrally far from the PU, has been given the highest power it will cause less interference and the interference threshold will not exceed the limit. However, we need to check the interference threshold time to time. If it exceeds the given threshold then the waterline has to be updated with a factor.

#### 7.4.2 Sensing Time Design

As already mentioned in section 7.4, power and sensing time cannot be jointly determined to maximize the throughput. Thus we develop another sub-problem of optimizing the sensing time while keeping the  $P_{fa}$  minimum. It is interesting to note the developed expression for interference is not depending on the sensing time as well, however the portion of the throughput that is due to the missed detection is multiplied by the term  $(1 - P_d)$  is neglected. The optimization problem becomes,

$$\max_{\tau} C = \left[ \sum_{n=1}^N \left( \frac{T - \tau}{T} \right) \Delta f (1 - P_{FA}^n) \log_2 \left( 1 + \frac{P_n |h_n^{ss}|^2}{\sigma_n^2} \right) \right]$$

$$P_{FA}(\tau) = \sum_{i=\frac{D}{2}}^D \binom{D}{i} P_{fa}^i (1 - P_{fa}^i)^{D-i} \leq \alpha \quad (7.32)$$

where  $\alpha$  is the  $P_{fa}^{tar}$ . The constraint here is multiplication of two Q functions we apply the majority rule in the fusion center. As we know that Q function is constantly decreasing we change the non convex problem in a linear problem. A careful analysis can be made while choosing the maximum and minimum value of the  $\tau$ . As already



shown in section 3.3 that  $\tau$  can be easily expressed in terms of the  $P_d^{tar}$  and  $P_{fa}^{tar}$  and the max and the min value of the can  $\tau$  be found following expression:

$$\tau_{max} = \frac{1}{f_s} \left\{ \frac{Q^{-1}(P_{fa}^{tar})}{\eta_i - 1} \right\}^2 \quad (7.33)$$

$$\tau_{min} = \frac{2\gamma_i + 1}{f_s} \left\{ \frac{Q^{-1}(P_d^{tar})}{\eta_i - \gamma_i - 1} \right\}^2 \quad (7.34)$$

## 7.5 Simulation Results

In simulation we consider the number of sub-carriers N is 15. The channel is considered as Raleigh fading channel. SNR is varied from -20 to 30 dB. The frame time T is 100 ms.

In Fig. 7.4, we plot, probability of detection of three different sensing schemes. Number of sensor, for OR and majority rule fusion schemes, are taken as 10. Based on the simulation, clearly the sensor network based schemes show better performance than the single sensor based scheme. The probability of detection increases as a function of SNR. Fig. 7.4 shows that OR based fusion rule has higher probability of detection than the majority rule for low SNR.

Fig. 7.5 shows performances of the three different power allocation schemes, equal power allocation, water filling traditional and DDMWF while keeping the sensing time constant. The initial water line is set by the (7.29)-(7.31). Clearly DDMWF out performs the traditional water-filling as well as the equal power allocation. This result proved the suboptimal power allocation in CR based OFDM system is a good method to increase the data rate of the spectrum and the cognitive radio user as a whole.

In Fig. 7.6 with a constant SNR of 10 dB, we plot the throughput of the cognitive radio as a function of the sensing time. We calculate the optimal power for

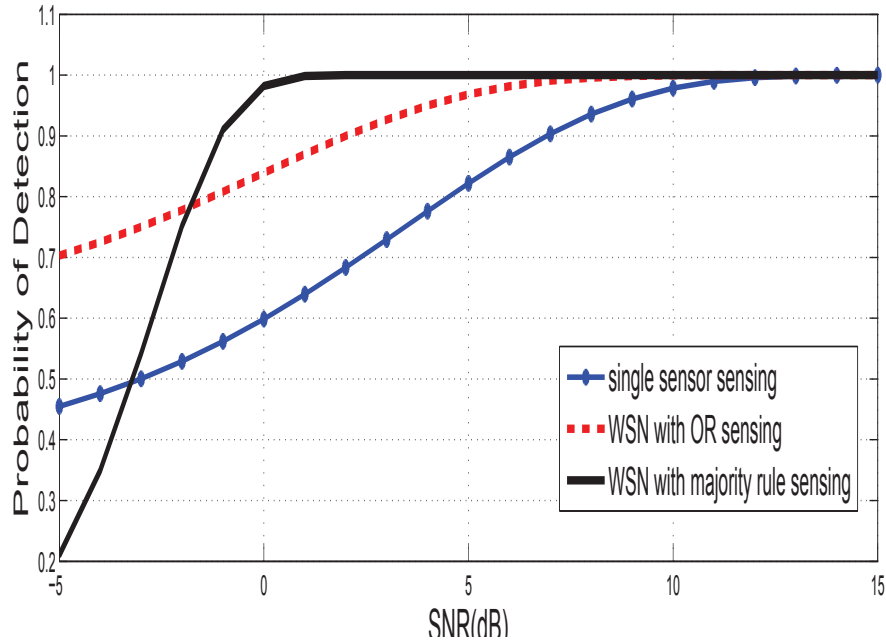


Figure 7.4. Probability of detection versus SNR for three different sensing schemes.

three different power allocation schemes. Clearly there exist a optimal sensing time that maximizes the throughput.

In Fig. 7.7 three dimensional representation of throughput is shown. Total throughput is plotted as a function of sensing time and SNR. This clarifies that we can maximize the throughput by power control and then design an optimal sensing time. For this figure we use DDMWF as our power allocation scheme.

## 7.6 Conclusion

In this study we consider an interweaved Cognitive radio network, which can sense the spectrum and communicate in the white space of the spectrum while keeping the interference due to the missed detection under limit. Throughput optimization while keeping the interference under the threshold is one of the most challenging issues in Cognitive Radio network. In this chapter, we combined the sensing schemes

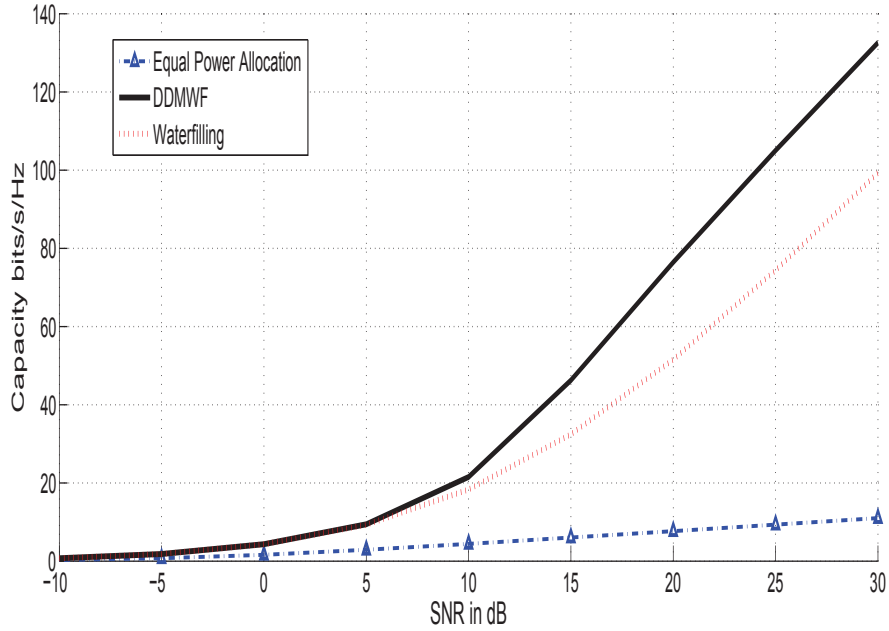


Figure 7.5. Capacity versus SNR for three different power allocation schemes.

along with sub optimal power allocation. We designed the optimal sensing time while initially applying the DDMWF scheme for power allocation. Results show that this method can greatly improve the overall throughput. We assume the threshold to be a constant, in this chapter. In future we shall apply this method where threshold can be dynamic and the sensors will apply the cognition from the learned environment. In this work we only apply the technology for the interweaved Cognitive network where communication for secondary is based on the white space, we can also extend this work for underlay cognitive network, where both primary and the secondary can coexist in the same frequency band. We can also extend this work for a macro femto network where the femtocell can work as a secondary device.

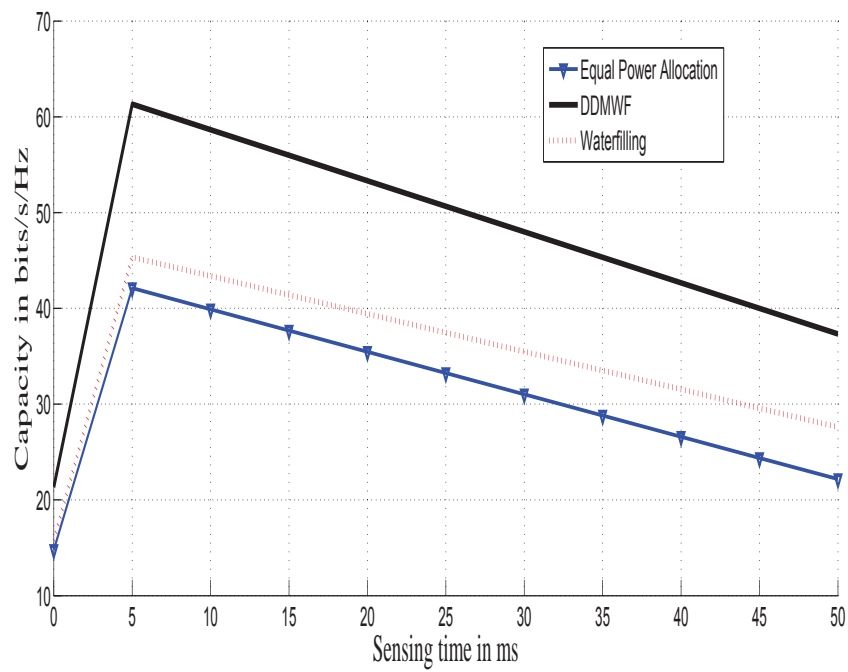


Figure 7.6. Throughput versus sensing time for three different power allocation schemes.

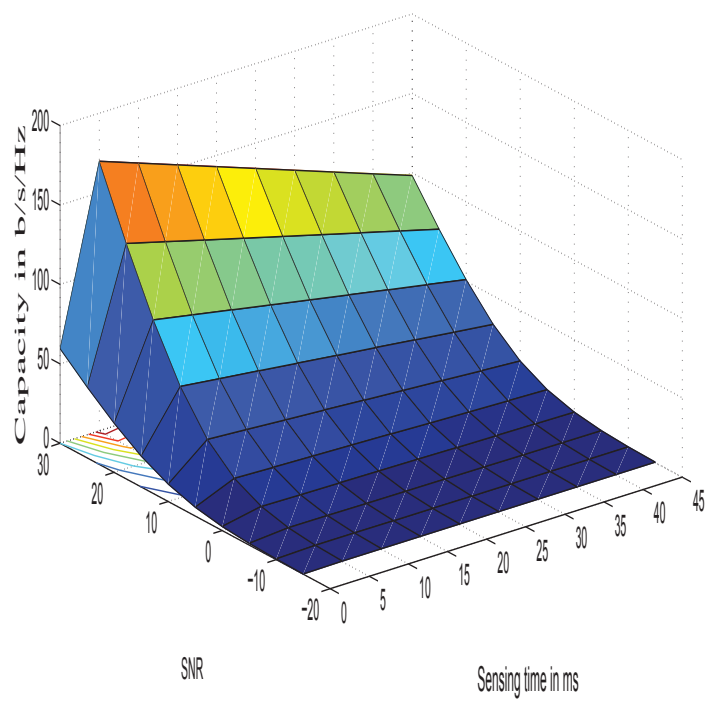


Figure 7.7. Three dimensional representation of throughput as a function of SNR and sensing time.

## Chapter 8

### Conclusion and Future Works

This chapter concludes the whole dissertation. It begins with a summary of the dissertation results and contributions, which will follow a discussion of future research directions for further investigation.

#### 8.1 Summary

This dissertation has focused on but not limited to Target detection using information theory and capacity analysis of the cognitive radio using sensor network. The contributions of this dissertation are:

- *Information Theory Based Target Detection* In this chapter we propose a new scheme for target detection using information theory. Dynamic nature of the foliage imposes lot of challenges to detect target, without statistical information. To enhance the performance of the poor signal we apply information theory to UWB radar. This work is based on sense through foliage data collected by AFOSR. First we analyzed the data and came into conclusion that, targeted region is more random than the region without target. Two information theory based metrics, entropy and mutual information are proposed to detect the target. For entropy based detection we proved that unless there is unique situation where each window has uniform distribution then entropy based target detection is possible using Maximum entropy method. The proposed algorithm is fundamentally different from the conventional wisdom, which assumes that we will have minimum information about the targeted region. It is nonconven-

tional that from data analysis we found uniform distribution of the targeted region, this will give higher entropy and lower conditional entropy, and will give higher mutual information in the targeted region. We also applied several quantization levels on the data for entropy based method and found best result in 32 level of quantization. Results show that our approach can work successfully for good signal of real world data. However entropy is more efficient in target detection than mutual information based detection [88] [89].

- *Radar Sensor Network and KL Based Preprocessing* When the pulse to pulse variability is high and the amplitude of the signal is low, then single radar is unable to detect the target. In order to deal with performance degradation, Radar sensor network (RSN) based detection with multi-step information fusion is proposed. Since two radars will not experience deep fading at the same time, RSN provides better signal quality when they are spaced sufficiently far apart. Also the collections of the reading from different position of the radar were not taken at the same time. This guarantees the time as well as spatial diversity in the proposed RSN. Information collected by individual radars are quantized and sent to fusion center to combine by using KL based weighting. Results show that our algorithm does provides huge improvement while it is compared with the existing method of power based weighting. This method can be an excellent alternative to signal processing based methods as it is computationally efficient and it has less processing load. We also calculated the upper bound of the false alarm probability for the clutter and target distribution using another information theoretic criterion known as method of types [90] [91].

- *Decision Fusion Based on Dempster Shafer's Theory and Bayesian Network*  
In this chapter, we propose three different schemes Dempster and Shafer (D-

S) theory of evidence, proportional conflict redistribution rule 5(PCR) and Bayesian network for decision fusion. In previous chapters, we propose to use information theory and mutual information based method to be applied to RSN and preprocessed the data using KL. However due to the complexity of the environment it is possible we might get conflicting result. We want to resolve the conflict of decision by applying different methods. Dempster-Shafer theory, deals with measures of belief as opposed to probability. For our target detection algorithms, two different propositions are target present (t) and target not present respectively(nt). Entropy (E) and mutual information (MI) provides two different evidential sources  $m_1$  and  $m_2$ . We can find the belief function from the threshold value. The combined belief of target present can be calculated by using the Dempster's rule of combination. Many researchers insist that normalization procedure in the DS combination rule involves counterintuitive result when there is high conflict in evidence. A lot of modified rule that can solve the problem are proposed. One of the popular one is Proportional Conflict Redistribution Rule 5 (PCR5). PCR5 is the most mathematically exact redistribution rule for conflicting mass than all other PCR methods. Bayesian network (BN), also known as belief networks, belongs to family of probabilistic graphical models (GMs). In our study we have a tree structured network with a root node T, which has no parent. T is the parent node with two children nodes  $E_h$  and  $MI_h$ , which represents high entropy and high Mutual information respectively. Among the decision fusion algorithms, Bayesian approach worked slightly better than PCR5 while combining evidential conflict. However PCR5 performed better than DS. Results show that accurate detection can be achieved by applying DS in case of low conflict [92].



- *Sensor Selection Based on Chernoff Information* We propose theory and algorithm for a new scheme of Opportunistic sensing(OS) that not only ensures effective utilization of sensing assets but also provides optimal performance. We propose to use Chernoff information as sensor selection scheme. Before the weighted average is applied in the fusion center, best sensors will be selected based on their Chernoff information. Chernoff information gives best error exponent for hypothesis testing in Bayesian approach. The higher the Chernoff information the lower the probability of error in detection. As an alternative to Bayesian approach, we can minimize one of the error subject to the constraint of the other error, which is known as Chernoff-Stein Lemma. From this we can say that the false alarm probability is inversely proportional to KL distance. This finding is consistent to Chapter 3. We derived the close form approximation for the Chernoff information and KL distance between uniform and Gaussian densities. This is a novel approach since it has not been investigated so far. Simulation results show that our approach can work successfully with real world data. Using this novel approach we could significantly reduce the number of radars from 9 to 1, while maintaining good performance [93] [94].
- *Human Detection Based on Information Theory* Detection of human hidden behind the walls is a challenging task. The transmission of electromagnetic waves through the wall causes decrease in velocity due to the dielectric constant of the wall. Higher the dielectric constant and more the thickness of the wall, larger will be the delay. This results in the targets behind the wall to appear farther away than they actually are. To overcome the attenuation in frequency bands, wide-band signal ensures that at least some of the energy will get through the wall and permit the processing of the target-reflected signals. In this chapter, we propose to use information theory to UWB radar to detect

human target. We applied relative entropy based preprocessing and entropy based detection. Results show that with this novel approach, accurate detection can be achieved when human is hidden behind the gypsum wall. This method could also detect human hidden behind the brick wall. However this method did not work for detecting human behind the wooden door [95].

- *Throughput Optimization of Cognitive Radio Using Sensor Network and Power Allocation* In this study we consider an interweaved Cognitive radio network, which can sense the spectrum and communicate in the white space of the spectrum while keeping the interference due to the missed detection under limit. Throughput optimization while keeping the interference under the threshold is one of the most challenging issues in Cognitive Radio network. In this dissertation, we combined the sensing schemes along with sub optimal power allocation. We designed the optimal sensing time while initially applying the DDMWF scheme for power allocation. From simulation result we found that OR based sensing scheme performed the best than any other sensing scheme. We also found that there exist an optimal sensing time where the throughput is maximum. Results show that this method can greatly improves the overall throughput. We can also extend this work for a macro femto network where the femtocell can work as a secondary device [96] [97].

## 8.2 Future Direction

### 8.2.1 Extending Information Theory Based Target Detection in Multi-target Environment

Using information theory based method, we successfully detected two different kinds of Target: Metallic reflector and human. In future this method can be success-

fully applied in multi-target environment. Various technical perspectives have been investigated by researchers in this domain, [98], [99], [100] and [101]. However none of these methods worked on information theory.

### 8.2.2 Applying Chernoff Information and KL Based Processing in Big Data

Big data has received increasing attention for its broad research and application prospects [102], [103], [104] and [105]. Big data refers to huge datasets that are difficult to acquire, store, search, visualize, and analyze. Nowadays the data scale expands rapidly and exceeds the current processing capability of computer. At present the global data storage and processing capability has already been far behind the growth of data. There are three basic steps for big data preprocessing, namely data Extraction, Transformation and Loading. ETL is responsible for extracting the data from the multiple data sources to a temporary intermediate layer for conversion, integrated, and finally loaded into the target database or the corresponding file in the storage system, which is the basis of data mining. Big data mining uses parallel processing such as MapReduce [102], it means resolving mass data and distributed storage, and then using data mining by parallel processing and finally outputting the results together.

Our method of KL based preprocessing can be applied in this scenario and Chernoff information can be applied in the stage of extracting the data. We can verify the integration error using Chernoff information.

### 8.2.3 Interweaved Cognitive Radio for Optimizing the Femto Macro Capacity

The demand for higher capacity in mobile network is unrelenting. The rapid development of the smart phone and tablet PCs has changed the cellular network from the voice network to mostly data network. Also due to attenuation of the

signal in indoor, some of the area in indoor has very poor coverage by macrocell. Femtocell provide the solution of these problems. The integrated femtocell/macrocell networks offer an efficient way to increase access capacity by improving coverage and quality of service, while on the other side the deployment cost of the service provider is kept in extremely low levels. A large wireless capacity can be increased by reducing the cell size and transmit distance. Femtocells are low cost, low power base stations, maintained by the consumer. It gives the opportunity to the service provider to extend the service indoors and other places where coverage is not available otherwise. However femtocell can cause interference to the macrocell user if they are both operating in the same channel, which in turn will reduce the capacity. In [106], the interference mitigation technique for the femtocell was presented by LDO method. In[107], a centralized resource management was proposed to mitigate the interference. In [108] authors presented CR as the solution, so there was cooperation between the macro and femtocell. Femtocell would share its information such as number of user, power and frequency. Resource would be allocated based on CR. Fractional frequency reuse was proposed as a method in [109]. In [110] the interference between macro and femtocell was presented for the open access, in heterogeneous tow-tier network. A cross layer interference control considering the QOS was proposed in [111]. In [112] the behavior of the macrocell and femtocell interference was modeled. In [113] beam forming was proposed as a method to manage the interference in femtocell by using directional antennas. In [114]self organizing method, was used where the network is based on Q learning and changed its parameter by self organization. Interference alignment was introduced as a technique to increase the multiplexing gain of a MIMO X channel [116],[117], [115] and [118]

In future, we can design the cognitive radio as an underlay cognitive radio instead of an interweave cognitive radio. In an attempt to get the information theo-

retic boundary of the capacity region, we propose to analyze the degree of freedom of the underlay cognitive radio network. We propose to investigate the interference alignment technique to manage the interference in a cognitive femto cell.

## Appendix A

Closed Form Approximation Between Rician and Gaussian for KL

### A.1 Closed Form Approximation Between Rician and Gaussian for KL

One of the popular indoor UWB channel model is S-V model. But the foliage environment differs from indoor and it has been already shown that the outdoor UWB channel follows a Rician distribution [4], whereas the target region is uniform [88]. Now KL distance for the continuous case can be written as

$$D(p(x)||q(x)) = \int_0^{\infty} p(x) \ln \frac{p(x)}{q(x)} dx \quad (\text{A.1})$$

For our case  $p(x)$  follows  $\mathbf{U}(a, b)$  and  $q(x)$  follows  $\mathbf{Rice}(\nu, \sigma)$  can be expressed as,

$$p(x) = \frac{1}{b-a} \quad (\text{A.2})$$

and

$$q(x) = \frac{x}{\sigma^2} e^{-\frac{x^2+\nu^2}{2\sigma^2}} I_0\left[\frac{x\nu}{\sigma^2}\right] \quad (\text{A.3})$$

Here  $I_0$  is the modified Bessel function of the first kind with order 0. Now the(A.1) becomes,

$$D(p(x)||q(x)) = \int_a^b \frac{1}{b-a} \ln \left( \frac{\frac{1}{b-a}}{\frac{x}{\sigma^2} e^{-\frac{x^2+\nu^2}{2\sigma^2}} I_0\left[\frac{x\nu}{\sigma^2}\right]} \right) dx \quad (\text{A.4})$$

After simplification this can be written as,

$$\begin{aligned} D(p(x)||q(x)) &= \frac{1}{b-a} \left[ \int_a^b \ln \frac{x}{\sigma^2} dx + \int_a^b \frac{x^2 + \nu^2}{2\sigma^2} dx \right] \\ &+ \frac{1}{b-a} \int_a^b \ln [I_0 \frac{x\nu}{\sigma^2}] dx + \ln(b-a) \end{aligned} \quad (\text{A.5})$$

Now the third term in (A.5) is difficult to integrate. So we need to approximate the closed form. The mean of Rician distribution is

$$E[x] = \sqrt{\frac{\pi\sigma^2}{2}} e^{-\frac{\nu^2}{4\sigma^2}} \left[ \left(1 + \frac{\nu^2}{2\sigma^2}\right) I_0\left(\frac{\nu^2}{4\sigma^2}\right) + \left(\frac{\nu^2}{2\sigma^2}\right) I_1\left(\frac{\nu^2}{4\sigma^2}\right) \right] \quad (\text{A.6})$$

and the variance is,

$$var(x) = \nu^2 + 2\sigma^2 - E^2(x) \quad (\text{A.7})$$

It is shown in Chapter 3 in (3.19) that the KL between a uniform and gaussian distribution can be written as,

$$D(p(x)||q(x)) = -\ln(b - a) + \ln\sqrt{2\pi}\sigma + \frac{\mu}{4\sigma^2} [\{a - \mu\}^2 + \{b - \mu\}^2] \tag{A.8}$$

Now using the mean and the variance from (A.6) and (A.7) in (A.8), the closed form expression of the KL for our target detection can be calculated.



## Appendix B

### Closed Form Approximation of Chernoff Information Between Rician and Uniform Distribution

### B.1 Closed Form Approximation of Chernoff Information Between Rician and Uniform Distribution

Chernoff information for continuous case can be defined as,

$$C(p(x), q(x)) = - \min_{0 \leq \lambda < 1} \left\{ \ln \int_x p(x)^\lambda q(x)^{1-\lambda} dx \right\} \quad (\text{B.1})$$

For our case  $p(x)$  follows  $\mathbf{U}(a, b)$  and  $q(x)$  follows  $\mathbf{Rice}(\nu, \sigma)$  can be expressed as,

$$p(x) = \frac{1}{b-a} \quad (\text{B.2})$$

and

$$q(x) = \frac{x}{\sigma^2} e^{-\frac{x^2 + \nu^2}{2\sigma^2}} I_0\left[\frac{x\nu}{\sigma^2}\right] \quad (\text{B.3})$$

Here  $I_0$  is the modified Bessel function of the first kind with order 0. Now if we define the natural log term as  $C(\lambda)$ , then using  $p(x)$  and  $q(x)$  from (B.2) and (B.3)

$$C(\lambda) = \ln \left\{ \int_a^b \left[ \frac{1}{b-a} \right]^\lambda \left[ \frac{x}{\sigma^2} e^{-\frac{x^2 + \nu^2}{2\sigma^2}} I_0\left[\frac{x\nu}{\sigma^2}\right] \right]^{1-\lambda} dx \right\} \quad (\text{B.4})$$

This can be further expanded and written as,

$$\begin{aligned} C(\lambda) = & -(\lambda)(b-a)\ln(b-a) + \lambda \left[ \int_a^b \ln \frac{x}{\sigma^2} dx \right] \\ & -(1-\lambda) \left[ \int_a^b \ln \frac{x^2 + \nu^2}{2\sigma} dx - \int_a^b \ln I_0\left(\frac{\nu^2}{\sigma^2}\right) dx \right] \end{aligned} \quad (\text{B.5})$$

Now we can find the closed form expression of Chernoff information between Uniform and Gaussian distribution from Chapter5. The expression is,

$$\begin{aligned} C(\lambda) = & -(b-a) \left[ \frac{1-\lambda}{2} \ln(2\pi\sigma^2) + (\lambda)\ln(b-a) \right] + \\ & -(1-\lambda) \frac{1}{6\sigma^2} [(b-\mu)^3 - (a-\mu)^3] \end{aligned} \quad (\text{B.6})$$

Now replacing the mean and variance from (A.6) and (A.7), we can get an approximate closed form expression for the Chernoff information for our target detection case.

## References

- [1] J. D. Taylor, *Introduction to Ultra-Wideband Radar Systems*, CRC Press, 1995.
- [2] J.D.Taylor, *Ultra-Wideband Radar Technology*, CRC Press, Newyork, 2001.
- [3] I. Y. Immoreev, "New practical application of ultra-wideband radars, *European Radar Conference*, pp. 216 - 219, Oct 2007.
- [4] Q. Liang, "Radar Sensor Wireless Channel Modeling in Foliage Environment: UWB Versus Narrowband," *IEEE Sensors J.* , vol. 11, no. 6, pp. 1448-1457, June 2011.
- [5] J. Liang, Q. Liang and S.W. Samn, "Foliage Clutter Modeling Using the UWB Radar," *IEEE Int. Conf. Communications*,pp. 1937-1941, May 2008.
- [6] R. Mayer, F. Bucholtz and D. Scribner, "Object detection by using whitening/dewhitening to transform target signatures in multitemporal hyperspectral and multispectral imagery," *IEEE Trans. Geosci. Remote Sens.*, vol. 41, no. 5, pp. 1136-1142, May 2003.
- [7] J. G. Nanis, S. D. Halversen, G. J. Owirka and L. M. Novak, "Adaptive filters for detection of targets in foliage," *IEEE Nat. Radar Conf.*, pp. 101-103, 29-31 Mar 1994.
- [8] D. E. Bar et al. "Target Detection and Verification via Airborne Hyperspectral and High-Resolution Imagery Processing and Fusion," *IEEE Sensors J.*, vol. 10, no. 3, pp. 707-711, March 2010.
- [9] J. Liang, Q. Liang, and S.W. Samn, "A Differential Based Approach for Sense-through-Foliage Target Detection Using UWB Radar Sensor Networks, *Proc. IEEE Intl Conf. Comm. (ICC 09)*, pp. 1952-1956, 2008.

- [10] J. Liang and Q. Liang, "UWB Radar Sensor Networks Detection of Targets in Foliage Using Short-Time Fourier Transform, *Proc. IEEE Intl Conf. Comm.* (ICC 09), pp. 1-5, 2009.
- [11] Q. Linag, B. Zhang and X. Wu, "UWB radar for target detection: DCT versus matched filter approaches," *IEEE Globecom Workshops (GC Wkshps)*, pp.1435,1439, 3-7 Dec. 2012.
- [12] Y. Kwon, R. M. Narayanan and M. Rangaswamy, "A multi-target detector using mutual information for noise radar systems in low SNR regimes," *Int. Waveform Diversity and Design Conf. (WDD)*, pp. 105-109, 8-13 Aug. 2010.
- [13] Y. Nijssure et al. "Information-theoretic algorithm for waveform optimization within ultra wideband cognitive radar network," *IEEE Int. Conf. Ultra-Wideband (ICUWB)*, vol. 2, pp. 1-4, 20-23 Sept. 2010.
- [14] S. Ji, X. Liao and L. Carin, "Adaptive multiaspect target classification and detection with hidden Markov models," *IEEE Sensors J.*, vol.5, no.5, pp. 1035-1042, Oct. 2005.
- [15] M. P. Kolba, W. R. Scott and L.M. Collins, "A Framework for Information-Based Sensor Management for the Detection of Static Targets", *IEEE Trans. Syst., Man., Cybern. A, Syst., Humans*, vol. 41, no. 1, pp.105-120, Jan. 2011.
- [16] C. Kreucher, K. Kastella, and A.O. Hero, "Information based sensor management for multitarget tracking," *Proc.SPIE*, vol. 5204, pp. 480-489, 2003.
- [17] J. M. Aughenbaugh and B. R. La Cour, "Metric selection for information theoretic sensor management," *11th Int. Conf. Information Fusion* pp. 1-8, June 30 2008-July 3 2008.
- [18] X. Wang, J. Liu and H. Liu "Small Target Detection in Sea Clutter Based on Doppler Spectrum Features," *International Conference on Radar*, pp.1-4, 16-19 Oct. 2006.

- [19] S. Li, F. Pu and D. Li , “An Improved Edge Detection Algorithm Based on Area Morphology and Maximum Entropy,”, *Second International Conference on Innovative Computing, Information and Control*, pp.536, 5-7 Sept. 2007.
- [20] A. Wagner and B. Plattner, “Entropy based worm and anomaly detection in fast IP networks,”, *14th IEEE International Workshops on Enabling Technologies: Infrastructure for Collaborative Enterprise*, pp. 172- 177, 13-15 June 2005.
- [21] L. He, Q. Pan, W. Di and Y. Li, “Anomaly detection in hyperspectral imagery based on maximum entropy and nonparametric estimation”, *Pattern Recognition Letter*, vol. 29, Issue 9, pp. 1392-1403, 2008.
- [22] T. M. Cover and J. A. Thomas *Elements of Information Theory*, Wiley-Interscience press, Newyork, 1991.
- [23] P.K. Dutta, A.K. Arora, and S.B. Bibyk, “Towards Radar-Enabled Sensor Networks, *Proc. Fifth Intl Conf. Information Processing in Sensor Networks*, pp. 467-474, Apr. 2006.
- [24] J. Liang and Q. Liang, “Design and analysis of distributed Radar Sensor Networks,” *IEEE Trans. Parallel and Distrib. Syst.*, vol. 22, no. 11, pp.1926-1933, Nov. 2011.
- [25] Q. Liang, “Automatic Target Recognition Using Waveform Diversity in Radar Sensor Networks, *Pattern Recognition Letters (Elsevier)*, vol. 29, no. 2, pp. 377-381, 2008.
- [26] Q. Liang, “Radar Sensor Networks: Algorithms for Waveform Design and Diversity with Application to ATR with Delay-Doppler Uncertainty, *EURASIP Journal on Wireless Communications and Networking*, Article ID: 89103, pp. 1-9, vol. 2007.

- [27] Q. Liang, X. Cheng, “KUPS: Knowledge-based Ubiquitous and Persistent Sensor networks for Threat Assessment, *IEEE Transactions on Aerospace and Electronic Systems*, vol. 44, no. 3, July 2008.
- [28] E. Fishler, A. Haimovich, R.S. Blum, L.J. Cimini, D. Chizhik, and A. Valenzuela, “Spatial Diversity in Radars Models and Detection Performance, *IEEE Trans. Signal Processing*, vol. 54, no. 3, pp. 823-838, Mar. 2006.
- [29] F.C. Robey, S. Coutts, D. Weikle, J.C. McHarg, and K. Cuomo, “MIMO Radar Theory and Experimental Results, *Proc. 38th Asilomar Conf. Signals, Systems and Computers*, vol. 1, pp. 300-304, Nov. 2004.
- [30] K. Forsythe, D. Bliss, and G. Fawcett, “Multiple-Input Multiple- Output (MIMO) Radar: Performance Issues, *Proc. 38th Asilomar Conf. Signals, Systems and Computers*, vol. 1, pp. 310-315, Nov. 2004
- [31] M. Kalandros, “Covariance control for multisensor systems,” *IEEE Trans. Aerosp. Electron. Syst.*, vol. 38, no. 4, pp. 1138-1157, Oct. 2002.
- [32] R. Mahler, “Multisensor -multitarget sensor management: A unified Bayesian approach,” *Proc.SPIE*, vol. 5096, pp. 222-233, 2003.
- [33] K. Kastella, “Discrimination gain to optimize detection and classification,” *IEEE Trans. Syst., Man., Cybern. A, Syst., Humans*, vol. 27, no. 1, pp. 112-116, Jan1997.
- [34] R. C. Luo and K. M. G. Kay, “A tutorial on multisensor integration and fusion,” *in Proc 16th Annual Conf. IEEE Ind. Electron*, pp. 707-722 vol. 1, Nov. 1990.
- [35] R. C. Luo, C. C. Chang, and C. C. Lai, “Multisensor Fusion and Integration: Theories, Applications, and its Perspectives,” *IEEE Sensors J.*, vol. 11, no. 12, pp. 3122-3138, Dec. 2011.

- [36] X. Li and W. Zhu, "Multi- feature fusion in weed recognition based on Dempster-Shafer's theory," *Int. Conf. Computer Application and System Modeling (IC-CASM)*, vol. 5, pp. 127-130, 22-24 Oct. 2010.
- [37] F. Smarandache, J. Dezert, "Information fusion based on new proportional conflict redistribution rules," *8th Int. Conf. Information fusion*, vol.2, pp. 8, 2005
- [38] S. J. Russell and P. Norvig, *Artificial Intelligence: A Modern Approach*, 3rd Edition, Pearson Education, Inc., Prentice Hall, Upper Saddle River, New Jersey, 2010.
- [39] V. Poulain, J. Inglada, M. Spigai, J. Y. Tourneret and P. Marthon, "High-Resolution Optical and SAR Image Fusion for Building Database Updating," *IEEE Trans. Geosci. Remote Sens.*, vol. 49, no. 8, pp. 2900-2910, Aug. 2011.
- [40] N. Nguyen-Thanh and I. Koo, "Evidence-Theory-Based Cooperative Spectrum Sensing With Efficient Quantization Method in Cognitive Radio," *IEEE Trans. Veh. Technol.*, vol.60, no.1, pp.185-195, Jan. 2011.
- [41] C. Cai and S. Ferrari, "Comparison of Information-Theoretic Objective Functions for Decision Support in Sensor Systems," *American Control Conf.*, pp. 3559-3564, 9-13 July 2007.
- [42] X. Chen; Y. Yang and H. Cheng, "Conflict problems of D-S evidence in multi-sensor information fusion technology," *Int. Conf. Computer Application and System Modeling (IC-CASM)*, vol. 4, pp. 314-318, Oct., 2010.
- [43] R.P.S. Mahler, *Statistical Multisource-Multitarget Information Fusion* Artech House, 2007.
- [44] A. Kirchner, F. Dambreville, F. Celeste, J. Dezert, and F. Smarandache, "Application of probabilistic PCR5 fusion rule for multisensor target tracking," *10th International Conference on Information Fusion*, pp.1,8, 9-12 July 2007.



- [45] H. Wen, X. Huang and X. Li, "A new tool applied to robot perception by selecting evidence sources," *IEEE International Conference on Automation and Logistics, (ICAL 2008)* pp.2364,2369, 1-3 Sept. 2008.
- [46] J. Dezert, Z. Liu and G. Mercier, "Edge detection in color images based on DSMT," *Proceedings of the 14th International Conference on Information Fusion* , pp.1,8, 5-8 July 2011.
- [47] Richard E. Neapolitan, *Probabilistic Reasoning in Expert Systems,theory and algorithms*, John Wiley & Sons, 1990.
- [48] B. Carbutar, A. Grama, J. Vitek, O. Carbutar, "Coverage Preserving Redundancy Elimination in Sensor Networks, *IEEE SECON 2004*, October 2004
- [49] Q. Liang, L. Wang, "Redundancy Reduction in Wireless Sensor Networks Using SVD-QR, *IEEE Military Communication Conference*, Atlantic City, NJ, Oct 2005.
- [50] Q. Liang, X. Cheng and D. Chen. "Opportunistic Sensing in Wireless Sensor networks: Theory and Application," *IEEE Global telecommunications conference (GLOBECOM'11)*, pp. 1-5, Dec 2011.
- [51] Q. Liang, X. Cheng, S Huang, and D. Chen. "Opportunistic Sensing in Wireless Sensor networks: Theory and Application, accepted by IEEE Trans on Computers.
- [52] G. Fabeck, and R. Mathar, "Chernoff information-based optimization of sensor networks for distributed detection," *IEEE International Symposium on Signal Processing and Information Technology (ISSPIT)*, 2009 , pp.606-611, 14-17 Dec. 2009.
- [53] S. Misra, Lang Tong and A. Ephremides, "Error Exponents for Target-Class Detection in a Sensor Network," *IEEE Conf. Military Commun.( MILCOM)* pp.1-7, 23-25 Oct. 2006.

- [54] B. M. Sadler, and A. Swami, "On the performance of episodic UWB and direct-sequence communication systems," *IEEE Transactions on Wireless Communications*, vol.3, no.6, pp.2246-2255, Nov. 2004.
- [55] Y. Lee and Y. Sung, "Generalized Chernoff Information for Mismatched Bayesian Detection and Its Application to Energy Detection," *IEEE Signal Processing Letters*, vol.19, no.11, pp.753-756, Nov. 2012.
- [56] A. Nezirovic, A.G. Yarovoy and L.P.Ligthart, "Experimental study on human being detection using UWB radar," *International Radar Symposium*, pp.1,4, 24-26 May 2006.
- [57] E. M. Staderini, E.M., "UWB radars in medicine, *IEEE Aerospace and Electronic Systems Magazine*, vol.17, no. 1, pp. 13 - 18., Jan. 2002.
- [58] G. Ossberger, I. Buchegger, E. Schimback, A. Stelzer and R. Weigel "Non-invasive respiratory movement detection and monitoring of hidden humans using ultra wideband pulse radar," *International Workshop on Ultra Wideband Systems*, pp. 395 - 399, May 2004.
- [59] S. Singh, Q. Liang, D. Chen and Li Sheng, "Sense through Wall Human Detection Using UWB Radar, *EURASIP Journal on Wireless Communications and Networking*, vol. 2011, no 20, June 2011.
- [60] A. Kumar, Q. Liang, Zhuo Li, B. Zhang and X. Wu, "Experimental study of through-wall human being detection using ultra-wideband (UWB) radar," *IEEE Globecom Workshops (GC Wkshps)*, pp.1455-1459, 3-7 Dec. 2012.
- [61] A. Kumar, Z. Li, Q. Liang, B. Zhang and X. Wu, "Experimental Study of through-wall Human Detection using Ultra Wideband Radar Sensors, *Elsevier Measurement*, vol. 47, pp. 869-879, January 2014.
- [62] Federal Communications Commission "Spectrum Policy Task Force Trans", Rep. ET Docket no. 02-135, 2002.

- [63] V. Fodore et. Al, "Sensor Networks for Cognitive Radio : Theory and System Design," *In proceedings of ICT mobile summit*, Stockholm, Sweden, 2010 .
- [64] D. Ruilong, J. Chen, C. Yuen, P. Cheng, and Y. Sun "Energy-Efficient Cooperative Spectrum Sensing by Optimal Scheduling in Sensor-Aided Cognitive Radio Networks," *IEEE Transactions on Vehicular Technology*, vol.61, no.2, pp.716-725,2012.
- [65] M. Chen, T. Kwon, S. Mao, Y. Yuan and C. M. V. Leung, "Reliable and energy-efficient routing protocol in dense wireless sensor networks," *International Journal of Sensor Networks*, vol. 4, no.1, pp. 104-117, 2008.
- [66] Q. Liang, L. Wang, and Q. Ren "Fault tolerant and energy efficient cross-layer design in wireless sensor networks," *International Journal of Sensor Networks*, vol. 2, no. 3/4, pp. 248-257, 2007.
- [67] X. Xia and Q. Liang "Latency-aware and Energy Efficiency Tradeoffs for Wireless Sensor Networks," *International Journal of Sensor Networks*, Vol. 5, No. 1, 2010.
- [68] L. Stabellini and J. Zander "Energy- efficient detection of intermittent interference in wireless sensor networks," *International Journal of Sensor Networks*, Vol. 8, No.1 pp. 27 - 40, 2010.
- [69] F. Hu, R. Patibandla and Y. Xiao, "Spectrum sensing in Cognitive Radio sensor networks: towards ultra low overhead, distributed channel findings," *International Journal of Sensor Networks*, Vol. 3, No.2 pp. 115 - 122, 2008.
- [70] S. Mosleh, A.A. Tadaion and M. Derakhtian, "Bayesian decision for the fusion center of a distributed network in Cognitive Radio," *IEEE International Conference on Signal and Image Processing Applications (ICSIPA)*, pp.508-513, 2009.

- [71] A. Singh, M.R. Bhatnagar and R.K. Mallik, "Cooperative Spectrum Sensing in Multiple Antenna Based Cognitive Radio Network Using an Improved Energy Detector," *IEEE Communications Letters*, vol.16, no.1, pp.64-67, 2012.
- [72] A. Liang, Nallanathan, H. K. Garg, R. Zhang, "Optimal power allocation for fading channels in cognitive radio networks: Ergodic capacity and outage capacity," *IEEE Trans. Wireless Commun.*, vol.8, no.2, pp.940-950, 2009.
- [73] Y. Hu and G. Kuo, "Space-Time-Frequency Domain Water-Filling in MIMO-OFDM Fading System," *IEEE conference on Vehicular Technology*, pp. 2475-2480, 2007.
- [74] G. Bansal, M. J. Hossain, and V. K. Bhargava "Optimal and Suboptimal Power Allocation Schemes for OFDM-based Cognitive Radio Systems," *IEEE Trans. Wireless Commun.*, vol.7, no.11, pp.4710-4718, 2008.
- [75] C. C. Chai, and Y. H. Che "Power Control for Cognitive Radios in Nakagami Fading Channels with Outage Probability Requirement," *IEEE Global Telecommun. Conf. (GLOBECOM 2010)*, pp.1-5, 2010
- [76] K. Hamdi and K. Ben Letaief "Power, Sensing Time, and Throughput Tradeoffs in Cognitive Radio Systems: A Cross-Layer Approach," *IEEE Wireless Communications and Networking Conference (WCNC)*, pp.1-5, 2009.
- [77] X. Huang, and B. Beferull-Lozano "Joint Optimization of Detection and Power Allocation for OFDM-Based Cognitive Radios," *IEEE Global Telecommunications Conference (GLOBECOM 2010)*, pp.1-5, 2010.
- [78] J. Shen, T. Jiang, S. Liu, and Z. Zhang, "Maximum channel throughput via cooperative spectrum sensing in cognitive radio networks," *IEEE Transactions on Wireless Communications*, vol.8, no.10, pp.5166-5175, 2009.

- [79] H. Yu, "The optimization of sensing-throughput in cognitive UWB networks," *2nd International Asia Conference on Informatics in Control, Automation and Robotics (CAR)*, vol.3, pp.1-4, 2010.
- [80] F. Li "Adaptive resource allocation in multiuser cooperative networks with proportional rate constraints," *International Journal of Sensor Networks*, Vol. 10, No. 1, pp. 104-110, 2011.
- [81] C. Dill, "Foliage Penetration(phase II) Field Test Narrow band versus Wideband Foliage Penetration," *Final report of contract number F41624-03-D-700/04*, July 2005 to Feb 2006.
- [82] Time Domain Corporation , "PulsON Technology Overview", July 2001.
- [83] Time Domain Corporation, "PulsON 220 SAM Users Manual", May 2008
- [84] Time Domain Corporation, "Monostatic Radar (MSR) Analysis Tool Application Note", May 2008.
- [85] A.G. Yarovoy, J. Matuzas, B. Levitas, L.P. Ligthart, "UWB radar for human being detection, 2009.
- [86] Lai, C. P., R.M. Narayanan and G. Culkowski, "Through Wall Surveillance Using Ultrawideband Random Noise Radar. Ft. Belvoir, Defense Technical Information Center", 2006.
- [87] R Chandra, Abhay N Gaikwad, Dharmendra Singh and M J Nigam, "An approach to remove the clutter and detect the target for ultra-wideband through-wall imaging," *Journal of Geophysics and Engineering*, December 2008.
- [88] I. Maherin and Q. Liang, "An entropy based approach for sense- through foliage target detection using UWB radar, *6th international conference of Wireless Algorithms, Systems and Applications (WASA )*, pp. 180-189, Chengdu, China, 2011.

- [89] I. Maherin and Q. Liang, "A mutual information based approach for target detection through foliage using UWB radar, *IEEE conference on Communications (ICC 2012)*, pp.6406-6410, 2012.
- [90] I. Maherin and Q. Liang, "Multi-step information fusion for target detection through UWB Radar Sensor Network, under review, *IEEE Sensors Journal*.
- [91] I. Maherin and Q. Liang, "Preprocessing in Radar Sensor Network using information theory, *IEEE Global Communications Conference*, 2014(submitted).
- [92] I. Maherin and Q. Liang, "Decision fusion in target detection using UWB radar sensor network, *In Proceedings of second International Conference on Communications, Signal processing and Systems, Lecture notes in Electrical Engineering*, vol. 246, pp 1013-1020, 2014.
- [93] I. Maherin and Q. Liang, "Radar sensor network based target detection using Chernoff information and relative entropy, *Physical Communication Journal*, Feb 2014.
- [94] I. Maherin and Q. Liang, "Information theory based opportunistic sensing in radar sensor network, *9th international conference of Wireless Algorithms, Systems and Applications (WASA 2014)* accepted.
- [95] I. Maherin and Q. Liang, "Human detection through wall using Information theory, *International Conference on Communications, Signal processing and Systems*, 2014, (submitted).
- [96] I. Maherin and Q. Liang, "Power allocation in OFDM based cognitive radio system, *International conference on Communications, Signal processing and Systems*, pp. 135-143, (CSPS)2012.
- [97] I. Maherin and Q. Liang, "Throughput optimization in sensor network aided Cognitive Radio, *Int. Journal of Sensor Networks*, vol.13, no. 4, pp. 234-240, 2013.

- [98] T. De Laet, H. Bruyninckx and J. De Schutter, "Shape-Based Online Multitarget Tracking and Detection for Targets Causing Multiple Measurements: Variational Bayesian Clustering and Lossless Data Association," *IEEE Transactions on Pattern Analysis and Machine Intelligence*, vol.33, no.12, pp.2477,2491, Dec. 2011.
- [99] H. Yong and G. Jian, "A track-before-detect algorithm for statistical MIMO radar multitarget detection," *IEEE Radar Conference*, pp.12,16, 10-14 May 2010.
- [100] K. Chang, "Adaptive detection thresholds for multitarget tracking," Proceedings of the American Control Conference, vol.1, no., pp.633,637 vol.1, 21-23 Jun 1995.
- [101] O. Songhwai, S. Russell and S. Sastry, "Markov Chain Monte Carlo Data Association for Multi-Target Tracking," *IEEE Transactions on Automatic Control*, vol.54, no.3, pp.481,497, March 2009.
- [102] J. Dean and S. Ghemawat, "MapReduce: Simplified Data Processing on Large Clusters", *CACM*, vol.51(1), pp.107-113, 2008.
- [103] L. Shi, Q. Liao, X. Sun, Y. Chen and C. Lin, "Scalable network traffic visualization using compressed graphs," *IEEE International Conference on Big Data* pp.606,612, 6-9 Oct. 2013.
- [104] Yifei Zhang; Guoren Wang, "SPTI: Efficient Answering the Shortest Path Query on Large Graphs," *IEEE International Congress on Big Data (BigData Congress)*, pp.195-202, June 27-July 2 2013.
- [105] S. Sakr, A. Liu, D. Batista, and M. Alomari, "A Survey of Large Scale Data Management Approaches in Cloud Environments," *IEEE Communications Surveys and Tutorials*, vol.13(3), pp.311-336, 2011.

- [106] H. Widiarti, S. Pyun and Dong-Ho Cho, "Interference Mitigation Based on Femtocells Grouping in Low Duty Operation," *IEEE 72nd Vehicular Technology Conference Fall (VTC 2010-Fall)* pp.1-5, 6-9 Sept. 2010.
- [107] Juyeop Kim; Dong-Ho Cho, "A Joint Power and Subchannel Allocation Scheme Maximizing System Capacity in Indoor Dense Mobile Communication Systems," *IEEE Trans. on Vehicular Techno.*, vol.59, no.9, pp.4340,4353, Nov. 2010.
- [108] D. Oh and Y. Lee, "Cognitive radio based resource allocation in femto-cells," *Journal of Communications and Networks*, vol.14, no.3, pp.252,256, June 2012.
- [109] H. Lei, L. Zhang, X. Zhang and D. Yang, "A Novel Multi-Cell OFDMA System Structure using Fractional Frequency Reuse," *IEEE 18th International Symposium on Personal, Indoor and Mobile Radio Communications (PIMRC 2007)*, pp.1-5, 3-7 Sept. 2007.
- [110] S. Wei, C. Chang, Y. Lin, H. Hsieh and H. Su, "Formulating and solving the femtocell deployment problem in two-tier heterogeneous networks," *IEEE International Conference on Communications (ICC)*, pp.5053-5058, 10-15 June 2012.
- [111] M. Cierny, R. Wichman, J. Hamalainen, C. Ribeiro, Z. Ding and X. Liu, "On TDD cross-tier in-band interference mitigation: A practical example," *7th International ICST Conference on Cognitive Radio Oriented Wireless Networks and Communications (CROWNCOM)*, pp.1-6, 18-20 June 2012.
- [112] A. Alexiou, C. Bouras, V. Kokkinos, K. Kontodimas and A. Papazois, "Interference behavior of integrated femto and macrocell environments," *IFIP Wireless Days (WD)*, pp.1-5, 10-12 Oct. 2011.
- [113] Ang-Hsun Tsai, Jane-Hwa Huang, Li-Chun Wang and Ruey-Bing Hwang, "Capacity comparison for CSG and OSG OFDMA femtocells," *IEEE GLOBECOM Workshops (GC Wkshps)*, pp.653-658, 6-10 Dec. 2010.



- [114] C. Dhahri and T. Ohtsuki "Learning-Based Cell Selection Method for Femtocell Networks," *75th IEEE Vehicular Technology Conference (VTC Spring)*, pp.1-5, 6-9 May 2012.
- [115] A. Goldsmith, S. A. Jafar, I. Maric and S. Srinivasa, "Breaking Spectrum Gridlock With Cognitive Radios: An Information Theoretic Perspective," *Proceedings of the IEEE*, vol.97, no.5, pp.894-914, May 2009.
- [116] V. R. Cadambe and S. A. Jafar, "Interference Alignment and Degrees of Freedom of the  $n$ -User Interference Channel," *IEEE Transactions on Information Theory*, vol.54, no.8, pp.3425-3441, Aug. 2008.
- [117] S. A. Jafar and S. Shamai, "Degrees of Freedom Region of the MIMO X Channel," *IEEE Transactions on Information Theory*, vol.54, no.1, pp.151-170, Jan. 2008.
- [118] O. El Ayach, S. W. Peters and R. W. Heath, "The practical challenges of interference alignment," *IEEE Transactions on Wireless Communications*, vol.20, no.1, pp.35-42, February 2013.

## Biographical Statement

Ishrat Maherin is a current Ph.D student in the Department of Electrical Engineering at the University of Texas at Arlington. Ishrat completed her Bachelor of Science Degree in Electrical Engineering from Bangladesh University of Engineering and Technology (BUET) in 1997. Her degree was awarded with Honours for outstanding academic performance. Ishrat completed her Masters of Science Degree from the University of Texas at Arlington in 2006. Ishrat joined UTA as a Ph.D. student in January, 2010. Her research interests include wireless communications, cognitive radio, information theory, UWB Radar Sensor Network, Target Detection and wireless sensor networks. She has been the author and co-author of several peer reviewed journal papers and conference proceedings. Ishrat received RIM Graduate Scholarship awards in 2013 and 2014.